

**Charles University in Prague
Faculty of Science**

Developmental biology



Mgr. Tereza Toralová

**Identification of genes crucially important for normal course of
fertilization and preimplantation development of cattle in *in vitro*
conditions**

**Identifikace genů nezbytně nutných pro normální průběh oplození
a preimplantačního vývoje skotu v podmínkách *in vitro***

PhD. thesis

Supervisor: RNDr. Jiří Kaňka, DrSc.

Prague, 2011

Declaration:

I declare that I have worked on this thesis independently. To the best of my knowledge and belief, this thesis contains no material previously published or written by another person, except where due reference has been made. This thesis contains no material which has been accepted for the award of any other degree or diploma in any University.

Prague

Tereza Toralová

The work was done at the Institute of Animal Physiology and Genetics AS CR, v.v.i. in Liběchov.

Acknowledgement

I would like to thank my supervisor RNDr. Jiří Kaňka, DrSc. for his support, guidance and encouragement throughout my study. I would also like to thank all the members of the Department of Reproductive and Developmental Biology who provided me with constant support and entertainment. Finally, I would like to thank my parents and my husband for always being there.

CONTENTS

1.	Abstract.....	2
2.	Abstrakt	3
3.	Introduction	4
1.1.	Oocyte maturation	4
1.2.	Fertilization.....	5
1.3.	Preimplantation development	6
1.4.	In vitro fertilization.....	8
2.	Characteristic of the most important used methods.....	10
2.1.	RNA interference.....	10
2.2.	Quantitative PCR.....	11
2.3.	Indirect immunofluorescent analysis.....	13
3.	Aims of the thesis	15
4.	Comments on publications	16
4.1.	Toralova T, Susor A, Nemcova L, Kepkova K, Kanka J. 2009 Silencing CENPF in bovine preimplantation embryo induces arrest at 8-cell stage. <i>Reproduction</i> 138: 783–791	16
4.2.	Susor A, Liskova L, Toralova T, Pavlok A, Pivonkova K, Karabinova P, Lopatarova M, Sutovsky P, Kubelka M. 2010 Role of UCHL1 in Anti-polyspermy Defense of Mammalian Eggs. <i>Biology of Reproduction</i> 82: 1151-1161	18
4.3.	Vodickova Kepkova K, Vodicka P, Toralova T, Lopatarova M, Cech S, Dolezel R, Havlicek V, Besenfelder U, Kuzmany A, Sirard M-A, Laurincik J, Kanka J. 2011 Transcriptomic analysis of <i>in vivo</i> and <i>in vitro</i> produced bovine embryos revealed a developmental change in cullin 1 expression during maternal-to embryonic transition. <i>Theriogenology</i> 75: 1582-1595.....	20
4.4.	Toralova T, Benesova V, Vodickova Kepkova K, Vodicka P, Susor A, Kanka J. Bovine preimplantation embryos with silenced nucleophosmin mRNA are able to develop until the blastocyst stage due to preservation of sufficient protein amount. Submitted to <i>Biology of Reproduction</i>	23
5.	Conclusions	25
6.	Abbreviation list	27
7.	References	29
8.	Publication list	42

1. ABSTRACT

The aim of this work was to find and characterize genes that seem to be important for normal preimplantation development. We characterized three genes in more detail – centromeric protein F (CENPF; mitotin), ubiquitin C-terminal hydrolase-L1 (UCHL1) and nucleophosmin (NPM1; B23; numatrin; NO38). CENPF and nucleophosmin were shown to start their expression at late 8-cell stage, i.e. at major embryonic genome activation (EGA), and were hence supposed to be important during bovine preimplantation development. CENPF plays crucial role during cell division, especially by mediating the interaction of kinetochores and microtubules. Nucleophosmin is a multifunctional nucleolar phosphoprotein, whose most important roles are rRNA processing, chaperoning, ribosome biogenesis and centriole duplication control. Further, we characterized the role of UCHL1 during fertilization of bovine oocytes. UCHL1 is a deubiquitinating enzyme that controls cytoplasmic protein degradation, recycling of free ubiquitin from proteasome products and is involved in regulation of physiological apoptosis.

We studied the function of CENPF and nucleophosmin using RNA interference approach. Since UCHL1 protein is very stable, this method is not suitable for studying the UCHL1 function. We thus used two UCHL1 inhibitors that block its hydrolase activity. The embryos with silenced *CENPF* mRNA arrest at 8-cell stage and have lower morphological quality than the control embryos. The development up until the 8-cell stage is likely enabled by the storage of maternal protein. In somatic cells and post-EGA embryos the protein is degraded at the end of each cycle, but we detected no such degradation in the pre-EGA embryos. Similarly, we confirmed the importance of UCHL1 for normal course of bovine fertilization. In oocytes matured in UCHL1 inhibitor, high rate of polyspermy was found after fertilization. This was likely caused by defects in cortical granule relocalization and extrusion. On the other hand, the embryos with silenced nucleophosmin mRNA were able to develop until the blastocyst stage. Even though a large portion of maternal protein was degraded a sufficient amount was still stored during whole preimplantation embryogenesis and enabled the development of embryos without any detectable defects.

Further, we have focused on identifying of new potentially important genes, whose role during preimplantation development will be determined in the following studies. Among these genes, especially cullin 1 seems to play an important role during bovine preimplantation development. Its transcription from embryonic genome starts at late 8-cells stage. Moreover, we detected two transcript variants of cullin 1 expressed from different genes, one of which (cullin 1-like; XM_589507.3) was present from MII oocytes to early 8-cell stage and the second one (cullin 1; XM_876699) was present from late 8-cell stage to the blastocyst stage. These two genes are 83% homologous in sequence, both present on chromosome 4 but localized to two different regions.

2. ABSTRAKT

Cílem této práce bylo nalézt a charakterizovat geny, které jsou potenciálně nezbytné pro normální preimplantační vývoj. Podrobněji jsme charakterizovali tři geny – CENPF (centromeric protein F; mitosin), UCHL1 (ubiquitin C-terminal hydrolase-L1) a nukleofosmin (NPM1, B23, numatrin; NO38). Embryonální transkripce *CENPF* a nukleofosminu je aktivována v pozdním 8-buněčném stádiu (tj. v době embryonální genomové aktivace – EGA), a proto lze předpokládat, že jsou pro normální preimplantační vývoj nezbytné. CENPF je důležitý pro buněčné dělení, především zprostředkuje interakci mezi kinetochorem a mikrotubuly. Nukleofosmin je multifunkční jadérový fosfoprotein, který se podílí zejména zpracování rRNA, biogenezi ribozómů, duplikaci centriol a uplatňuje se také jako chaperon. Dále jsme na základě předpokládané úlohy během fertilizace vybrali gen UCHL1 a popsali jeho úlohu během oplození bovinních oocytů. UCHL1 je deubikvitinylační enzym, který koordinuje degradaci cytoplazmatických proteinů, recyklaci volného ubikvitinu z proteazomu a podílí se na regulaci fyziologické apoptózy.

Úlohu CENPF a nukleofosminu jsme sledovali pomocí RNA interference (RNAi). Protein UCHL1 je velmi stabilní, a proto není pro jeho studium RNAi vhodná. Místo toho jsme využili dvou UCHL1 specifických inhibitorů, které inhibují jeho hydrolázovou aktivitu. Embrya s umlčenou *CENPF* mRNA se zastavují v 8-buněčném stádiu a vykazují nižší morfologickou kvalitu než odpovídající kontrolní embrya. Vývoj embryí až do 8-buněčného stádia je pravděpodobně umožněn díky uchování maternálního proteinu. Zatímco u embryí po EGA a u somatických buněk je CENPF na konci každého buněčného cyklu degradován, u embryí před EGA jsme takovouto degradaci proteinu nenašli. Podobně jsme potvrdili úlohu UCHL1 během fertilizace bovinních oocytů. U oocytů maturovaných s UCHL1 inhibitorem jsme po oplození našli velké množství dispermičtých zygot. To bylo pravděpodobně způsobeno defekty relokalizace a vylití obsahu kortikálních granulí. Naopak embrya s umlčenou mRNA nukleofosminu byla schopna se vyvíjet až do stádia blastocysty. Přestože velká část maternálního proteinu byla degradována, dostatečné množství proteinu zůstalo uchováno během celé preimplantační embryogeneze a umožnilo tak vývoj embryí bez detekovatelných defektů.

Dále jsme se zaměřili na identifikaci nových potenciálně důležitých genů, jejichž exprese a funkce bude určena v navazujících studiích. Z těchto genů zejména cullin 1 pravděpodobně hraje během preimplantačního vývoje velmi podstatnou úlohu. Exprese cullinu 1 z embryonálního genomu je zahájena v pozdním 8-buněčném stádiu. Nedochází však pouze k přechodu z maternální na embryonální transkripci, ale také ke změně ve využití dvou různých genů – z cullin 1-like (XM_589507.3) na cullin 1 (XM_876699). Tyto geny jsou z 83% homologní, oba jsou přítomné na chromozomu 4, avšak v odlišných oblastech.

3. INTRODUCTION

The preimplantation development is probably the most important period of mammalian life. It comprises the period from fusion of gametes to implantation into the maternal uterus. The transformation from resting oocyte into rapidly proliferating embryo demands a great change in the molecular processes in the cell. The steps foregoing the creation of the embryo are however no less important. The faultless oocyte maturation is essential for normal embryo development, since all the material necessary for the first embryonic divisions is stored in the oocyte. However, as soon as the embryo activates the transcription from its own genome, it takes over the responsibility for itself. The developmental potential is determined especially by the gene expression. Hence, it is necessary to characterize the gene expression in oocytes and preimplantation embryos and to identify the most important genes that can be used as markers of the embryo quality.

1.1. Oocyte maturation

During the prenatal development, approximately 7 million of precursor germ cells are formed. Nevertheless, the majority of the cells die and only 2-3 million of these cells continue maturation and enter the first meiotic division (Baker, 1963; Rüsse, 1983). These so-called primary oocytes proceed in meiosis until the diplotene stage of prophase (dictyate state; germinal vesicle (GV) stage oocyte) (Byskov and Hoyer, 1994) and maintain at this stage until the adolescence. The number of primary oocytes further decreases and only a fragment of the starting amount survives until the puberty (Baker, 1963). Once the female matures, the hormonally stimulated oocytes periodically resume their maturation (germinal vesicle break down, GVBD). By contrast, the *in vitro* isolated oocytes resume their meiosis spontaneously (Pincus and Enzmann, 1935; Edwards, 1965a).

The dictyate-state oocyte is placed in a so-called primordial follicle which is characterized by a single layer of granulosa cells. Follicular cells keep the oocyte in the dictyate state, but also mediate its contact with the environment. They transfer stimulating signals for the reinitiation of the meiosis (Byskov and Lintern-Moore, 1973; Eppig, 1976; Carabatsos et al., 2000; Picton, 2001; Mehlmann et al., 2004) and signals controlling its maturation. The follicular cells are later important for fertilization of the oocyte.

The oocyte, even though arrested, is both transcriptionally and translationally active (Wassarman and Kinloch, 1992). It has to produce and store all material and organelles needful for the initial stages of embryo development. Thus during maturation, oocyte severalfold enlarges its volume due to amassing of cytoplasm and synthesis and accumulation of mRNAs, proteins and other essential components.

As the follicular cells proliferate, the follicle grows and transforms to the antral follicle. The oocyte finishes the first meiotic division and extrudes first polar body, but keeps almost the entire volume of cytoplasm. The generated cell is then called the MII stage oocyte. The second meiotic division is finished only after successful fertilization of the oocyte.

1.2. Fertilization

In contrast to the oocyte, sperm throw off almost all its cytoplasm during its development. It retains only the nucleus and material and organelles needed for sperm motion. During its maturation no entities like polar bodies arise, however four sperms are established from one primary spermatocyte. The paternal genetic material is carried in the sperm head together with the acrosomal vesicle, the centriole is placed into the neck and components necessary for the sperm motility follow in the flagellum – midpiece with mitochondria and axonemes; the tail and the endpiece.

The matured oocyte is arrested at metaphase of the second meiotic division and is fertilized at a region of the oviduct called the ampulla. For successful fertilization a sequence of events is needed. At first, to become capable of recognizing the oocyte, the sperm must undergo the capacitation. The capacitation is stimulated by the environment of female reproductive tract or *in vitro* by the culture media (Austin, 1951, 1952; Chang, 1951; Austin et al., 1973). It results in presenting and unmasking of several receptor proteins at the anterior sperm site, accumulation of Ca^{2+} and HCO_3^- ions and preparation of the outer acrosome membrane for acrosome reaction (Lopez et al., 1985; Visconti et al., 1995; Galantino-Hommer et al., 1997; Cross, 1998; Arnoult et al., 1999). The capacitated sperm is attracted by the thermotactic and chemotactic signals from ampulla and the oocyte respectively.

The first contact of sperm and oocyte takes place at zona pellucida. The zona pellucida consists of 3 or 4 zona proteins (ZP); its composition is species specific (e.g.:cattle - ZPA/ZP2, ZPB/ZP4, and ZPC/ZP3; human - ZPA/ZP2, ZPB/ZP4, ZPC/ZP3 and ZP1; mouse - ZPA/ZP2, ZPC/ZP3, and ZP1) (Goudet et al., 2008; Izquierdo-Rico et al., 2009). The key attachment is done by binding of the spermatid galactosyltransferase (GalT) to ZP3. It is generally supposed that binding of a sperm to zona pellucida initiates the acrosome reaction (AR). However, some authors suggest that the AR occurs already as a consequence of entering the cumulus oophorus (reviewed in Sun et al., 2011). As a consequence of sperm binding to the zona, the calcium concentration reaches even higher levels than during capacitation (Fukami et al., 2001; Breitbart et al., 2010) and thus the outer acrosome and inner spermatid plasmatic membranes merge together so that the content of acrosome spills out (Brucker and Lipford, 1995; Ikawa et al., 2010). The enzymes that were included in the acrosome (like acrosin or hyaluronidase) help the spermatozoon to penetrate through zona pellucida (Colwin and Colwin, 1963; Tulsiani et al., 1998). Simultaneously, the inner acrosome membrane is uncovered, whereby a secondary zona pellucida binding is enabled. Once the acrosome reaction has passed, the fusion of the gametes can begin.

For the development of healthy embryo, fusion of the oocyte with only one spermatozoon is needed. Polyspermy has been evidenced in 10-20% spontaneous abortions (Hassold et al., 1980; Michelmann et al., 1986) and it is the most frequent cause of triploidy. Polyspermy is prevented by two different mechanisms - the zona-pellucida-mediated and the plasma-membrane-mediated polyspermy blocking. It is supposed that in most mammalian species, the zona-pellucida mediated block is the more important one (Yanagimachi, 1994). As the sperm enters the oocyte, the Ca^{2+} ions are released from

endoplasmic reticulum of the egg, which results in the extrusion of cortical granules (Miyazaki et al., 1993; Stricker, 1999). The released enzymes modify zona pellucida (e.g. cleavage of N-acetylglucosamine) so that no other spermatozoon is able to enter the oocyte (Ducibella, 1996). This change of zona pellucida is permanent and the zona further works as a protective layer for the embryo (Dale and DeFelice, 2010). The rate of polyspermy is species-specific; the highest frequency is in pig. The differences are likely caused by diversity in zona pellucida constitution (Goudet et al., 2008; Dale and DeFelice, 2010). Moreover, it is supposed that a minor contribution in polyspermy prevention plays the binding of sperms to oviduct cells, which prevents all spermatozoa to reach the ampulla at the same time (Töpfer-Petersen et al., 2002)

Since at the time of sperm entry the oocyte is arrested at metaphase of second meiotic division, it has to be activated to become the dividing embryo. This is mediated by the Ca^{2+} wave. A very important role in this oscillation plays a sperm-delivered protein phospholipase C zeta (PLC ζ) (Rice et al., 2000; Cox et al., 2002; Saunders et al., 2002, Yoon et al., 2008; Ross et al., 2009). The release of Ca^{2+} ions further causes the inhibition of cytostatic factor and decrease of CDK1 activity (CDK1/cyclin B complex is called M-phase promoting factor, i.e. MPF) (Brunet and Maro, 2005). As a consequence, the meiotic division is finalized, the second polar body is extruded and the oocytal genome is prepared for fusion with the spermatid one.

Similarly, the spermatozoon has to undergo changes, so that the two haploid genomes can become a diploid one. The sperm DNA is stabilized by protamines, the spermatid analogues of histones. The protamines form both intra- and inter-molecular disulphide bonds that are responsible for dense packaging of the sperm DNA. However, the DNA has to be decompressed before the genome fusion and thus the disulphide bonds are reduced by the oocyte-derived glutathione (Calvin and Bedford, 1971; Perreault et al., 1988).

The majority of proteins and other “building material” are of maternal origin, the only important sperm-borne organelle is the centriole which organizes the formation of mitotic spindle.

During the preparation for the first embryo division, the pronuclei migrate to each other and once they approximate, the pronuclear envelopes break down. However, the actual embryonic nucleus emerges by the 2-cell stage in mammals.

1.3. Preimplantation development

The preimplantation development covers the period from fertilization of the oocyte to the implantation of the embryo to the maternal endometrium. The newly formed zygote has to transform from the state of resting differentiated oocyte to rapidly proliferating totipotent embryo within a short time. This transformation is a stepwise process performed by several cascading events like first cleavage, embryonic genome activation (EGA), compaction or differentiation of trophectoderm (TE) and inner cell mass (ICM) at the blastocyst stage.

In comparison to resembling developmental period in other animals, the preimplantation development of mammals proceeds very slowly. It takes about 24 h until the first cleavage occurs. The timing of the first cleavage is used for assessment of embryo quality, since the earlier dividing embryos have higher potential to reach the blastocyst stage (Lonergan et al., 1999). The lately dividing embryos usually arrest their development before reaching the blastocyst stage.

At the beginning of development, the embryo is transcriptionally silent and relies on maternal reserves of mRNAs and proteins. The timing of EGA is species-specific and takes place in two waves called minor and major EGA. In bovines, the minor EGA is supposed to start at 2-cell stage (Kues et al., 2008), but some authors suggest that it happens already at the zygote (Memili and First, 1999). However, the vast majority of genes are started to be transcribed during the major genome activation. The earliest major EGA occurs at the 2-cell stage in mice, the latest happens at 8-16-cell stage in rabbit, in bovines the activation takes place at late 8-cell stage (Camous et al., 1986; Telford et al., 1990). However, it cannot be said that the transcription of all genes is started during one of these two waves. EGA is a stepwise process and minor and major waves rather represent its peaks.

The EGA proper is preceded by the degradation of maternal mRNAs and hence the overall mRNA level decreases even though the blastomere number increases. As was demonstrated in mice (Piko and Clegg, 1982), much of maternal mRNAs are degraded at 2-cell stage. Later it was shown that this degradation is fertilization-activated (Alizadeh et al., 2005). Moreover, the embryo synthesizes proteins and miRNAs that are involved in degradation of maternal mRNAs (Tadros and Lipshitz, 2009). Similarly, the maternal proteins are degraded, but the degradation is not so rapid and some maternal proteins are preserved even after EGA (Ohsugi et al., 2008; Vigneault et al., 2009).

As a consequence of transcription commencement during EGA, the functionally active nucleoli emerge in the nucleus. Before the transcription initiation, only nucleolar precursor bodies (NPBs) are present in the nucleus and the embryonic translation is dependent on maternally derived ribosomes (Kopecny et al., 1989). In cattle, only vacuolized fibrillar spheres are present in the nucleus during first three cell cycles (Hyttel et al., 2000). At late 8-cell stage, the dense fibrillar component (DFC) and fibrillar centres (FC) emerge for the first time. Initially, both of them are present at the periphery of the sphere, later the DFC emerges also at the rim of the central vacuole. Subsequently, also the granular component (GC) emerges and replaces the fibrillar sphere. At this time the FCs and DFCs are already fully developed (Hyttel et al., 2000).

As soon as the embryo reaches the 8-cell stage, the blastomeres that have held together above all due to zona pellucida until now, start to adhere to each other. For the compaction of the cells, the expression of cadherins is especially important (Peyrieras et al., 1983). Following compaction, the first cellular differentiation occurs at the morula stage. The blastomeres that are hidden in the middle of the embryo and that are surrounded by another layer of cells will become the inner cell mass (the future entire embryo and part of extraembryonic tissues). On the other hand, the surrounding blastomeres form even more tight junctions and become the trophoblast (embryonic part of the future

placenta). This is the first differentiation of embryonic cells and the blastomeres lose their totipotency (Rossant and Cross, 2001). From now on, the two layers play completely different roles during embryogenesis. The trophoblastic cells actively increase the concentration of Na⁺ ions inside the embryo, which causes secretion of fluid and formation of a cavity called blastocoel (Borland et al., 1977). With the cavitation, the morula differentiates into the blastocyst, where trophoblast encloses both the ICM and the whole embryo. The ICM is placed to one side of this circle. In order that the two layers stay distinct and perform their different functions, the ICM and TE blastomeres express diverse, reciprocally interacting genes. The ICM is characterized mainly by expression of POU5F1 (formerly Oct4), Nanog and Sox2 genes (Boyer et al. 2005). Those transcription factors are critical not only for embryo development, but first of all for maintaining the pluripotency of the cells. For trophectoderm cells, the expression especially of eomesodermin and Cdx2 is crucial (Strumpf et al. 2005). Provided the expression of Cdx2 is diminished, the cells start to express POU5F1 and Nanog and lose their trophectoderm feature (Strumpf et al. 2005). However, these data are based on experiments performed on murine model and some contradictory results were published for example in pig (Keefer et al., 2007; Kuijk et al., 2008; Magnani and Cabot, 2008; Oestrup et al., 2009), human (reviewed in Rossant, 2007) and recently even cows (Berg et al., 2011).

Before implantation into the maternal endometrium the embryo has to hatch from the zona pellucida (Enders and Schlafke, 1967). In most mammals the time of hatching is more or less synchronized with reaching the uterus at the blastocyst stage. During the way through the oviduct, the embryo is protected from implantation by the glycoproteinous zona pellucida and thus the ectopic gestation is prevented. The hatching of the blastocyst is enabled by trypsin-like protease strypsin that digests a small hole in the zona pellucida through which the embryo creeps (Perona and Wassarman, 1986; O'Sullivan et al, 2001; Sharma et al., 2006). During *in vivo* development, also the uterine-derived proteases contribute to the lysis of zona pellucida and it was shown that the implantation immediately follows the hatching in mouse (O'Sullivan et al, 2001; Sharma et al., 2006).

1.4. In vitro fertilization

Since the number of couples that are dependent on assisted reproduction is still increasing, the *in vitro* fertilization (IVF) is generally known as a method for overcoming human infertility. However, the technique is also used for reproduction of domestic animals and endangered species.

The first experiments with *in vitro* maturation of oocytes and *in vitro* cultivation of preimplantation embryos have been done even before the Second World War. The development of entire assisted reproduction was set in 1960s and 1970s. At the beginning, the scientists and physicians solved problems especially with ovarian hyperstimulation (Edwards 1957a,b; Fowler and Edwards, 1957) and oocyte maturation and fertilization (Edwards 1965a,b). The first child after *in vitro* fertilization was born in 1978 in England (Steptoe a Edwards, 1978), in our country this was realized four years later in 1982. In cattle, the first successful embryo transfer was performed in 1981 (Brackett et al., 1982).

The *in vitro* fertilization comprises of three separate steps: *in vitro* maturation of oocytes (IVM), fertilization and *in vitro* embryo culture (IVC). In human IVF, the oocyte maturation is usually skipped, since the pregnancy rates after usage of IVM oocytes are much poorer (De Vos et al., 1999; Chen et al., 2000; Trounson et al., 2001; Balakier et al., 2004; Strassburger et al., 2004). The patients are hormonally stimulated and matured oocytes at the MII stage are isolated. The oocytes are then fertilized by coincubation of the cumulus-oocyte complexes with wash semen. Especially in human medicine, this conventional fertilization approach is often replaced by intracytoplasmic sperm injection (ICSI). This method is suitable above all for men with low sperm numbers or poor sperm morphology, moreover it is useful in oocytes with polyspermy block defects or some other fertilization abnormalities. Since no ways for fertilization defects prediction have been developed up to now, even a half of healthy oocytes are often fertilized using ICSI. After IVC, embryos at stages from 8-cell stage to blastocyst stage are transferred to the recipient females. To select the embryo of the highest developmental potential, several methods of quality evaluation are performed. Currently, the most exploited approach is the first cleavage timing and morphology assessment (Lonergan et al., 2000). However, several defects that are not expressed at this developmental stage can be revealed only by gene expression analysis. Even though several potentially important genes were identified up to now, their proper expression during preimplantation development and even their entire function during this specific period have not been determined up to now. The identification of genes that are crucially important for correct preimplantation development is thus the objective of scientists all over the world.

The identification of potentially important genes is based on their expression. It is supposed that transcription of genes that are crucial for early embryogenesis is activated as the first. Thus we select the genes whose mRNA amount increases during embryonic genome activation, providing this increase is α -amanitin sensitive. Alfa-amanitin is an inhibitor of RNA-polymerase II and thus in correct concentration prevents the transcription of mRNA precursors. The selected genes are further thoroughly studied to verify their importance for early embryogenesis.

To identify the candidate genes, the suppressive subtractive hybridization (SSH) was used at first. With the progress in molecular biology methods, the microarray techniques are preferred. The results of both of these methods have to be further verified by quantitative RT-PCR which ensures much more accurate results. The subsequent verification of importance and function of selected genes is performed by a variety of methods with RNA interference analysis as a pilot technique.

Genes that will be shown to be necessary for normal preimplantation development can be later used as marker of high developmental potential.

2. CHARACTERISTIC OF THE MOST IMPORTANT USED METHODS

2.1. RNA interference

RNA interference (RNAi) has been discovered in *Caenorhabditis elegans* as a natural mechanism leading to sequence-specific degradation of mRNA (Fire et al., 1998). The authors Andrew Z. Fire and Craig C. Mello received Nobel Prize in Physiology or Medicine in 2006 for their discovery. As usual, this phenomenal discovery was made by a coincidence. For silencing of expression of the studied gene, the transfection of an antisense RNA was used first. The research group led by C.C.Mello however gained a better silencing effect in control samples transfected with sense RNA. By a sequence of experiments they gradually showed that the control sense RNA was likely contaminated by antisense strand, which led to formation of a double stranded RNA (dsRNA) and that this dsRNA has a higher silencing potential than the antisense RNA alone. They showed that the transfection of dsRNA into *C. elegans* cells causes sequence specific post-transcriptional silencing of gene expression, reduces the targeted mRNA level and that the mechanism is likely self-reproducing, since only a few molecules of dsRNA are needed for long-term silencing effect.

Consequently a large number of papers showed that the RNAi is a conserved mechanism occurring throughout all eukaryotes (Ngô et al., 1998; Misquitta and Paterson, 1999; Lohmann et al., 1999; Wargelius et al., 1999; Wianny and Zernicka-Goetz, 2000 and others). Since the dsRNA triggers anti-viral interferon response in mammals, it was initially assumed that it cannot work in this group. However, it was shown that, firstly, the interferon response is not developed in oocytes and early embryos and, secondly, the interferon response is not triggered after transfection of the silencing effectors – the siRNAs (Wianny and Zernicka-Goetz, 2000; Svoboda et al., 2000; Elbashir et al., 2001a).

The finding how to induce RNA interference in mammalian cell was enabled by deciphering of its mechanism. It was shown that the long dsRNA is cleaved by a RNase Dicer into 21-23 nt long siRNAs (Hamilton and Baulcombe 1999; Zamore et al. 2000; Elbashir et al. 2001b), one strand (called guide strand) is then incorporated into RISC (i.e. RNA-induced silencing complex) composed further of an Argonaute protein, TRBP (i.e. TAR RNA binding protein) and Dicer (Hammond et al. 2000; Zamore et al. 2000). The RISC then induces the cleavage of mRNA according to the sequence of incorporated guide strand.

In addition to siRNAs several other small RNAs trigger the RNAi pathway. The most explored small RNAs, miRNAs, play an important role in development, but also e.g. in cancerogenesis (Banerjee and Slack, 2002; Ryazansky and Gvozdev 2008). Lately, the expression of several miRNAs was characterized during bovine oocyte maturation and early embryogenesis (Tsfaye et al., 2009). The miRNAs rise from endogenous, originally single-stranded, pri-miRNAs that, by forming stem-loops, forms double-stranded structures. The pri-miRNAs are cleaved by enzyme Drosha to smaller (c. 70bp) pre-miRNAs that are finally cleaved to miRNAs (Lee et al., 2003; Murchison and Hannon, 2004). The final miRNAs are identical to the siRNAs. It is generally accepted that siRNAs

cause degradation of target mRNA and miRNAs cause the cap-dependent suppression of synthesis of the corresponding protein. However, the only thing that distinguishes miRNAs and siRNAs is their origin. The feature that determines the manner of gene expression silencing is the sequence similarity of the small RNA and its mRNA counterpart (Hutvagner and Zamore, 2002; Doench et al., 2003). Provided the sequence is completely homologous, the mRNA is targeted to degradation. On the other hand, if the sequence of small RNA is only similar to the sequence of mRNA, the suppression of translation is applied. In this case a perfect homology of the so-called seed region is required (Lewis et al. 2003, 2005; Brennecke et al. 2003). The seed region is a heptamer of nucleotides 2 – 8 and because of the homology, it is often used for search for miRNA targets. From the most important miRNAs, I will mention the lin4 and let7 miRNAs that regulate development of *C. elegans* (Lee et al., 1993; Wightman et al., 1993); bantam that controls tissue formation during development of *D.melanogaster* (Brennecke et al., 2003) or mammalian miR196 that downregulates mRNA level of homeobox genes HoxB8, HoxC8, HoxD8 and HoxA7 (Yekta et al., 2004). miR196 was the first miRNA that was found to degrade the targeted mRNA rather than suppress protein translation (Kim, 2005).

From other small RNAs the Piwi-interacting RNAs (piRNAs), small-scan RNAs (scRNAs), trans-acting siRNAs (tasiRNAs) and repeat associated siRNAs (rasiRNAs) are worth noting. The piRNAs are 26-31nt long and participate in mammalian spermatogenesis (Aravin et al., 2006; Girard et al., 2006; Grivna et al., 2006; Watanabe et al., 2006; Kim, 2006; Lau et al., 2006); scRNAs are 28 nt long and are possibly involved in genome rearrangements of *Tetrahymena thermophila* (Mochizuki and Gorovsky, 2004); the 21nt long tasiRNAs are involved in silencing in plants (Peragine et al., 2004; Vazquez et al., 2004) and the rasiRNAs perform gene silencing in *S. pombe* and *A. thaliana* (Reinhart et al., 2002; Volpe et al., 2002; Carrington, 2005).

In our studies, we used RNAi to silence mRNA of *CENPF* and nucleophosmin. We have performed the microinjection of long dsRNA into zygotes 20 h post fertilization. Two control groups were established, the uninjected group and the green fluorescent protein (*GFP*) dsRNA injected group. Zygotes were microinjected with ~ 5 pl of the dsRNA using an MIS-5000 micromanipulator (Burleigh, Exfo Life Sciences, Canada) and PM2000B microinjector (MicroData Instrument, South Plainfield, NJ). The embryos were then cultivated under standard conditions, the number of embryos that reached each developmental stage was counted and the morphological state of each embryo was determined using phase-contrast technique. The efficiency and specificity of silencing of the targeted mRNA was verified using single-embryo quantitative RT-PCR and the downregulation of protein expression was verified using immunofluorescence and western blot.

2.2. Quantitative PCR

The polymerase chain reaction (PCR) was invented during years 1983-1987 by Kary Mullis in cooperation with mathematician Fred Faloona (Mullis et al., 1986; Mullis and Faloona, 1987). The principle of the reaction is based on cyclical changes of

temperature resulting in repeated steps of DNA template denaturation, annealing of oligonucleotide primers and product extension. A great progress in improving the PCR technique was done after introduction of a thermophilous DNA polymerase that does not degrade during high temperatures of the denaturation step. This polymerase was initially isolated from bacteria *Thermus aquaticus*. Nowadays it is usually replaced by a modified or synthetic polymerase.

Since the RNA is needed for analysis of gene expression, a reverse transcription (RT) foregoing the entire PCR has to be performed. The reverse transcription can be performed in the same tube with the following PCR (i.e. one-step RT-PCR) or the reaction can be performed separately in two tubes (i.e. two-step RT-PCR). The one-step protocol is faster and more precise since it provides less occasions for handling errors and contamination. On the other hand, the two-step PCR offers more suitable conditions for each reaction, allows amplification of multiple products from the same amount of RNA and enables to store the more stable cDNA rather than the labile RNA.

The real-time detection allows precise quantification of the starting amount of RNA (DNA). The reaction mix is enriched by a fluorescent dye or probe that fluoresces only if bound to the dsDNA. The emitted fluorescence is measured during each amplification cycle. As the concentration of the amplified DNA rises, the intensity of the fluorescence increases and the cycle at which the fluorescence exceeds the background noise is detected (Wittwer et al., 1997). This enables the accurate quantification of the starting amount of the nucleic acid.

The fluorescence can be emitted either by a fluorescent dye (SYBR Green I) that generally binds to dsDNA or by a sequence-specific DNA probe. The advantage of SYBR Green I is its universality. It is suitable especially for laboratories that quantify large number of different molecules. However, the universality is also the disadvantage of this approach. In addition to the intended product, SYBR Green I detects non-specific products or primer dimers. Thus, the melting analysis and electrophoresis is necessary for verifying the specificity of the product. Moreover it cannot be used for multiplex PCR.

On the other hand the fluorescently labeled probes are sequence specific and thus amplify only the desired template. There are several types of probes used for real-time detection; the principle of the function is based on cooperation of a fluorophore and a quencher (e.g. QuantiProbes, TaqMan probes or Molecular Beacons). When unbound, the molecules are in close proximity and thus the quencher hampers the emitting of fluorescence signal. After binding to the DNA, the quencher and fluorophore draw away and the fluorescence can be emitted. The FRET probes work in a similar way, however the principle is based on two fluorophores – donor and acceptor that get near to each other when bound to the DNA. The usage of probes is favourable for multiplex analysis, when each probe emits fluorescence at different wavelength or for laboratories that study one gene in the long-term.

For precise quantification of DNA starting concentration, the accurate normalization of the data is necessary. The normalization is performed either to expression level of an endogenous gene, known level of an exogenously added mRNA or to a standard curve. Originally the normalization to the expression level of one endogenous gene was the

first choice. However since only a few genes have stable expression during some treatments or developmental conditions, the normalization to set of genes is currently preferred (Vandesompele et al., 2002). The genes are selected precisely for needs of the concrete cells or treatments. When there are no genes expressed with stable level or the amount of accessible material is very low (both are truth for preimplantation embryos), the normalization to externally added mRNA (e.g. luciferase; *GFP*) is preferred (Livak a Schmittgen, 2001). In cases where no handling lost threatens (such as whole single-cell-lysate analysis) the normalization to a standard curve is applicable.

In our studies, the single-embryo qRT-PCR was used for verification of mRNA silencing as mentioned above. Single embryos were lysed using FastLane Cell SYBR Green Kit (Qiagen, Hilden, Germany) and immediately used for the qRT-PCR. The reaction was performed using OneStep RT-PCR kit (Qiagen) with real time detection using SybrGreen I fluorescent dye. The experiments were carried out on Rotor-Gene 3000 (Corbett Research/Qiagen). Fluorescence data were acquired at 3 °C below the melting temperature to distinguish the possible primer dimers. The qRT-PCR data were determined using serial dilutions; the standard curve was created using the takeoff points. The takeoff points were calculated by Internal RotorGene software (Corbett Research/Qiagen). The starting amount of corresponding RNA in analysed samples was determined by appointing the takeoff points to the curve. Products were verified by melting analysis and gel electrophoresis on 1.5% agarose gel with ethidium bromide staining.

2.3. Indirect immunofluorescent analysis

The indirect immunofluorescent analysis is used for monitoring of protein localization. It is based on detecting the protein with a primary antibody which is further visualised by fluorescently labeled secondary antibody. The secondary antibody binds to the complement region of the primary antibody, the specificity of this binding is ensured by usage of a secondary antibody targeted to species in which the primary antibody was derived. The emitted fluorescence is than detected using a fluorescent microscope. Each fluorophore is characterized by two wavelength values, the excitation wavelength and the emission wavelength. The excitation wavelength determines the physical properties of light which causes the emission of fluorescent signal. The emission wavelength determines at which values the emission is detectable. Thus, the fluorescence microscope has to have two filters: 1) dismissing only light of the excitation wavelength and 2) dismissing only light of the emission wavelength. By utilization of set of different filters the usage of two or more fluorescent dyes at once is enabled.

The invention of confocal microscope brought a great advance in the applicability of fluorescent microscopy. In contrast to the conventional microscope, the confocal microscope cuts off signals from unsharpened planes and thus brings signal only from the focal plane. The thick sample is scanned through in many stacks (z-stacks) and the precise site where the signal comes from can be determined. The 3D figure of the sample can be then reversely reconstructed. The focusing on the smallest possible spot is enabled by a so-called pinhole - a slit in front of the detector which sets the amount of light incidenting at

the detector. The smaller the diameter of the pinhole is the better resolution can be achieved. On the other hand, the small pinhole lowers the amount of detected signal.

Thus, the proper apparatus adjustment is even more essential for achievement of high quality and truthful results during the confocal microscopy experiments than in other methods.

In our experiments, embryos for immunofluorescent analysis were fixed using 4% paraphormaldehyde and permeabilized using 0.5% TritonX-100. Embryos were blocked with 2% normal serum according to the origin of the secondary antibody and consequently incubated with the primary antibody overnight at 4°C. After thorough washing the embryos were incubated with secondary antibody for 1 h at room temperature darkling. During the double-staining protocol the staining with primary antibodies was performed separately. The nuclei were stained and the embryos were mounted on glass slides using VECTASHIELD HardSet Mounting Medium with DAPI (Vector Laboratories, Peterborough, UK). The samples were examined with a confocal laser-scanning microscope Leica TCS SP (Leica Microsystems AG, Wetzlar, Germany). The images were processed using the ImageJ software (NIH, Betsheda, MD; <http://rsb.info.nih.gov/ij>).

3. AIMS OF THE THESIS

- To find candidate genes that could be used as markers of high developmental potential for *in vitro* fertilization techniques
- To characterize expression and function of these genes during bovine fertilization and preimplantation development
- To confirm the necessity of these genes for proper course of *in vitro* fertilization and embryo culture

4. COMMENTS ON PUBLICATIONS

4.1. Toralova T, Susor A, Nemcova L, Kepkova K, Kanka J. 2009 Silencing CENPF in bovine preimplantation embryo induces arrest at 8-cell stage. *Reproduction* 138: 783–791

The aim of this paper was to characterize the role of CENPF (centromeric protein F; mitosin) in bovine preimplantation development. This study continued another paper from our laboratory (Kanka et al., 2009), in which several differentially expressed genes, including *CENPF*, were identified. CENPF is a large multifunctional protein, which is above all known because of its role in cell division, when it helps kinetochore-microtubule interaction, chromosome condensation and cell cycle progression (Liao et al., 1995, Zhu et al., 1995, Holt et al., 2005). Much like many other cell-cycle regulators, CENPF is expressed and localized in cell-cycle dependent manner and is degraded at the end of each cycle. Depletion of *CENPF* in somatic cells causes frequent aneuploidies due to incorrect chromosome alignment, attenuated tension between sister chromatids and instable kinetochore-microtubule interaction. Since the results concerning CENPF protein expression throughout cell cycle are very heterogeneous in different species (Wei et al. 1996, Goodwin et al. 1999, Redkar et al. 2002, Cheeseman et al. 2005, Dees et al. 2005, Soukolis et al. 2005, Evans et al. 2007, Hajeri et al. 2008), we examined whether bovine embryonic CENPF is expressed in cell-cycle dependent manner.

We treated 4-cell and late 8-cell stage embryos with general translational inhibitor cycloheximide (CHX) and cultivated them for 24 h. This time period enabled all the embryos to pass through the cell cycle. The embryos were then tested using immunofluorescence and we found a wide difference between both treatment groups. Whilst we did not detect a staining decrease in embryos cultivated with CHX from 4-cell stage in comparison to controls, a considerably lower staining intensity was found in embryos cultivated from late 8-cell stage in comparison to controls (Fig.6). This denotes the expression of CENPF protein throughout whole cell cycle in embryos before EGA. On the other hand, in bovine post-EGA embryos, CENPF is expressed in the same manner as in human somatic cells – in interphase blastomeres, the protein is dispersed in the nucleoplasm, relocalizes to kinetochores at the beginning of M-phase and is degraded at the end of mitosis (Fig.7).

Further, we used *CENPF* dsRNA to silence corresponding mRNA, so that we could compare the role of CENPF in bovine preimplantation embryos and somatic cells. The embryonic cell cycle is profoundly different from somatic cells in many respects. In addition to *CENPF* dsRNA injected group, two control groups were established – an uninjected group and a *GFP* dsRNA injected group. We silenced *CENPF* mRNA by 96.0% in comparison to uninjected control and by 94.9% in comparison to *GFP* dsRNA injected control in 8-cell stage embryos and by 97.8% in comparison to uninjected control and by 98.5% in comparison to *GFP* dsRNA injected control in 16-cell stage embryos (Fig.1). No significant difference between the experimental groups was found in mRNA expression level of two other genes – nucleophosmin and *H2AFZ* (Fig.2). Similarly, the

intensity of immunofluorescence staining was markedly decreased in *CENPF* dsRNA injected embryos (Fig.3).

The embryos of all three experimental groups were cultivated under standard conditions. No significant difference in developmental competence between the treatment groups was found until 8-cell stage. However, significantly lower number of 8-cell embryos was able to develop to 16-cell stage or further (72% in both control groups vs. 28% in *CENPF* dsRNA injected group). Moreover, the *CENPF* dsRNA injected embryos were of lower morphological quality, some of the blastomeres even did not have nucleus or the nuclei were fragmented. Our results were in agreement with findings in somatic cells, where most of the cells arrested. Nevertheless some rare survivors were able to proceed in cell division despite the unaligned chromosomes or another similarly substantial defect. Interestingly, there are significant discrepancies in results published by different groups (Holt et al. 2005, Laoukili et al. 2005, Yang et al. 2005, Feng et al. 2006). In our opinion, the inconsistencies are caused mainly by usage of different cell-lines. Since the embryos are pushed into rapid cell division, they will more likely divide even with a severe defect.

Taken together, our results show that until EGA, the embryo utilizes maternal reserves of *CENPF* protein, which is, in contrast to the embryonic protein, expressed throughout the whole cell cycle. However, for subsequent preimplantation development, the start of *CENPF* transcription at the EGA stage is crucial. The silencing of *CENPF* mRNA causes arrest at around the 8-cell stage in cattle.

4.2. Susor A, Liskova L, Toralova T, Pavlok A, Pivonkova K, Karabinova P, Lopatarova M, Sutovsky P, Kubelka M. 2010 Role of UCHL1 in Anti-polyspermy Defense of Mammalian Eggs. *Biology of Reproduction* 82: 1151-1161

Fertilization represents the beginning of preimplantation development. Successful fertilization can be hindered either by inability of sperm to enter the oocyte or on the other hand by penetration of more than one spermatozoon. The latter one - polyspermy - is a serious fertilization defect that usually causes early embryonic death. Hence, several active mechanisms blocking polyspermic fertilization were developed in oocytes. Even though a participation of ubiquitin C-terminal hydrolase-L1 (UCHL1) in polyspermy blocking was shown recently (Sekiguchi et al., 2006; Yi et al., 2007), the entire role of UCHL1 in polyspermy prevention is still not known. The aim of this study was to find the role of UCHL1 in the prevention of polyspermic fertilization in bovines.

There are two types of active polyspermy defence in mammals – the zona-pellucida-mediated and the plasma-membrane-mediated polyspermy blocking. After fertilization, the nature of zona pellucida is modified by enzymes released from cortical granules, so that no other spermatozoon is able to bind to the newly formed zygote (Ducibella 1996). The precise mechanisms of the plasma-membrane-mediated polyspermy blocking were not clarified up to now.

UCHL1 is a deubiquitinating enzyme which is highly abundant in mammalian oocytes but is also present in some other tissues and certain types of cancer. It seems to be important especially for cytoplasmic protein degradation, recycling of free ubiquitin from proteasome products (Larsen et al., 1996 and 1998) and physiological apoptosis (Kwon et al., 2004, 2005; Wang et al., 2006; Yu et al., 2008).

To examine the role of UCHL1 during bovine fertilization, we at first wanted to characterize the expression and localization pattern of the protein. Using western blot analysis, we showed that the expression level did not change during oocyte maturation. The localization was monitored using two different approaches (immunofluorescence and microinjection of *EGFP*-tagged *UCHL1* mRNA) and we showed that UCHL1 is localized to subcortical region in MII and GV oocytes and to the nucleus in GV stage oocytes (Fig. 2 and 3).

Because of the low turnover of UCHL1 protein during oocyte maturation, we used UCHL1 inhibitor instead of the RNAi approach. Two specific inhibitors of UCHL1 hydrolase activity were used: C16, which is an uncompetitive inhibitor of UCHL1 that binds only to the Michaelis complex and not to free enzyme; and C30, which is a reversible, competitive, active site-directed isatin oxime with consistent preference for UCHL1 over UCHL3 by 28-fold. Meiotic progression or UCHL1 level was not changed in the treated oocytes.

No significant difference in fertilization rates between UCHL1-inhibitor treated oocytes and controls was found. However a considerable increase in polyspermy rate in zygotes with downregulated UCHL1 activity was found (C16 - 60%; C30 – 66%; controls – 10%). This shows that even though the inhibition of UCHL1 activity does not alter the maturation and fertilization competence of oocytes, the anti-polyspermy defence is highly

decreased and the majority of such oocytes are not able to form healthy embryo. However the consequent development of diploid embryos evolved from oocytes cultivated in UCHL1 inhibitor is not diminished, as was shown using parthenogenetically activated bovine embryos (Fig.5).

Next, we wanted to know whether the failure of polyspermy defence was caused by defect in behaviour of cortical granules (CGs). The CG localization pattern changes from oocyte-like (CGs in clusters, typical for GV stage oocytes) through intermediate pattern (dissociation of clusters) to egg-like pattern (cortical localization; typical for MII stage oocytes) (Wang et al., 1997; Connors et al., 1998). In C16/C30-treated oocytes, the CGs showed oocyte-like localization during whole maturation and the CGs did not invade the cortex. Similarly, high overexpression of UCHL1 (injection of 250ng/μl concentrated *EGFP-UCHL1* mRNA) blocked the redistribution of CGs during oocyte maturation (Fig.6). Further, the cortical granules were not extruded in 66% and 56% of C16 and C30 treated oocytes respectively, whereas the same was true only for 12.5% of control oocytes. Moreover we found a coincidence between polyspermy ratio and ratio of non-extruded CGs at 20 h after IVF (Fig.10).

Since UCHL1 maintains the cytoplasmic monoubiquitin pool by recycling the polyubiquitin chains, we wanted to know whether the monoubiquitin levels are changed in C16/C30-treated oocytes. Using western blot, we found a significant decrease in monoubiquitin level and in connection with that an increase in polyubiquitin level and protein ubiquitination in UCHL1-inhibitor treated oocytes (Fig.11). As expected, the overexpression of UCHL1 has an opposite effect on monoubiquitin level, but surprisingly did not influence the level of protein ubiquitination.

In C16/C30-treated oocytes an increased formation of presumptive UCHL1 oligomers (75-150kDa) was found. Bands at 50, 75, 100 and 150 kDa were detected, of which 100 and 150 kDa bands were likely linked by disulphide bonds. These bands seem to represent UCHL1 oligomers (Fig.12). The increased amount of UCHL1 oligomers in inhibitor-treated oocytes led us to supposition that the inhibition of UCHL1-hydrolase activity stimulates its ligase activity. In dimeric or oligomeric form, UCHL1 functions as an ubiquitin ligase that promotes formation of K63-linked polyubiquitin chains (Liu et al., 2002; Setsuie and Wada, 2007). The immunofluorescent analysis revealed a markedly brighter staining for K63-linked polyubiquitin chains in comparison to controls (Fig.13), which supported our above mentioned hypothesis.

In conclusion, we showed that UCHL1 is needful for normal fertilization in mammals. Inhibition of the hydrolase activity avoids the relocalization of CGs to cortical region, which is likely the cause of high rate of polyspermic embryos. However the development of embryos parthenogenetically derived from UCHL1-inhibitor treated oocytes was not affected.

4.3. Vodickova Kepkova K, Vodicka P, Toralova T, Lopatarova M, Cech S, Dolezel R, Havlicek V, Besenfelder U, Kuzmany A, Sirard M-A, Laurincik J, Kanka J. 2011 Transcriptomic analysis of *in vivo* and *in vitro* produced bovine embryos revealed a developmental change in cullin 1 expression during maternal-to embryonic transition. *Theriogenology* 75: 1582-1595

Even though a great progress has been done in the field of embryo culture over the last years, the *in vitro* prepared (IVP) embryos still do not reach the same developmental competence as their *in vivo* derived (IVD) counterparts. In this study, we wanted to characterize the differences in gene expression in IVP and IVD embryos using a microarray constructed from bovine oocyte- and preimplantation embryo-specific cDNAs (BlueChip, Université Laval, Québec) and to find genes, whose expression is influenced by the culture environment. Based on the microarray results, several genes were selected for further analysis.

For preparation of three cDNA libraries a suppression subtractive hybridization (SSH) was used. SSH is a PCR-based technology suited to identify transcripts differentially expressed between two samples. We confronted 4-cell stage embryos to MII stage oocytes (Kanka et al., 2009), 8-cell stage to 4-cell stage embryos and 4-cell stage to 8-cell stage embryos. Selected clones from these libraries were then included in the bovine oocyte and embryo specific BlueChip version 3 array design (Sirard et al., 2005).

We then used the BlueChip for comparison of 4-cell stage IVP vs. IVD embryos and in second experiment 8-cell stage IVP vs. IVD embryos. In total 134 candidate genes differentially expressed in the 4-cell stage embryos and 97 candidate genes differentially expressed in the 8-cell stage embryos were identified. The available Protein/Swiss-Prot accession numbers of human orthologs of identified candidate genes were then inserted into Interlogous Interaction Database (I2D) (Brown and Jurisica, 2005) and the protein-protein interaction network was constructed (Fig.1). Four groups of highly interconnected nodes were identified in the resulting network by an automated computational algorithm. One candidate gene from each of three of these nodes (fibrillarin, *CNOT4*, cullin1) and 4 other candidate genes with reported or presumptive role in preimplantation development (*BUB3*, *NOLC1*, *PCAF* and *GABPA*) were chosen for further analysis using qRT-PCR. At first the microarray-detected difference in transcript abundance between IVP and IVD embryos (4- and 8-cell stage) was confirmed and then the gene expression in IVP embryos from MII oocyte to hatched blastocyst was determined. The embryos for qRT-PCR analysis were cultivated in two different types of media – Menezo B2 and COOK BVC/BVB. The results for the selected genes are presented below:

NOLC1 (nucleolar and coiled-body phosphoprotein 1)

NOLC1 was selected based on its supposed role in embryonic nucleogenesis (Baran et al., 2001). In the microarray study, an overexpression of *NOLC1* mRNA was found in IVP 8-cell embryos in comparison to IVD embryos. This was confirmed also using qRT-PCR technique in both culture media. The overall level of *NOLC1* mRNA in

IVP embryos was low at 2- and 4-cell stage, started to increase at early 8-cell stage and kept increasing up until the blastocyst stage (Fig.4B).

BUB3 (budding uninhibited by benzimidazoles 3 homolog)

BUB3 is a spindle checkpoint component essential for kinetochore-microtubule interaction (Logarinho et al., 2008). It has been identified to be upregulated in both human and bovine oocytes (Adjaye et al., 2007; Gasca et al., 2007). In our study, we have detected upregulation at 8-cell stage IVP embryos. The gene expression in IVP embryos gradually decreased from oocytes to early 8-cell stage and then increased in morula and blastocyst stage in both culture conditions (Fig.4C).

PCAF (p130/CBP associated-factor)

PCAF regulates transcriptional activation by interaction with transcription factors and chromatin remodelling and has an essential role in early embryonic transcription control (Yang et al., 1996; Yamauchi et al., 2000). Analogously to the above mentioned genes, *PCAF* was identified to be upregulated in IVP embryos. Only a very low expression was detected in embryos until 4-cell stage, a slight increase was found in early 8-cell stage followed by steeper increase in late 8-cell stage that persisted until blastocyst stage (Fig.4D).

GABPA (GA binding protein transcription factor, alpha subunit)

GABPA is a transcription factor regulating expression of mitochondrial respiration chain genes that is essential for preimplantation embryo development (Ristevski et al., 2004). *GABPA* mRNA was found to be upregulated in 8-cell IVP embryos. The levels of mRNA in IVP embryos were low from oocytes to 4-cell stages, however they steeply increased in early 8-cell embryos and maintained high up until the blastocyst stage (Fig.4E).

CNOT4 (CCR4-NOT transcription complex, subunit 4)

CNOT4 is an E3 ubiquitin ligase which plays role in many processes crucially important for cell living. In the microarray study, *CNOT4* transcripts were detected to be more abundant in 4-cell stage IVP embryos; however this upregulation was not confirmed using qRT-PCR. On the contrary, in late 8-cell stage the *CNOT4* transcripts were significantly more abundant in IVD embryos. Generally, the mRNA level was gradually decreasing in IVP embryos from 2-cell stage to morula stage and slightly increased thereafter (Fig.4F).

Fibrillarin

Fibrillarin (*FBL*) is a nucleolar protein that is involved in early rRNA processing. The de novo synthesis of *FBL* mRNA is needful for formation of functional nucleoli in bovine preimplantation embryos (Svarcova et al., 2007). We have detected only low levels of *FBL* mRNA in embryos until 4-cell stage. The amount started to increase in early 8-cell stage. The mRNA was more abundant in 4-cell IVP embryos than in IVD embryos (Fig.4A). Moreover, we have performed immunofluorescence analysis. The protein was found to be present in GV stage oocytes; however there was no detectable staining from MII oocyte to 4-cell stage embryos. The protein reemerged at early 8-cell stage (Fig.3).

Cullin1

Cullin1 (*cull1*) is an invariable member of SCF complex which mediates ubiquitination of proteins involved in cell-cycle progression (Pernetier et al., 2005). It was shown that *cull1*^{-/-} embryos die at E5.5 – E7.5 and that it is not possible to establish *cull1*^{-/-} stem cells (Dealy et al, 1999; Wang et al., 1999).

The microarray study revealed an overexpression of cullin1 mRNA in both 4-cell and 8-cell stage IVP embryos compared to IVD embryos. Using qRT-PCR, we detected two distinct products with the same length but different melting temperatures (Fig.2A). The first one, expressed from MII oocytes to early 8-cell stage, was identified as *Bos taurus* cullin 1-like, transcript variant 1 (XM_589507.3); the second one, expressed from late 8-cell stage to blastocyst stage, was identified as *Bos taurus* cullin 1, transcript variant 3 (XM_876699) (Fig.2B). After cultivation of 1-cell or 4-cell stage up to late 8-cell stage in α -amanitin, no cullin 1 mRNA was detectable in late 8-cell embryos, which confirmed the observed switch (Fig.2A). Both transcripts represent two different genes from cullin family, both of them localized on chromosome 4, only to distinct regions. According to alignment studies, cullin 1 like transcript possibly originated by duplication in bovine genome. Using immunofluorescence, cullin 1 protein was detected in all embryonic stages and was dispersed throughout the whole cytoplasm (Fig.2C).

In conclusion, we have found significant differences in gene expression of *BUB3*, *NOLCI*, *PCAF*, *GABPA* and *CNOT4* between IVP and IVD embryos and also between both culture media in the blastocyst stage. The further analysis of fibrillarin and cullin 1 revealed interesting results. In contrast to other study (Svarcova et al., 2007), we detected fibrillarin already in early 8-cell stage. These results correlated with the increased amount of fibrillarin mRNA. In cullin 1, we detected two transcript variants, one of which (cullin 1-like; XM_589507.3) was present from MII oocytes to early 8-cell stage and likely represents the maternal transcript. The second one (cullin 1; XM_876699) was present from late 8-cell stage to the blastocyst stage and hence likely represents the embryonic variant. The switch between these two transcripts just around the EGA stage likely denotes the importance of cullin 1 in preimplantation development. Thus, the role of cullin 1 in bovine preimplantation development will be further analysed.

4.4. Toralova T, Benesova V, Vodickova Kepkova K, Vodicka P, Susor A, Kanka J. Bovine preimplantation embryos with silenced nucleophosmin mRNA are able to develop until the blastocyst stage due to preservation of sufficient protein amount. Submitted to Biology of Reproduction

The aim of this paper was to characterize the role of nucleophosmin during bovine preimplantation development. Using SSH, nucleophosmin was previously found to be differentially expressed during bovine preimplantation development and hence was supposed to be important for early embryogenesis of cattle. It is a multifunctional nucleolar protein involved in rRNA processing, ribosome biogenesis, centrosome duplication control and chaperoning (Borer et al., 1989; Savkur & Olson 1998; Hingorani et al., 2000; Okuwaki et al., 2002; Swaminathan et al. 2005). As it shuttles between nucleoli and cytoplasm it also participates in transport of several proteins (Borer et al., 1989; Yung et al., 1990; Fankhauser et al., 1991; Adachi et al. 1993; Valdez et al., 1994; Li et al., 1996).

At first, we wanted to verify the results from SSH by qRT-PCR and determine the expression of nucleophosmin mRNA during the whole preimplantation period. We found out that the expression gradually decreased up until the early 8-cell stage and slightly increased in late 8-cell stage. This increase was α -amanitin sensitive and hence signs the activation of transcription from embryonic genome. After EGA the nucleophosmin mRNA level remains approximately at the same grade up until the blastocyst stage (Fig. 1).

During preimplantation development the nucleoli are not functionally active at the very early stages. The fully-evolved nucleolus emerges as late as after the embryonic genome activation. Because there were some contradictory results concerning nucleophosmin expression and localization during these early stages (Laurincik et al., 2000; Fair et al., 2001), we performed the immunofluorescent and western blot analyses. We showed that the protein was detectable from the beginning of embryonic development. At the pre-EGA stages, it showed diffused localization in the nucleoplasm and during mitosis it was dispersed throughout the whole blastomere (Fig. 2B,C). This localization pattern was likely caused by the absence of functional nucleolus. The nucleolar localization emerged at early 8-cell stage when it showed a shell-like structures that reflected the formation of nucleolus (Fig. 2D,E). From late 8-cell stage on, when the nucleoli started to be functionally active, the localization was typically nucleolar, comparable to the localization in somatic cells (Fig. 2F-H). In blastocyst stage, nucleophosmin tended to localize especially to the trophectoderm (Fig. 2I,J). Interestingly, we did not detect an immunofluorescent signal in MII oocytes (Fig. 2A). However, when we verified the results using western blot analysis, we found a clear band, which displayed a mobility shift in comparison to 4-cell stage and morulas (Fig. 3). This suggests that nucleophosmin protein in MII oocytes is likely phosphorylated and that the phosphorylation prevents the antibody to bind to the epitope during immunofluorescent analysis.

Further we wanted to see, for how long is the maternal protein preserved and whether it is able to supply the role of the newly synthesized nucleophosmin. Bjerregaard et al. (2004) and Svarcova et al. (2007) showed that nucleophosmin is stored at least over the EGA stage in porcine and bovine embryos, respectively. Nevertheless, the protein was

not able to localize to the nucleoli. Since they both used the α -amanitin treatment, the inhibition of nucleophosmin expression was not specific. Hence, we microinjected the nucleophosmin dsRNA into the zygotes, which caused silencing of the nucleophosmin mRNA by 86.8% in comparison to the uninjected embryos and by 83.6% in comparison to the embryos injected with *GFP* dsRNA ($p < 0.001$ in both cases) (Fig. 4). No significant difference was found in expression of two other genes (*CENPF* and *CLEC2D*) between the treatment groups ($p > 0.05$ in each case) (Fig. 5).

Surprisingly, we did not detect any differences neither in expression nor localization of the protein between the treatment groups (Fig. 6). We only noted a slight delay in relocalization of the protein from nucleoplasm to nucleoli in the nucleophosmin dsRNA injected group. However, when we analysed the protein level using western blot, we found a dramatic decrease in the protein amount in the nucleophosmin injected embryos in comparison to the uninjected embryos (Fig. 7). This likely suggests that the protein is largely degraded, however the preserved amount is sufficient for coverage of the needs for nucleoli functioning and normal preimplantation development. Indeed, even though we detected a visible decrease in number of embryos that reached the blastocyst stage, the difference was significant only in comparison to the uninjected group and reached only a boundary value $p = 0.05$ (Fig. 8). Moreover, the embryos with silenced nucleophosmin mRNA did not show any defects that were detected in *Npm*^{-/-} cells (Fig. 9) (Colombo et al., 2005; Grisendi et al., 2005; Amin et al., 2008A,B).

Taken together, we found that the transcription of nucleophosmin mRNA from embryonic genome is activated at late 8-cell stage. The protein is present from the beginning of embryonic development and its localization reflects the maturity of the nucleoli. A small amount of maternal protein is preserved throughout the whole preimplantation development and enables almost normal growth of embryos with silenced nucleophosmin mRNA.

5. CONCLUSIONS

- We found out that the expression of mRNA in preimplantation embryos is greatly influenced by the culture conditions. The IVD embryos often showed totally different expression profile in comparison to IVP embryos, whether the expression in IVP embryos was increased (e.g. in *CNOT4* in late 8-cell embryos) or decreased (e.g. *PCAF*). Moreover, the expression levels were different also in diverse *in vitro* culture media, especially at the blastocyst stage. The gained results call for further optimization and standardization of the *in vitro* fertilization techniques.
- Two genes differentially expressed during bovine preimplantation development, *CENPF* and nucleophosmin, were studied in more detail. The embryonic transcription of both these genes is started during major EGA at late 8-cell stage. However, the consequences of silencing of their mRNAs are profoundly different. On one hand, the initiation of expression of *CENPF* mRNA seems to be necessary for normal development and the silencing of *CENPF* mRNA causes arrest of the majority of embryos at 8-cell stage. On the other hand, the maternal protein nucleophosmin is stored throughout the whole preimplantation period and enables the development of bovine embryos even after the silencing of nucleophosmin mRNA. In contrast to embryos with silenced *CENPF* dsRNA, we did not find decrease in morphological quality of embryos with silenced nucleophosmin mRNA.
- We showed that both *CENPF* and nucleophosmin maternal proteins have higher stability during early embryogenesis. *CENPF* is not degraded at the end of each cell cycle before EGA and a considerable amount of maternal nucleophosmin is stored up until the blastocyst stage.
- We monitored the embryonic expression and localization of two nucleolar proteins – nucleophosmin and fibrillarin. Whilst nucleophosmin is largely inherited from oocyte and is present from the beginning of the embryogenesis, fibrillarin is not detectable at the early stages of preimplantation development and emerges as late as at early 8-cell stage. Nevertheless, during the first three cycles, even nucleophosmin is not localized to the nucleoli and is dispersed throughout the nucleoplasm. Its relocalization occurs at the same time as the appearance of fibrillarin. The expression and localization of both proteins thus reflect the functional activity of the nucleolus.
- We showed that the hydrolase activity of *UCHL1* is not necessary for oocyte maturation. However, it is crucially important for correct fertilization. The *UCHL1* protein prevents polyspermy, likely by controlling the relocalization and extrusion of cortical granules. The activity of *UCHL1* during maturation of bovine oocytes is not needful for normal preimplantation development, nevertheless the creation of a healthy zygote is very unlikely.
- We showed that correct expression and function of *CENPF* and *UCHL1* is crucial for proper course of *in vitro* fertilization and *in vitro* embryo culture and thus these genes might be in future used as markers of high developmental potential.

- New genes potentially important for normal preimplantation development of bovine embryo were identified. These genes will be thoroughly studied in the follow-up projects. In some of the genes the mRNA expression and eventually even the protein expression was already determined. We detected the expression of both fibrillarin mRNA and protein at early 8-cell stage, which shows the activation of fibrillarin transcription before the major EGA. Even more interesting was the revelation of the expression switch between two genes coding for cullin 1. Since this switch takes place at the EGA stage, we give a great importance to the role of cullin 1 during bovine preimplantation development and the role of cullin 1 will be analysed as the first.

6. ABBREVIATION LIST

BUB3	budding uninhibited by benzimidazoles 3 homolog
Cdk1	cyclin dependent kinase 1
CENPF	centromeric protein F
CG	cortical granule
CHX	cycloheximide
CNOT4	CCR4-NOT transcription complex, subunit 4
cul1	cullin 1
DFC	dense fibrillar component
dsRNA	double stranded RNA
EGA	embryonic genome activation
EGFP	enhanced green fluorescent protein
GABPA	GA binding protein transcription factor, alpha subunit
GC	granular component
GFP	green fluorescent protein
GV	germinal vesicle
GVBD	germinal vesicles break down
FBL	fibrillarin
FC	fibrillar centre
ICM	inner cell mass
ICSI	intracytoplasmic sperm injection
IVC	<i>in vitro</i> culture
IVD	<i>in vivo</i> derived
IVF	<i>in vitro</i> fertilization
IVM	<i>in vitro</i> maturation
IVP	<i>in vitro</i> prepared
miRNA	micro RNA
MPF	mitosis promotion factor
NOLC1	nucleolar and coiled-body phosphoprotein 1
NPB	nucleolar precursor body
Npm	nucleophosmin
PCAF	p130/CBP associated-factor
piRNA	Piwi-interacting RNA
PLC ζ	phospholipase C zeta
POU5F1	POU class 5 homeobox 1
qRT-PCR	quantitative reverse transcriptase-polymerase chain reaction
rasi RNA	repeat associated small interfering RNA
RISC	RNA-induced silencing complex
RNAi	RNA interference
scRNA	small-scan RNA
siRNA	small interfering RNA

SSH	suppressive subtractive hybridization
TE	trophectoderm
tasiRNA	trans-acting small interfering RNA
TRBP	TAR RNA binding protein
UCHL1	ubiquitin C-terminal hydrolase-L1
ZP	zona protein

7. REFERENCES

- Adachi Y, Copeland TD, Hatanaka M, Oroszlan S. 1993 Nucleolar targeting signal of Rex protein of human T-cell leukemia virus type I specifically binds to nucleolar shuttle protein B-23. *Journal of Biological Chemistry* 268:13930-13934.
- Adjaye J, Herwig R, Brink TC, Herrmann D, Greber B, Sudheer S, Groth D, Carnwath JW, Lehrach H, Niemann H. 2007 Conserved molecular portraits of bovine and human blastocysts as a consequence of the transition from maternal to embryonic control of gene expression. *Physiol Genomics* 31:315-327.
- Alizadeh Z, Kageyama S, Aoki F. 2005 Degradation of maternal mRNA in mouse embryos: selective degradation of specific mRNAs after fertilization. *Mol Reprod Dev* 72:281-290.
- Aravin A, Gaidatzis D, Pfeffer S, Lagos-Quintana M, Landgraf P, Iovino N, Morris P, Brownstein MJ, Kuramochi-Miyagawa S, Nakano T, Chien M, Russo JJ, Ju J, Sheridan R, Sander C, Zavolan M, Tuschl T. 2006 A novel class of small RNAs bind to MILI protein in mouse testes. *Nature* 442:203–207
- Arnoult C, Kazam IG, Visconti PE, Kopf G, Villaz M, Florman H. 1999 Control of the lowvoltage-activated calcium channel of mouse sperm by egg ZP3 and by membrane hyperpolarization during capacitation. *Proc Natl Acad Sci USA* 96: 6757–6762.
- Austin CR. 1951 Observations on the penetration of the sperm into the mammalian egg. *Aust I Sci Res B* 4:581-589.
- Austin CR. 1952 The capacitation of mammalian sperm. *Nature* 170:326.
- Austin CR, Bavister BD, Edwards RG. 1973 Components of capacitation. In: Segal SJ et al. *The regulation of mammalian reproduction*. Springfield 247-254.
- Baker TG. 1963 A quantitative and cytological study of germ cells in the human ovaries. *Proc R Soc London, Ser B*. 158:417–433.
- Bernstein E, Caudy AA, Hammond SM, Hannon GJ. 2001 Role for a bidentate ribonuclease in the initiation step of RNA interference. *Nature* 409: 363–366.
- Balakier H, Sojecki A, Motamedi G, Librach C. 2004 Time-dependent capability of human oocytes for activation and pronuclear formation during metaphase II arrest. *Hum Reprod* 19:982–987.
- Banerjee D, Slack F. 2002 Control of developmental timing by small temporal RNAs: a paradigm for RNA-mediated regulation of gene expression. *Bioessays* 24:119-129.
- Baran V, Brochard V, Renard JP, Flechon JE, 2001 Nopp 140 involvement in nucleologenesis of mouse preimplantation embryos. *Molecular Reproduction and Development* 59:277-284.
- Berg DK, Smith CS, Pearton DJ, Wells DN, Broadhurst R, Donnison M, Pfeffer PL. 2011 Trophectoderm lineage determination in cattle. *Dev Cell* 20:244-255.
- Bjerregaard B, Wrenzycki C, Strejcek F, Laurincik J, Holm P, Ochs RL, Rosenkranz C, Callesen H, Rath D, Niemann H, Maddox-Hyttel P. 2004

Expression of Nucleolar-Related Proteins in Porcine Preimplantation Embryos Produced *In vivo* and *In vitro*. Biol Reprod 70:867-876

- Borer RA, Lehner CF, Eppenberger HM, Nigg EA. 1989 Major nuclear proteins shuttle between nucleus and cytoplasm. Cell 56:379-390
- Borland RM, Biggers JD, Lechene CP. 1977 Fluid transport by rabbit preimplantation blastocysts *in vitro*. J Reprod Fertil. 51:131-135.
- Boyer LA, Lee TI, Cole MF, Johnstone SE, Levine SS, Zucker JP, Jacob P, Guenther MG, Kumar RM, Murray HL, Jenner RG, Gifford DK, Melton DA, Jaenisch R, Young RA. 2005 Core transcriptional regulatory circuitry in human embryonic stem cells. Cell 122:947–956.
- Brackett BG, Bousquet D, Boice ML, Donawick WJ, Evans JF, Dressel MA. 1982 Normal development following *in vitro* fertilization in the cow. Biol Reprod 27:147-158.
- Breitbart H, Rotman T, Rubinstein S, and Etkovitz N. 2010 Role and regulation of PI3K in sperm capacitation and the acrosome reaction. Mol Cell Endocrinol 314:234–238.
- Brennecke J, Hipfner DR, Stark A, Russell RB, Cohen S. 2003 M. bantam encodes a developmentally regulated microRNA that controls cell proliferation and regulates the proapoptotic gene hid in Drosophila. Cell 113:25–36
- Brown KR, Jurisica I, 2005 Online predicted human interaction database. Bioinformatics 21:2076-2082.
- Brucker C, Lipford GB. 1995 The human sperm acrosome reaction: physiology and regulatory mechanisms. An update. Hum Reprod Update 1:51–62.
- Brunet S, Maro B. 2005 Cytoskeleton and cell cycle control during meiotic maturation of the mouse oocyte: integrating time and space. Reproduction 130:801-811.
- Byskov AG, Lintern-Moore S. 1973 Follicle formation in the immature mouse ovary: the role of the rete ovarii. J Anat 116:207-217.
- Byskov AG, Hoyer PE. 1994 Embryology of mammalian gonads and ducts. In The Physiology of Reproduction (E. Knobil and J. D. Neill, Eds), 2nd ed, Raven Press, New York 487–531.
- Calvin HI and Bedford JM. 1971 Formation of disulfide bonds in the nucleus and accessory structures of mammalian spermatozoa during maturation in the epididymis. J Reprod Fertil [Suppl.] 13:65–75.
- Camous S, Kopecny V, Flechon JE. 1986 Autoradiographic detection of the earliest stage of [3H]-uridine incorporation into the cow embryo. Biology of the Cell 58:195-200.
- Carabatsos MJ, Sellitto C, Goodenough DA, Albertini DF. 2000 Oocyte-granulosa cell heterologous gap junctions are required for the coordination of nuclear and cytoplasmic meiotic competence. Dev Biol 226:167-179.
- Carrington JC. 2005 Small RNAs and *Arabidopsis*. A fast forward look. Plant Physiol 138:565–566.

- Chang MC. 1951 Fertilizing capacity of spermatozoa deposited into the Fallopian tubes. *Nature*, London 168:697.
- Cheeseman IM, MacLeod I, Yates JR 3rd, Oegema K, Desai A. 2005 The CENP-F-like proteins HCP-1 and HCP-2 target CLASP to kinetochores to mediate chromosome segregation. *Current Biology* 5:771-777.
- Chen SU, Chen HF, Lien YR, Ho HN, Chang HC, Yang YS. 2000 Schedule to inject *in vitro* matured oocytes may increase pregnancy after intracytoplasmic sperm injection. *Arch Androl* 44:197–205.
- Colwin AL, Colwin LH. 1963 Role of the gamete membranes in fertilization in *Saccoglossus Kowalevskii* (Enteropneusta). I. The Acrosomal Region and Its Changes in Early Stages of Fertilization. *J Cell Biol* 19:477-500.
- Connors A, Kanatsu-Shinohara M, Schultz RM, Kopf RS. 1998 Involvement of the cytoskeleton in the movement of cortical granules during oocyte maturation, and cortical granule anchoring in mouse eggs. *Dev Biol* 200:103–115.
- Cox LJ, Larman MG, Saunders CM, Hashimoto K, Swann K, Lai FA. 2002 Sperm phospholipase C zeta from humans and cynomolgus monkeys triggers Ca²⁺ oscillations, activation and development of mouse oocytes. *Reproduction* 124:611-623.
- Cross NL. 1998 Role of cholesterol in sperm capacitation. *Biol. Reprod.* 59: 7–11.
- Dale B, DeFelice L. 2011 Polyspermy prevention: facts and artifacts? *J Assist Reprod Genet.* 28:199-207.
- Dees E, Robertson JB, Ashe M, Pabon-Pena L, Bader D, Goodwin RL. 2005 LEK1 Protein Expression in Normal and Dysregulated Cardiomyocyte Mitosis. The anatomical record. Part A, Discoveries in molecular, cellular, and evolutionary biology 286:823-832.
- Dealy MJ, Nguyen KV, Lo J, Gstaiger M, Krek W, Elson D, Arbeit J, Kipreos ET, Johnson RS. 1999. Loss of Cull1 results in early embryonic lethality and dysregulation of cyclin E. *Nature Genetics* 23:245-248.
- De Vos A, Van de Velde H, Joris H, Van Steirteghem A. 1999 In-vitro matured metaphase-I oocytes have a lower fertilization rate but similar embryo quality as mature metaphase-II oocytes after intracytoplasmic sperm injection. *Hum Reprod* 14:1859–1863.
- Doench JG, Petersen CP, Sharp PA. 2003 siRNAs can function as miRNAs. *Genes Dev* 17:438-442.
- Ducibella T. 1996 The cortical reaction and development of activation competence in mammalian oocytes. *Hum Reprod Update* 2:29-42.
- Edwards RG. 1957a The experimental induction of gynogenesis in the mouse. I. Irradiation of the sperm by X rays. *Proc Roy Soc Lond, B* 146: 469-487
- Edwards RG. 1957b The experimental induction of gynogenesis in the mouse. II. Ultra-violet irradiation of the sperm. *Proc R Soc Lond, B Biol Sci.* 146:488-504.
- Edwards RG. 1965a Maturation *in vitro* of mouse, sheep, cow, pig, rhesus monkey and human ovarian oocytes. *Nature* 208:349-351

- Edwards RG. 1965b Maturation *in vitro* of human ovarian oocytes. *Lancet* ii:926-929.
- Elbashir SM, Harborth J, Lendeckel W, Yalcin A, Weber K, Tuschl T. 2001a Duplexes of 21-nucleotide RNAs mediate RNA interference in cultured mammalian cells. *Nature* 411:494-498.
- Elbashir, S.M., Martinez, J., Patkaniowska, A., Lendeckel, W., and Tuschl, T. 2001b Functional anatomy of siRNAs for mediating efficient RNAi in *Drosophila melanogaster* embryo lysate. *EMBO J* 20:6877–6888.
- Enders AC, Schlafke S. 1967 A morphological analysis of the early implantation stages in the rat. *Am J Anat* 120:185–226.
- Eppig JJ. 1976 Analysis of mouse oogenesis *in vitro*. Oocyte isolation and the utilization of exogenous energy sources by growing oocytes. *J Exp Zool* 198:375-382.
- Evans HJ, Edwards L, Goodwin RL. 2007 Conserved C-terminal domains of mCenpf (LEK1) regulates subcellular localization and mitotic checkpoint delay. *Experimental Cell Research* 313:2427-2437.
- Fair T, Hyttel P, Lonergan P, Boland MP. 2001 Immunolocalization of nucleolar proteins during bovine oocyte growth, meiotic maturation, and fertilization. *Biology of Reproduction*, 64:1516-1525.
- Feng J, Huang H, Yen TJ. 2006 CENPF is a novel microtubule-binding protein that is essential for kinetochores attachments and affects the duration of the mitotic delay. *Chromosoma* 115 320-329.
- Fire A, Xu S, Montgomery MK, Kostas SA, Driver SE, Mello CC. 1998 Potent and specific genetic interference by double-stranded RNA in *Caenorhabditis elegans*. *Nature* 391:806-811.
- Fowler RE, Edwards RG. 1957 Induction of superovulation and pregnancy in mature mice by gonadotrophins. *J Endocrinol* 15:374-384.
- Fankhauser C, Izaurralde E, Adachi Y, Wingfield P, Laemmli UK. 1991 Specific complex of human immunodeficiency virus type 1 rev and nucleolar B23 proteins: dissociation by the Rev response element. *Mol Cell Biol* 11:2567-2575
- Fukami K, Nakao K, Inoue T, Kataoka Y, Kurokawa M, Fissore RA, Nakamura K, Katsuki M, Mikoshiba K, Yoshida N, Takenawa T. 2001 Requirement of phospholipase Cdelta4 for the zona pellucida-induced acrosome reaction. *Science* 292:920–923.
- Galantino-Homer HL, Visconti PE, Kopf GS. 1997 Regulation of protein tyrosine kinase phosphorylation during bovine capacitation by a cyclic adenosine 3',5'-monophosphate-dependent pathway. *Biol. Reprod* 56:707–719.
- Gasca S, Pellestor F, Assou S, Loup V, Anahory T, Dechaud H, De Vos J, Hamamah S. 2007 Identifying new human oocyte marker genes: a microarray approach. *Reprod Biomed Online* 14:175-183.
- Girard A, Sachidanandam R, Hannon GJ, Carmell MA. 2006 A germline-specific class of small RNAs binds mammalian Piwi proteins. *Nature* 442:199–202.

- Goudet G, Mugnier S, Callebaut I, Monget P. 2008 Phylogenetic analysis and identification of pseudogenes reveal a progressive loss of zona pellucida genes during evolution of vertebrates. *Biol Reprod* 78:796–806.
- Goodwin RL, Pabón-Peña LM, Foster GC, Bader D. 1999 The Cloning and Analysis of LEK1 Identities Variations in the LEK/Centromere Protein F/Mitotin Gene Family. *Journal of Biological Chemistry* 274:18597-18604.
- Grivna ST, Beyret E, Wang Z, Lin HA. 2006 A novel class of small RNAs in mouse spermatogenic cells. *Genes Dev* 20:1709–1714
- Hajeri VA, Stewart AM, Moore LL, Padilla PA. 2008 Genetic analysis of the spindle checkpoint genes *san-1*, *mdf-2*, *bub-3* and the CENP-F homologues *hcp-1* and *hcp-2* in *Caenorhabditis elegans*. *Cell Division* 3:6.
- Hamilton AJ, Baulcombe DC. 1999 A species of small antisense RNA in posttranscriptional gene silencing in plants. *Science* 286: 950–952.
- Hammond SM, Bernstein E, Beach D, Hannon GJ. 2000 An RNA-directed nuclease mediates post-transcriptional gene silencing in *Drosophila* cells. *Nature* 404: 293–296.
- Hassold T, Chen N, Funkhouser J, Jooss T, Manuel B, Matsuura J, Matsuyama A, Wilson C, Yamane JA, Jacobs PA. 1980 A cytogenetic study of 1000 spontaneous abortions. *Ann Hum Genet* 44:151-178.
- Hingorani K, Szebeni A, Olson MO. 2000 Mapping the functional domains of nucleolar protein B23. *J Biol Chem* 275:24451-24457.
- Holt SV, Vergnolle MA, Hussein D, Wozniak MJ, Allan VJ, Taylor SS. 2005 Silencing Cenpf weakens centromeric cohesion, prevents chromosome alignment and activates the spindle checkpoint. *Journal of Cell Science* 18:4889-4900.
- Hutvagner G, Zamore PD. 2002 A microRNA in a Multiple-Turnover RNAi Enzyme Complex. *Science* 297:2056-2060.
- Hyttel P, Laurincik J, Viuff D, Fair T, Zakhartchenko V, Rosenkranz C, Avery B, Rath D, Niemann H, Thomsen PD, Schellander K, Callesen H, Wolf E, Ochs RL, Greve T. 2000 Activation of ribosomal RNA genes in preimplantation cattle and swine embryos. *Anim Reprod Sci* 60-61:49-60.
- Ikawa M, Inoue N, Benham AM, Okabe M. 2010 Fertilization: a sperm's journey to and interaction with the oocyte. *J Clin Invest* 120:984–994.
- Izquierdo-Rico MJ, Jimenez-Movilla M, Llop E, Perez-Oliva AB, Ballesta J, Gutierrez-Gallego R, Jimenez-Cervantes C, Aviles M. 2009 Hamster zona pellucida is formed by four glycoproteins: ZP1, ZP2, ZP3, and ZP4. *J Proteome Res* 8:926–941.
- Kanka J, Kepkova K, Nemcova L. 2009 Gene expression during minor genome activation in pre-implantation bovine development. *Theriogenology* 72:572–583.
- Keefer CL, Pant D, Blomberg L, Talbot NC. 2007 Challenges and prospects for the establishment of embryonic stem cell lines of domesticated ungulates. *Anim Reprod Sci* 98:147–168.

- Kim VN. 2005 MicroRNA biogenesis: coordinated cropping and dicing. *Nat Rev Mol Cell Biol* 6:376-385.
- Kim VN. 2006 Small RNAs just got bigger: Piwi-interacting RNAs (piRNAs) in mammalian testes. *Genes Dev* 20:1993-1997.
- Kopečný V, Fulka J Jr, Pivko J, Petr J. 1989 Nucleologenesis and the onset of transcription in the eight-cell bovine embryo: fine-structural autoradiographic study. *Mol Reprod Dev* 1:79-90.
- Kues WA, Sudheer S, Herrmann D, Carnwath JW, Havlicek V, Besenfelder U, Lehrach H, Adjaye J, Niemann H. 2008 Genome-wide expression profiling reveals distinct clusters of transcriptional regulation during bovine preimplantation development *in vivo*. *Proc Natl Acad Sci USA* 105:19768-19773.
- Kuijk EW, Du Puy L, Van Tol HTA, Oei CHY, Haagsman HP, Colenbrander B, Roelen BA. 2008 Differences in early lineage segregation between mammals. *Dev Dyn* 237:918–927.
- Kwon J, Wang YL, Setsuie R, Sekiguchi S, Sato Y, Sakurai M, Noda M, Aoki S, Yoshikawa Y, Wada K. 2004 Two closely related ubiquitin C-terminal hydrolase isozymes function as reciprocal modulators of germ cell apoptosis in cryorchid testis. *Am J Pathol* 165:1367-1374.
- Kwon J, Mochida K, Wang YL, Sekiguchi S, Sankai T, Aoki S, Ogura A, Yoshikawa Y, Wada K. 2005 Ubiquitin C-terminal hydrolase L-1 is essential for the early apoptotic wave of germinal cells and for sperm quality control during spermatogenesis. *Biol Reprod* 73:29-35.
- Laoukili J, Kooistra MR, Bras A, Kauw J, Kerkhoven RM, Morrison A, Clevers H, Medema RH. 2005 FoxM1 is required for execution of the mitotic programme and chromosome stability. *Nature Cell Biology* 7:126-136.
- Larsen CN, Price JS, Wilkinson KD. 1996 Substrate binding and catalysis by ubiquitin C-terminal hydrolases: Identification of two active site residues. *Biochemistry* 35:6735-6744.
- Larsen CN, Krantz BA, Wilkinson KD. 1998 Substrate specificity of deubiquitinating enzymes: ubiquitin C-terminal hydrolases. *Biochemistry* 37:3358–3368.
- Lau NC, Seto AG, Kim J, Kuramochi-Miyagawa S, Nakano T, Bartel DP, Kingston RE. 2006 Characterization of the piRNA complex from rat testes. *Science* 313:363-367.
- Laurincik J, Thomsen PD, Hay-Schmidt A, Avery B, Greve T, Ochs RL, Hyttel P. 2000 Nucleolar proteins and nuclear ultrastructure in preimplantation bovine embryos produced *in vitro*. *Biol Reprod* 62:1024-1032.
- Lee RC, Feinbaum RL, Ambros V. 1993 The *C. elegans* heterochronic gene *lin-4* encodes small RNAs with antisense complementarity to *lin-14*. *Cell* 75:843–854.
- Lee Y, Ahn C, Han J, Choi H, Kim J, Yim J, Lee J, Provost P, Rådmark O, Kim S, Kim VN. 2003 The nuclear RNase III Drosha initiates microRNA processing. *Nature* 425:415–419.

- Lewis BP, Shih IH, Jones-Rhoades MW, Bartel DP, Burge CB. 2003 Prediction of mammalian microRNA targets. *Cell* 115:787–798.
- Lewis BP, Burge CB, Bartel DP. 2005 Conserved seed pairing, often flanked by adenosines, indicates that thousands of human genes are microRNA targets. *Cell* 120:15–20.
- Li YP, Busch RK, Valdez BC, Busch H. 1996 C23 interacts with B23, a putative nucleolar-localization-signal-binding protein. *European Journal of Biochemistry* 237:153-158.
- Liao H, Winkfein RJ, Mack G, Rattner JB, Yen TJ. 1995 CENPF Is a Protein of The Nuclear Matrix That Assembles onto Kinetochores at Late G2 and Is Rapidly Degraded After Mitosis. *The Journal of Cell Biology* 130:507-518.
- Liu Y, Fallon L, Lashuel HA, Liu Z, Lansbury PT Jr. 2002 The UCH-L1 Gene Encodes Two Opposing Enzymatic Activities that Affect α -Synuclein Degradation and Parkinson's Disease Susceptibility. *Cell* 111:209–218.
- Livak KJ, Schmittgen TD. 2001 Analysis of relative gene expression data using real-time quantitative PCR and the 2(-Delta Delta C(T)) Method. *Methods* 25:402-408.
- Logarinho E, Resende T, Torres C, Bousbaa H. 2008 The human spindle assembly checkpoint protein Bub3 is required for the establishment of efficient kinetochore-microtubule attachments. *Molecular Biology of the Cell* 19:1798-813.
- Lohmann JU, Endl I, Bosch TC. 1999 Silencing of developmental genes in Hydra. *Dev Biol* 214:211-214.
- Lonergan P, Khatir H, Piumi F, Rieger D, Humblot P, Boland MP. 1999 Effect of time interval from insemination to first cleavage on the developmental characteristics, sex ratio and pregnancy rate after transfer of bovine embryos. *J Reprod Fertil* 117:159-167.
- Lonergan P, Gutiérrez-Adán A, Pintado B, Fair T, Ward F, Fuente JD, Boland M. 2000 Relationship between time of first cleavage and the expression of IGF-I growth factor, its receptor, and two housekeeping genes in bovine two-cell embryos and blastocysts produced *in vitro.*, *Mol Reprod Dev* 57:146-152.
- Lopez LC, Bayna EM, Litoff D, Shaper NL, Shaper JH, Shur BD. 1985 Receptor function of mouse sperm surface galactosyltransferase during fertilization. *J Cell Biol* 101:1501–1510.
- Magnani L, Cabot RA. 2008 *In vitro* and *in vivo* derived porcine embryos possess similar, but not identical, patterns of Oct4, Nanog, and Sox2 mRNA expression during cleavage development. *Mol Reprod Dev* 75:1726–1735.
- Mehlmann LM, Saeki Y, Tanaka S, Brennan TJ, Evsikov AV, Pendola FL, Knowles BB, Eppig JJ, Jaffe LA. 2004 The Gs-linked receptor GPR3 maintains meiotic arrest in mammalian oocytes. *Science* 306:1947-1950.
- Memili E, First NL. 1999 Control of gene expression at the onset of bovine embryonic development. *Biol Reprod* 61:1198-1207.
- Michelmann HW, Bonhoff A, Mettler L. 1986 Chromosome analysis in polyploid human embryos. *Hum Reprod* 1:243-246.

- Misquitta L, Paterson BM. 1999 Targeted disruption of gene function in *Drosophila* by RNA interference (RNA-i): a role for nautilus in embryonic somatic muscle formation. *Proc Natl Acad Sci USA* 96:1451-1456.
- Miyazaki S, Shirakawa H, Nakada K, Honda Y. 1993 Essential role of the inositol 1,4,5-trisphosphate receptor/Ca²⁺ release channel in Ca²⁺ waves and Ca²⁺ oscillations at fertilization of mammalian eggs. *Dev Biol* 158:62–78.
- Mochizuki K, Gorovsky MA. 2004 Small RNAs in genome rearrangement in *Tetrahymena*. *Curr Opin Genet Dev* 14:181–187.
- Mullis K, Faloona F, Scharf S, Saiki R, Horn G, Erlich H. 1986 Specific enzymatic amplification of DNA *in vitro*: the polymerase chain reaction. *Cold Spring Harb Symp Quant Biol* 51 Pt 1:263-273.
- Mullis KB, Faloona FA. 1987 Specific synthesis of DNA *in vitro* via a polymerase-catalyzed chain reaction. *Meth Enzymol* 155:335-350.
- Murchison EP, Hannon GJ. 2004 miRNAs on the move: miRNA biogenesis and the RNAi machinery. *Curr Opin Cell Biol* 16:223–229.
- Ngô H, Tschudi C, Gull K, Ullu E. 1998 Double-stranded RNA induces mRNA degradation in *Trypanosoma brucei*. *Proc Natl Acad Sci USA* 95:14687-14692.
- O'Sullivan CM, Rancourt SL, Liu SY, Rancourt DE. 2001 A novel murine tryptase involved in blastocyst hatching and outgrowth. *Reproduction* 122:61-71.
- Oestrup O, Hall V, Petkov SG, Wolf XA, Hyldig S, Hyttel P. 2009 From zygote to implantation: morphological and molecular dynamics during embryo development in the pig. *Reprod Domest Animl* 3:39-49.
- Ohsugi M, Zheng P, Baibakov B, Li L, Dean J. 2008 Maternally derived FILIA-MATER complex localizes asymmetrically in cleavage-stage mouse embryos. *Development* 135:259-269.
- Okuwaki M, Tsujimoto M, Nagata K. 2002 The RNA Binding Activity of a Ribosome Biogenesis Factor, Nucleophosmin/B23, Is Modulated by Phosphorylation with a Cell Cycle-dependent Kinase and by Association with Its Subtype. *Mol Biol Cell* 13:2016-2030
- Pennetier S, Uzbekova S, Guyader-Joly C, Humblot P, Mermillod P, Dalbès-Tran R. 2005 Genes preferentially expressed in bovine oocytes revealed by subtractive and suppressive hybridization. *Biology of Reproduction* 73:713-720.
- Peragine A, Yoshikawa M, Wu G, Albrecht HL, Poethig RS. 2004 SGS3 and SGS2/SDE1/RDR6 are required for juvenile development and the production of trans-acting siRNAs in *Arabidopsis*. *Genes Dev* 18:2368–2379.
- Perona RM, Wassarman PM. 1986 Mouse blastocysts hatch *in vitro* by using a trypsin-like proteinase associated with cells of mural trophectoderm. *Dev Biol* 114:42-52.
- Perreault SD, Barbee RR, Slott VL. 1988 Importance of glutathione in the acquisition and maintenance of sperm nuclear decondensing activity in maturing hamster oocytes. *Dev Biol* 125:181–187.

- Peyrieras N, Hyafil F, Louvard D, Ploegh HL, Jacob F. 1983 Uvomorulin: a nonintegral membrane protein of early mouse embryo. *Proc Natl Acad Sci USA* 80:6274-6277.
- Picton HM. 2001 Activation of follicle development: the primordial follicle. *Theriogenology* 55:1193-1210.
- Piko L, Clegg K B. 1982 Quantitative changes in total RNA, total poly(A), and ribosomes in early mouse embryos. *Dev Biol* 89:362-378.
- Pincus G, Enzmann EV. 1935. The comparative behavior of mammalian eggs *in vivo* and *in vitro*. I. The activation of ovarian eggs. *J Exp Med* 62:665–675.
- Redkar A, deRiel JK, Xu Y-S, Montgomery M, Patwardhan V, Litvin J. 2002 Characterization of cardiac muscle factor 1 sequence motifs: retinoblastoma protein binding and nuclear localization. *Gene* 282:53-64.
- Reinhart BJ, Bartel DP. 2002 Small RNAs correspond to centromere heterochromatic repeats. *Science* 297:1831.
- Rice A, Parrington J, Jones KT, Swann K. 2000 Mammalian sperm contain a Ca(2+)-sensitive phospholipase C activity that can generate InsP(3) from PIP(2) associated with intracellular organelles. *Dev Biol* 228:125-135.
- Ristevski S, O'Leary DA, Thornell AP, Owen MJ, Kola I, Hertzog PJ, 2004 The ETS transcription factor GABPalpha is essential for early embryogenesis. *Molecular and Cellular Biology* 24:5844-5849.
- Ross PJ, Rodriguez RM, Iager AE, Beyhan Z, Wang K, Ragina NP, Yoon SY, Fissore RA, Cibelli JB. 2009 Activation of bovine somatic cell nuclear transfer embryos by PLCZ cRNA injection. *Reproduction* 137:427-437.
- Rossant J. 2007 Stem cells and lineage development in the mammalian blastocyst. *Reprod Fertil* 19:111-118
- Rossant J, Cross JC. 2001 Placental development: lessons from mouse mutants. *Nat Rev Genet* 2:538-548.
- Rüsse I. 1983 Oogenesis in cattle and sheep. *Bibl Anat* 24:77-92.
- Ryazansky SS, Gvozdev VA. 2008 Small RNAs and cancerogenesis. *Biochemistry (Mosc)* 73:514-527.
- Saunders CM, Larman MG, Parrington J, Cox LJ, Royse J, Blayney LM, Swann K, Lai FA. 2002 PLC zeta: a sperm-specific trigger of Ca(2+) oscillations in eggs and embryo development. *Development* 29:3533-3544.
- Savkur RS, Olson MO. 1998 Preferential cleavage in pre-ribosomal RNA by protein B23 endoribonuclease. *Nucleic Acid Res* 26:4508-4515
- Sekiguchi S, Kwon J, Yoshida E, Hamasaki H, Ichinose S, Hideshima M, Kuraoka M, Takahashi A, Ishii Y, Kyuwa S, Wada K, Yoshikawa Y. 2006 Localization of ubiquitin C-terminal hydrolase L1 in mouse ova and its function in the plasma membrane to block polyspermy. *Am J Pathol* 169:1722-1729.
- Setsuie R, Wada K. 2007 The functions of UCH-L1 and its relation to neurodegenerative diseases. *Neurochem Int* 51:105-111.

- Sharma N, Liu S, Tang L, Irwin J, Meng G, Rancourt DE. 2006 Implantation Serine Proteinases heterodimerize and are critical in hatching and implantation. *BMC Dev Biol* 6:61.
- Sirard, MA, Dufort, I, Vallee M, Massicotte L, Gravel C, Reghenas H, Watson AJ, King WA, Robert C, 2005 Potential and limitations of bovine-specific arrays for the analysis of mRNA levels in early development: preliminary analysis using a bovine embryonic array. *Reproduction, Fertility, and Development* 17:47-57.
- Steptoe PC, Edwards RG. 1978 Birth after the reimplantation of human a embryo. *The Lancet* 312:366.
- Stricker SA. 1999. Comparative biology of calcium signaling during fertilization and egg activation in animals. *Dev Biol* 211:157–176.
- Strassburger D, Friedler S, Raziel A, Kasterstein E, Schachter M, Ron-El R. 2004 The outcome of ICSI of immature MI oocytes and rescued *in vitro* matured MII oocytes. *Hum Reprod* 19:1587–1590.
- Strumpf D, Mao CA, Yamanaka Y, Ralston A, Chawengsaksophak K, Beck F, Rossant J. 2005 Cdx2 is required for correct cell fate specification and differentiation of trophectoderm in the mouse blastocyst. *Development* 132:2093-2102.
- Sun TT, Chung CM, Chan HC. 2011 Acrosome reaction in the cumulus oophorus revisited: involvement of a novel sperm-released factor NYD-SP8. *Protein Cell* 2:92-98.
- Svarcova O, Laurincik J, Avery B, Mlyncek M, Niemann H, Maddox-Hyttel P. 2007 Nucleolar development and allocation of key nucleolar proteins require de novo transcription in bovine embryos. *Molecular Reproduction and Development* 74:1428-1435.
- Svoboda P, Stein P, Hayashi H, Schultz RM. 2000 Selective reduction of dormant maternal mRNAs in mouse oocytes by RNA interference. *Development* 127:4147-4156.
- Swaminathan V, Kishore AH, Febitha KK Kundu TK. 2005 Human histone chaperone nucleophosmin enhances acetylation-dependent chromatin transcription. *Molecular and Cellular Biology* 25:7534-7545.
- Tadros W, Lipshitz HD. 2009 The maternal-to-zygotic transition: a play in two acts. *Development* 136:3033-3042.
- Telford NA, Watson AJ, Schultz GA. 1990 Transition from maternal to embryonic control in early mammalian development: a comparison of several species. *Mol Reprod Dev* 26:90-100.
- Tesfaye D, Worku D, Rings F, Phatsara C, Tholen E, Schellander K, Hoelker M. 2009 Identification and expression profiling of microRNAs during bovine oocyte maturation using heterologous approach. *Mol Reprod Dev* 76:665-677.
- Töpfer-Petersen E, Wagner A, Friedrich J, Petrunkina A, Ekhlasi-Hundrieser M, Waberski D, Drommer W. 2002 Function of the mammalian oviductal sperm reservoir. *J Exp Zool* 292:210-215.

- Trounson A, Anderiesz C, Jones G. 2001 Maturation of human oocytes *in vitro* and their developmental competence. *Reproduction* 121:51-75.
- Tulsiani DRP, Abou-Haila A, Loeser CR, Pereira BM. 1998 The biological and functional significance of the sperm acrosome and acrosomal enzymes in mammalian fertilization. *Exp Cell Res* 240:151–164.
- Valdez BC, Perlaky L, Henning D, Saijo Y, Chan PK, Busch H. 1994 Identification of the nuclear and nucleolar localization signals of the protein p120. Interaction with translocation protein B23. *J Biol Chem* 269:23776-23783.
- Vandesompele J, De Preter K, Pattyn F, Poppe B, Van Roy N, De Paepe A, Speleman F. 2002 Accurate normalization of real-time quantitative RT-PCR data by geometric averaging of multiple internal control genes. *Genome Biol* 3:RESEARCH0034.
- Vazquez F, Vaucheret H, Rajagopalan R, Lepers C, Gascioli V, Mallory AC, Hilbert JL, Bartel DP, Cr  t   P. 2004 Endogenous *trans*-acting siRNAs regulate the accumulation of Arabidopsis mRNAs. *Mol. Cell* 16:69–79.
- Visconti PE, Moore GD, Bailey JL, Leclerc P, Connors SA, Pan D, Olds-Clarke P, Kopf GS. 1995 Capacitation of mouse spermatozoa. II. Protein tyrosine phosphorylation and capacitation are regulated by a cAMP-dependent pathway. *Development* 121:1139–1150.
- Vigneault C, McGraw S, Sirard MA. 2009 Spatiotemporal expression of transcriptional regulators in concert with the maternal-to-embryonic transition during bovine *in vitro* embryogenesis. *Reproduction* 137:13-21.
- Volpe TA, Kidner C, Hall IM, Teng G, Grewal SI, Martienssen RA. 2002 Regulation of heterochromatin silencing and histone H3 lysine-9 methylation by RNAi. *Science* 297:1833–1837.
- Wang WH, Sun QY, Hosoe M, Shioya Y, Day BN. 1997 Quantified analysis of cortical granule distribution and exocytosis of porcine oocytes during meiotic maturation and activation. *Biol Reprod* 56:1376-1382.
- Wang Y, Penfold S, Tang X, Hattori N, Riley P, Harper JW, Cross JC, Tyers M. 1999 Deletion of the Cull1 gene in mice causes arrest in early embryogenesis and accumulation of cyclin E. *Current Biology* 9:1191-1194.
- Wang YL, Liu W, Sun YJ, Kwon J, Setsuie R, Osaka H, Noda M, Aoki S, Yoshikawa Y, Wada K. 2006 Overexpression of ubiquitin carboxyl-terminal hydrolase L1 arrests spermatogenesis in transgenic mice. *Mol Reprod Dev* 73:40-49.
- Wargelius A, Ellingsen S, Fjose A. 1999 Double-stranded RNA induces specific developmental defects in zebrafish embryos. *Biochem Biophys Res Commun* 263:156-161.
- Wassarman PM, Kinloch RA. 1992 Gene expression during oogenesis in mice. *Mutation Research/Reviews in Genetic Toxicology* 296:3-15.
- Watanabe T, Takeda A, Tsukiyama T, Mise K, Okuno T, Sasaki H, Minami N, Imai H. 2006 Identification and characterization of two novel classes of small

RNAs in the mouse germline: retrotransposon-derived siRNAs in oocytes and germline small RNAs in testes. *Genes* Dec 20:1732–1743.

- Wei Y, Bader D, Litvin J. 1996 Identification of a novel cardiac-specific transcript critical for cardiac myocyte differentiation. *Development* 122:2779-2789.
- Wianny F, Zernicka-Goetz M. 2000 Specific interference with gene function by double-stranded RNA in early mouse development. *Nat Cell Biol* 2:70-75.
- Wightman B, Ha I, Ruvkun G. 1993 Posttranscriptional regulation of the heterochronic gene *lin-14* by *lin-4* mediates temporal pattern formation in *C. elegans*. *Cell* 75:855-862.
- Wittwer CT, Herrmann MG, Moss AA, Rasmussen RP. 1997 Continuous fluorescence monitoring of rapid cycle DNA amplification. *BioTechniques* 22:130-131, 134-138.
- Yamauchi ., Yamauchi J, Kuwata T, Tamura T, Yamashita T, Bae N, Westphal H, Ozato K, Nakatani Y. 2000 Distinct but overlapping roles of histone acetylase PCAF and of the closely related PCAF-B/GCN5 in mouse embryogenesis. *Proceedings of the National Academy of Sciences of the United States of America* 97:11303-11306.
- Yanagimachi R. 1994 Mammalian Fertilization. In: Knobil E, Neill JD, editors. *The physiology of reproduction*. New York: Raven Press 261–268.
- Yang XJ, Ogryzko VV, Nishikawa J, Howard BH, Nakatani Y. 1996 A p300/CBP-associated factor that competes with the adenoviral oncoprotein E1A. *Nature* 382:319-324.
- Yang Z, Guo J, Chen Q, Ding C, Du J, Zhu X. 2005 Silencing Mitosin Induces Misaligned Chromosomes, premature Chromosome Decondensation before Anaphase Onset, and Mitotic Cell Death. *Molecular and Cellular Biology* 25:4062-4074.
- Yekta S, Shih IH, Bartel DP. 2004 MicroRNA-directed cleavage of *HOXB8* mRNA. *Science* 304:594–596.
- Yi YJ, Manandhar G, Sutovsky M, Li R, Jonáková V, Oko R, Park CS, Prather RS, Sutovsky P. 2007 Ubiquitin C-terminal hydrolase-activity is involved in sperm acrosomal function and anti-polyspermy defense during porcine fertilization. *Biol Reprod* 77:780-793.
- Yoon SY, Jellerette T, Salicioni AM, Lee HC, Yoo MS, Coward K, Parrington J, Grow D, Cibelli JB, Visconti PE, Mager J, Fissore RA. 2008 Human sperm devoid of PLC, zeta 1 fail to induce Ca(2+) release and are unable to initiate the first step of embryo development. *J Clin Invest* 118:3671-3681.
- Yu J, Tao Q, Cheung KF, Jin H, Poon FF, Wang X, Li H, Cheng YY, Röcken C, Ebert MP, Chan AT, Sung JJ. 2008 Epigenetic identification of ubiquitin carboxyl-terminal hydrolase L1 as a functional tumor suppressor and biomarker for hepatocellular carcinoma and other digestive tumors. *Hepatology* 48:508-518.
- Yung BYM, Bor AMS, Yang YH. 1990 Immunolocalization of phosphoprotein B23 on proliferating and non-proliferating HeLa cells. *International Journal of Cancer* 46:272-275.

- Zamore PD, Tuschl T, Sharp PA, Bartel DP. 2000 RNAi: Double-stranded RNA directs the ATP-dependent cleavage of mRNA at 21 to 23 nucleotide intervals. *Cell* 101:25–33.
- Zhu X, Mancini MA, Chang K-H, Liu C-Y, Chen C-F, Shan B, Jones D, Yang-Feng TL, Lee W-H. 1995 Characterization of a Novel 350-Kilodalton Nuclear Phosphoprotein That Is Specifically Involved in Mitotic-Phase Progression. *Molecular and Cellular Biology* 15:5017-5029.

8. PUBLICATION LIST

P1: Silencing CENPF in bovine preimplantation embryo induces arrest at 8-cell stage.

Toralova T, Susor A, Nemcova L, Kepkova K, Kanka J.

Reproduction. 2009 Nov;138(5):783-91. Epub 2009 Aug 3.; IF: 2.579

P2: Role of UCHL1 in Anti-polyspermy Defense of Mammalian Eggs.

Susor A, Liskova L, Toralova T, Pavlok A, Pivonkova K, Karabinova P, Lopatarova M, Sutovsky P, Kubelka M.

Biol Reprod. 2010 Jun;82(6):1151-61. Epub 2010 Feb 17.; IF: 3.300

P3: Transcriptomic analysis of *in vivo* and *in vitro* produced bovine embryos revealed a developmental change in cullin 1 expression during maternal-to embryonic transition.

Vodickova Kepkova K, Vodicka P, Toralova T, Lopatarova M, Cech S, Dolezel R, Havlicek V, Besenfelder U, Kuzmany A, Sirard M-A, Laurincik J, Kanka J.

Theriogenology. 2011 Jun;75(9):1582-95. Epub 2011 Mar 15.; IF: 2.073

P4: Bovine preimplantation embryos with silenced nucleophosmin mRNA are able to develop until the blastocyst stage due to preservation of sufficient protein amount.

Toralova T, Benesova V, Vodickova Kepkova K, Vodicka P, Susor A, Kanka J.

Submitted to Biology of Reproduction

Publication 1:

Silencing CENPF in bovine preimplantation embryo induces arrest at 8-cell stage.

Toralova T, Susor A, Nemcova L, Kepkova K, Kanka J.

Reproduction. 2009 Nov;138(5):783-91. Epub 2009 Aug 3.; IF: 2.579

Silencing *CENPF* in bovine preimplantation embryo induces arrest at 8-cell stage

Tereza Toralová, Andrej Šušor, Lucie Němcová, Kateřina Kepková and Jiří Kaňka

Department of Reproductive and Developmental Biology, Institute of Animal Physiology and Genetics, v.v.i., Academy of Sciences of the Czech Republic, Rumburská 89, 277 21 Liběchov, Czech Republic

Correspondence should be addressed to T Toralová; Email: moravcova@iapg.cas.cz

Abstract

Identification of genes that are important for normal preimplantation development is essential for understanding the basics of early mammalian embryogenesis. In our previous study, we have shown that *CENPF* (mitosin) is differentially expressed during preimplantation development of bovine embryos. *CENPF* is a centromere–kinetochore complex protein that plays a crucial role in the cell division of somatic cells. To our best knowledge, no study has yet been done on either bovine model, or oocytes and preimplantation embryos. In this study, we focused on the fate of bovine embryos after injection of *CENPF* double-stranded RNA (dsRNA) into the zygotes. An average decrease of *CENPF* mRNA abundance by 94.9% or more and an extensive decline in immunofluorescence staining intensity was detected relative to controls. There was no disparity between individual groups in the developmental competence before the 8-cell stage. However, the developmental competence rapidly decreased then and only 28.1% of *CENPF* dsRNA injected 8-cell embryos were able to develop further (uninjected control: 71.8%; green fluorescent protein dsRNA injected control: 72.0%). In conclusion, these results show that depletion of *CENPF* mRNA in preimplantation bovine embryos leads to dramatic decrease of developmental competence after embryonic genome activation.

Reproduction (2009) **138** 783–791

Introduction

Identification of genes that are important for normal preimplantation development of mammals is essential for studying early mammalian embryogenesis. A large number of genes expressed from the embryonic genome during embryonic genome activation (EGA) were identified using all sorts of molecular genetic methods including microarray analysis (Hamatani *et al.* 2004, Wang *et al.* 2004, Misirlioglu *et al.* 2006, Kanka *et al.* 2009, Vigneault *et al.* 2009). However, the functions of many transcripts during mammalian embryogenesis are still not known. This study concerns one of these genes encoding *CENPF* (centromeric protein F; mitosin).

CENPF is a large human protein (> 350 kDa; 3113 amino acids), which plays a crucial role in cell division by controlling microtubule dynamics, maintaining chromosome condensation, transcription regulation, and cell cycle progression (Liao *et al.* 1995, Zhu *et al.* 1995, Holt *et al.* 2005, Zhou *et al.* 2005). It is expressed and localized in a cell-cycle-dependent manner (Liao *et al.* 1995, Zhu *et al.* 1995). The protein starts to be expressed in the G1/S phase when it is dispersed in nucleoplasm with the exception of nucleolus (Zhu *et al.* 1995). During late G2 phase, it also relocalizes to the inner site of nuclear membrane and consequently to

the outer plate of the forming prekinetochores (Liao *et al.* 1995, Zhu *et al.* 1995). *CENPF* is one of the earliest proteins associated with kinetochores (Bomont *et al.* 2005, Yang *et al.* 2005, Pouwels *et al.* 2007) and helps to form the correct kinetochore–microtubule interactions (Yang *et al.* 2005). The protein remains associated with kinetochores until chromosome segregation when it subsequently relocalizes to the spindle mid-zone and intracellular bridge (Liao *et al.* 1995, Zhu *et al.* 1995). *CENPF* reaches its maximum level at the G2/M transition and is rapidly degraded after the cell division (Zhu *et al.* 1995). Several studies have shown that the depletion of *CENPF* in somatic cells prevents correct chromosome alignment, destabilizes the microtubule–kinetochore interaction and weakens the tension between sister centromeres (Bomont *et al.* 2005, Holt *et al.* 2005, Yang *et al.* 2005).

The cell cycle during mammalian preimplantation development is very specific in many ways. The cycle is markedly shortened – especially the G1 phase – and at the same time, mitosis occupies longer part of the cycle (Bolton *et al.* 1984, Iwamori *et al.* 2002). The transcription of embryonic genome starts in bovines in the late 8-cell stage (8c; Camous *et al.* 1986, King *et al.* 1988, Kopecny *et al.* 1989, Pavlok *et al.* 1993) and this event is called EGA. Until EGA, all the mRNAs

and proteins are of maternal origin (Bilodeau-Goeseels & Schultz 1997). Some authors suggest that there is also a so-called minor genome activation between 1- and 4c, which is followed by major genome activation in the 8c (Memili & First 2000, Jakobsen *et al.* 2006). We have recently proved that in bovine embryos the transcription of embryonic *CENPF* starts during major genome activation at late 8c. Until then, all the *CENPF* mRNA is of maternal origin and its amount gradually decreases from 2- to early 8c. After EGA, the expression level increases again and remains almost the same up until the blastocyst stage (Kanka *et al.* 2009).

Even though the embryo develops without any need of exogenous mitogens, it is very sensitive to changes of external environment. This is the cause of decreased developmental competence of *in vitro* produced embryos compared to embryos produced *in vivo* and a significant negative impact on the offspring (Hales & Barker 2001, DeBaun *et al.* 2003, Ecker *et al.* 2004).

In this study, we used the *CENPF*-specific double-stranded RNA (dsRNA) to silence the corresponding mRNA, so that we could monitor the developmental competence of the embryos and consequently compare the role of *CENPF* in mammalian preimplantation development with somatic cells.

Results

Effect of *CENPF* dsRNA injection on embryonic *CENPF* mRNA expression

To confirm that *CENPF* expression is needful for correct preimplantation development, we employed the RNA interference (RNAi) method. The dsRNA used was homologous to nucleotides 8971–9383 at the 3' end of bovine *CENPF* mRNA. The microinjection of *CENPF* dsRNA efficiently and specifically causes degradation of *CENPF* mRNA in bovine preimplantation embryos (Fig. 1).

At late 8c, the *CENPF* mRNA was reduced by 96.0% ($P < 0.001$) in comparison to uninjected control and by 94.9% ($P < 0.001$) in comparison to green fluorescent protein (*GFP*) dsRNA injected control (Fig. 1A). At late

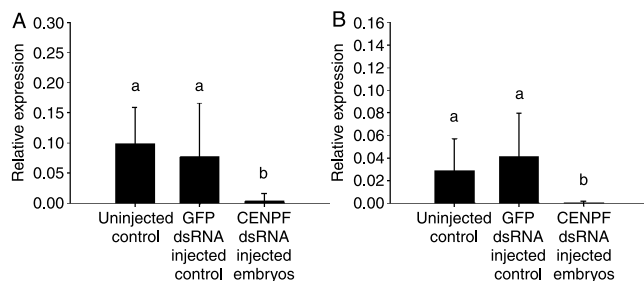


Figure 1 Relative abundance of *CENPF* mRNA after injection of *CENPF* dsRNA. *CENPF* mRNA expression (A) in 8-cell stage embryos and (B) in 16-cell stage embryos. The relative abundance (y-axis) represents the amount of *CENPF* mRNA in a single embryo normalized to one blastomere. Bars show mean \pm s.d. ^{a,b}Values with different superscripts indicate statistical significance ($P < 0.05$).

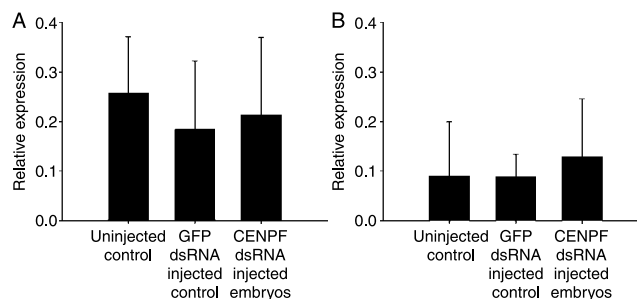


Figure 2 The expression of control genes after injection of *CENPF* dsRNA. The relative abundance of (A) *NPM1* mRNA and (B) *H2AFZ* mRNA. The relative abundance (y-axis) represents the amount of mRNA in a single embryo normalized to one blastomere. Bars show mean \pm s.d.

16-cell stage (16c), the *CENPF* mRNA was reduced by 97.8% ($P < 0.02$) in comparison to uninjected control and by 98.5% ($P < 0.002$) in comparison to *GFP* dsRNA injected control (Fig. 1B). No significant difference was found in the abundance of *CENPF* mRNA between the uninjected group and the *GFP* dsRNA injected group ($P > 0.05$).

To verify the specificity of *CENPF* mRNA degradation, we measured the level of mRNA of two control genes: H2A histone family, member Z (*H2AFZ*) and nucleophosmin (*NPM1*). No significant distinction between individual groups was detected ($P > 0.05$ in each case; Fig. 2).

Effect of *CENPF* dsRNA injection on protein expression

To monitor the effect of *CENPF* mRNA silencing on protein expression, we performed the immunofluorescence analysis using the polyclonal anti-*CENPF* antibody specific for C-terminus of the protein (Fig. 3). In uninjected embryos and embryos injected with *GFP* dsRNA, *CENPF* clearly colocalizes with the nuclei of blastomeres (Fig. 3A and B). In *CENPF* dsRNA injected embryos, we did not detect a similar localization pattern and fluorescence intensity was dramatically decreased (Fig. 3C).

Effect of *CENPF* mRNA silencing on developmental competence of the embryo

We monitored the number of embryos arrested at individual developmental stages in each treatment group. No developmental impairment was noticed until EGA (8c; $P > 0.05$ in each case; Fig. 4). However, a significantly lower number of *CENPF* dsRNA injected 8-cell embryos (8c) was capable to develop to 16c or beyond when compared with control groups (mean \pm s.e.m.: uninjected control: 71.8% \pm 3.55; *GFP* dsRNA injected control: 72.0% \pm 2.62; *CENPF* dsRNA injected group: 28.1% \pm 6.19; $P < 0.001$ in both cases; Fig. 5). Moreover, the embryos in both control groups were of

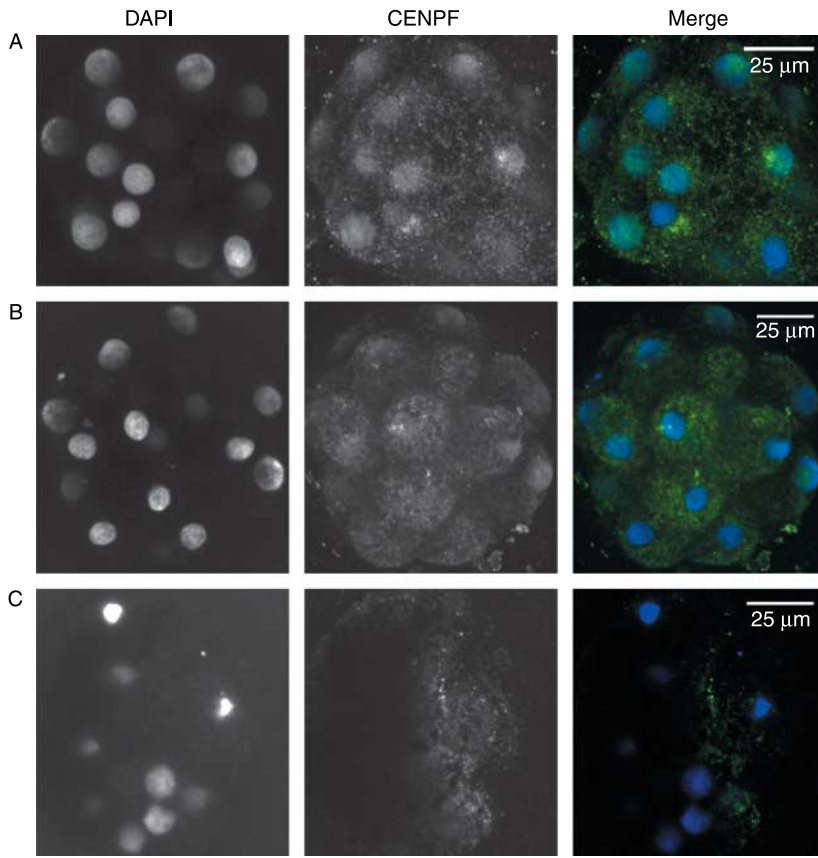


Figure 3 The immunofluorescence detection of CENPF after injection of *CENPF* dsRNA. CENPF expression (A) in uninjected embryos; (B) in embryos injected with *GFP* dsRNA; (C) in embryos injected with *CENPF* dsRNA. The embryos were stained using specific anti-CENPF antibody against C-terminus (CENPF, green; DNA, blue). The embryos were fixed at 4.5 days post fertilization.

higher morphological quality. The most frequent defect in *CENPF* dsRNA injected embryos was an unequal size of blastomeres, indistinct boundaries of blastomeres and partial transparency of blastomeres. Immunofluorescence analysis revealed that some of the *CENPF* dsRNA injected embryos had fragmented nuclei or even the blastomeres did not have any nucleus (Fig. 3C). Only $33.02\% \pm 3.684$ (mean \pm S.E.M.) of *CENPF* dsRNA injected embryos corresponded to the appropriate phenotype, whilst $68.88\% \pm 6.26$ of uninjected embryos and $69.38\% \pm 10.38$ *GFP* dsRNA injected embryos were of high quality ($P < 0.05$ in both cases).

***CENPF* is not degraded before EGA in bovine preimplantation embryos**

To find out whether CENPF is cyclically degraded and resynthesized in pre-EGA embryos, we blocked the protein synthesis using translation inhibitor cycloheximide (CHX) during cultivation from late 4c to 8c embryos (4c–8c group) and from late 8c to 16c (8c–16c group). The embryos were then examined for CENPF presence using immunofluorescence analysis. No significant difference in staining intensity was found between CHX-treated and non-treated embryos in 4c–8c group

(Fig. 6A and B). This suggests that CENPF is not degraded at the end of cell cycle in bovine preimplantation embryos before EGA. However, the results were considerably different in 8c–16c group. We did not observe complete degradation of CENPF, though, but the staining intensity was markedly weaker and the protein was not present in all the nuclei (Fig. 6C and D).

The localization of CENPF in bovine preimplantation embryos after EGA is cell cycle dependent

We employed immunofluorescence analysis for the monitoring of CENPF localization during early embryo cell cycle. Our data suggest that bovine CENPF is expressed and localized in the same pattern as the human protein. Most of the blastomeres of the analysed embryos were in interphase. In consistence with the immunofluorescence staining in somatic cells (Liao *et al.* 1995, Zhu *et al.* 1995, Hussein & Taylor 2002, Feng *et al.* 2006), CENPF was detected in the whole nucleus except nucleoli (Fig. 7A and C; non-marked blastomeres). As the chromosomes gradually condense, fluorescent dots begin to appear on chromosomes (Fig. 7A; blastomere marked by arrowhead and B), which is consistent with the kinetochore localization during prophase and prometaphase in somatic cells

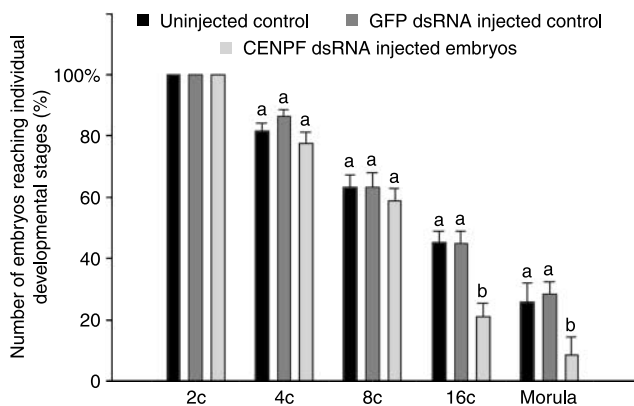


Figure 4 Developmental competence of embryos after injection of *CENPF* dsRNA. Number of embryos reaching individual developmental stages (y-axis). The number of 2-cell stage embryo is considered as 100%. The development competence was followed up during 12 independent experiments. ^{a,b}Values with different superscripts indicate statistical significance ($P < 0.05$). 2c, 2-cell stage embryos, 4c, 4-cell stage embryos, 8c, 8-cell stage embryos, 16c, 16-cell stage embryos.

(Liao *et al.* 1995, Zhu *et al.* 1995, Hussein & Taylor 2002, Feng *et al.* 2006). At the end of mitosis, *CENPF* ceases to be detectable by immunofluorescence (Fig. 7C; blastomere marked by arrowhead), which corresponds to the degradation of *CENPF* in somatic cells (Liao *et al.* 1995, Zhu *et al.* 1995, Hussein & Taylor 2002, Feng *et al.* 2006). The cell cycle stage of the blastomere was determined by DAPI staining.

Discussion

Although *CENPF* is known to be crucially important for cell division and cell cycle progression, no study concerning early mammalian embryo development has been done, up to now. We have recently shown that *CENPF* mRNA expression from embryonic genome is activated at late 8c (Kanka *et al.* 2009), which suggest importance of *CENPF* expression during preimplantation development. To confirm this, we included *CENPF* in a more thorough study. The bovine model has been chosen

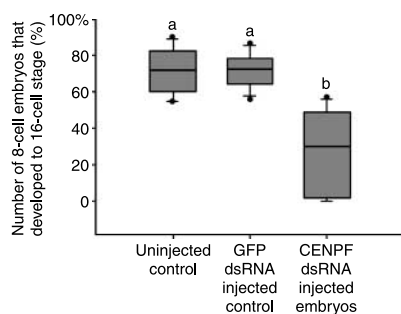


Figure 5 Developmental competence of 8-cell embryos. Number of 8 cell stage embryos that developed to 16-cell stage or beyond (y-axis). The graph plots the median and 10th, 25th, 75th and 90th percentiles and outliers (dots). ^{a,b}Values with different superscripts indicate statistical significance ($P < 0.05$).

because of the similarity of human and bovine preimplantation development (Telford *et al.* 1990, Adjaye *et al.* 2007, Kues *et al.* 2008).

The RNAi using dsRNA was used to silence the *CENPF* expression. The RNAi causes specific degradation of mRNA and is in fact the only applicable method for studying gene function in early mammalian embryo. Since the quality of early mammalian embryo unwinds from the quality of oocyte and the internal maternal environment, it is not feasible to use knockout for our purpose. For the assessment of degradation efficiency in single embryos we employed the FastLane Cell SYBR Green Kit (Qiagen) and the procedure that was first used by P Šolc for analysing single oocytes (personal communication; details described in Materials and Methods).

The absolute majority of studies concerning *CENPF* have been done on human somatic cells. Only four of its orthologs – murine *CENPF* (Goodwin *et al.* 1999, Ashe *et al.* 2003, Dees *et al.* 2005, Soukolis *et al.* 2005, Evans *et al.* 2007), avian CMF1 (Wei *et al.* 1996, Redkar *et al.* 2002) and worm *hcp1* and *hcp2* (Cheeseman *et al.* 2005, Hajeri *et al.* 2008) have been studied slightly more intensively. However, these proteins are expressed throughout the whole cell cycle, do not strictly localize to the nucleus or have a somewhat different function (Wei *et al.* 1996, Goodwin *et al.* 1999, Redkar *et al.* 2002, Cheeseman *et al.* 2005, Dees *et al.* 2005, Soukolis *et al.* 2005, Evans *et al.* 2007, Hajeri *et al.* 2008). This suggests that bovine *CENPF* does not necessarily have to be expressed in a cell-cycle-dependent manner. Moreover, some of the physiological activators and inhibitors of somatic cell cycle do not play the same role during preimplantation development and may even not be needed (Iwamori *et al.* 2002).

In somatic cells, *CENPF* participates in the kinetochore–microtubule interaction and is required for chromosome condensation, alignment and segregation. The silencing of *CENPF* in human somatic cells causes weakened centromere cohesion, premature chromosome decondensation and aneuploidy or metaphase arrest (Bomont *et al.* 2005, Holt *et al.* 2005, Yang *et al.* 2005).

The immunofluorescence analysis of bovine preimplantation embryo at the 16c exhibits the same expression and localization of *CENPF* as human somatic cells (Liao *et al.* 1995, Zhu *et al.* 1995, Hussein & Taylor 2002, Feng *et al.* 2006). In non-mitotic blastomeres we detected *CENPF* dispersed in nucleoplasm; in prophase and prometaphase blastomeres distinct foci of *CENPF* staining were detected on chromosomes. The protein was not detectable at the end of mitosis in preimplantation embryos after EGA (Fig. 7C). In somatic cells *CENPF* is degraded at the end of mitosis (Zhu *et al.* 1995). However, in preimplantation embryos before EGA, we did not detect any observable fall of protein amount after 24 h treatment with translation inhibitor CHX, which

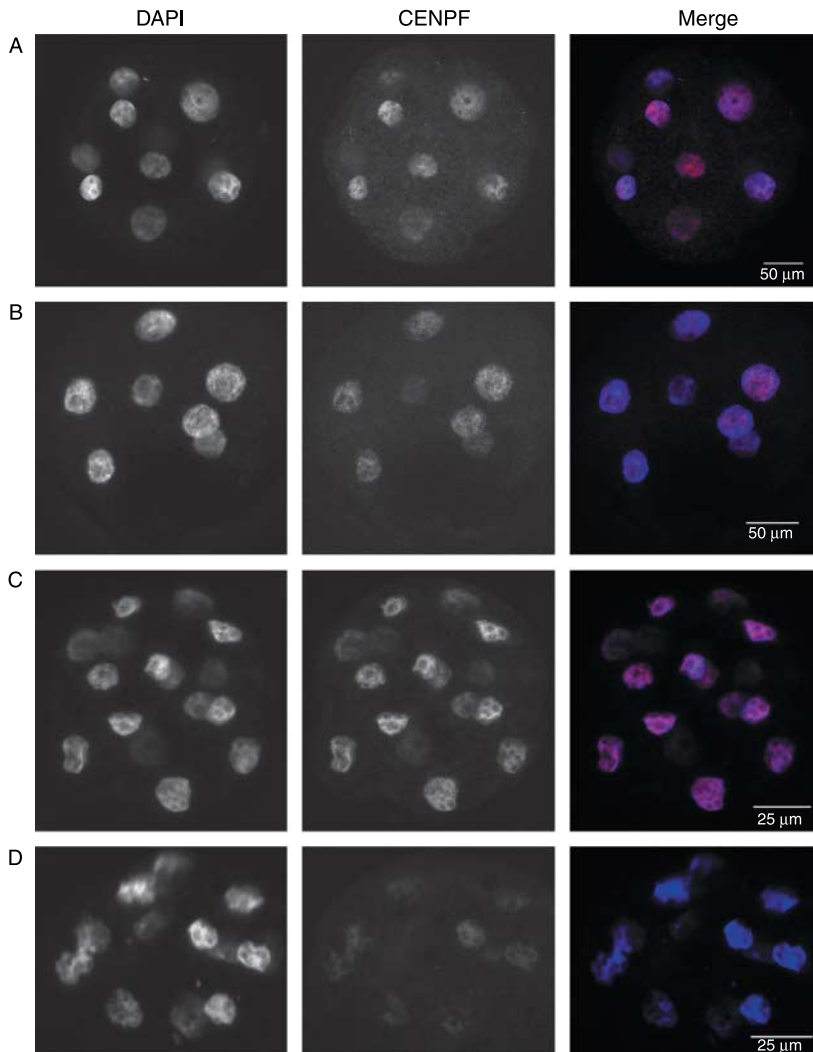


Figure 6 CENPF expression in cycloheximide treated embryos. Immunofluorescence analysis of (A) non-treated 8-cell embryos, (B) embryos cultivated from late 4-cell stage to 8-cell stage (for 24 h) in 10 $\mu\text{g/ml}$ cycloheximide, (C) non-treated 16-cell embryos, (D) embryos cultivated from late 8-cell stage to 16-cell stage (for 24 h) in 10 $\mu\text{g/ml}$ cycloheximide. The embryos were stained using specific mouse anti-CENPF antibody against N-terminus (DAPI, blue; CENPF, red).

poses a sufficiently long period for passing through the cell cycle (Fig. 6A and B). On the other hand, after CHX treatment of embryos post EGA, we detected a considerable decline of staining intensity (Fig. 6C and D). Hence, we suppose the preservation of maternal CENPF protein until the EGA in the late 8c. On the basis of the data mentioned above, we supposed that the CENPF-depleted embryos might arrest after EGA.

To confirm this, we performed the dsRNA mediated specific degradation of CENPF mRNA. We did not notice any differences in developmental competence between individual treatment groups until the 8c ($P > 0.05$ in each case; Fig. 4). However, the developmental competence of CENPF dsRNA injected embryos steeply decreased after the 8c; lesser than one-third of 8c embryos reached the 16c (Fig. 5) and only rare embryo-survivors further developed. Similarly, POU5F1 (Oct-4)-depleted embryos are able to develop until the morula stage without any significant differences in developmental competence, although the maternal mRNA can be detected in embryos before EGA and the first embryonic

transcript in bovine can be detected at the morula stage (Nganvongpanit *et al.* 2006a, 2006b). In our previous study (Kanka *et al.* 2009), we have shown that CENPF transcription from embryonic genome is activated during major genome activation, i.e. at late 8c. The arrest of CENPF-mRNA-depleted embryos just at the 8c suggests that until then, the embryos utilize maternal reserves of the protein. In addition, this is in agreement with our CHX experimental data.

In the CENPF dsRNA injected 16c embryos, the CENPF mRNA was silenced too. This suggests that embryos are to some extent able to compensate the decreased level of CENPF mRNA. The depletion of CENPF in somatic cells causes incorrect distribution of chromosomes during mitosis, since the cells form an interaction that is too weak between kinetochores and microtubules (Holt *et al.* 2005, Yang *et al.* 2005, Feng *et al.* 2006). Some of the CENPF-depleted cells progress through mitosis without chromosome segregation in anaphase or form a tripolar spindle resulting in multinucleated cells or aneuploidies (Holt *et al.* 2005,

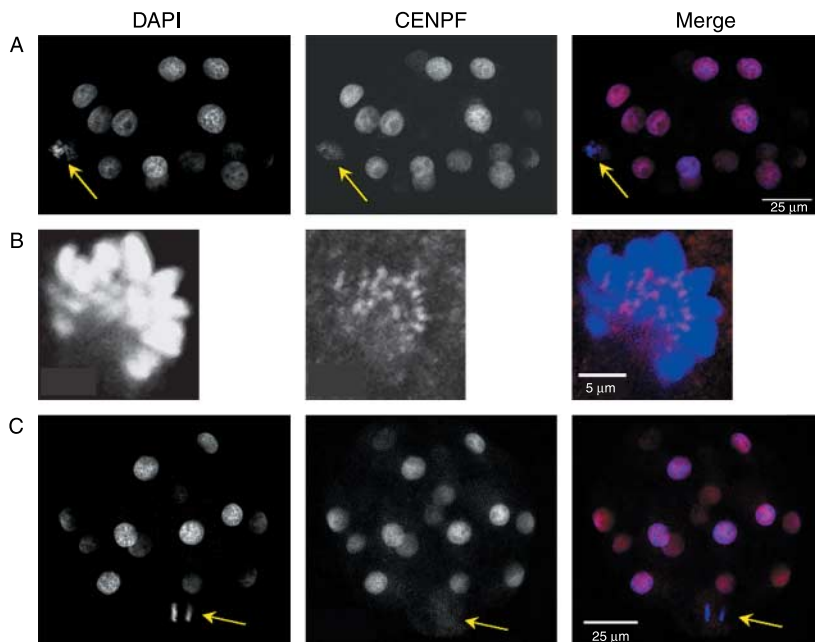


Figure 7 Localization of CENPF protein in a non-treated bovine preimplantation embryo throughout the cell cycle. (A) and (C) whole embryos, (B) detail of nucleus of a single blastomere in prometaphase; (A) localization on kinetochores in prophase (indicated by arrowhead); (B) localization on kinetochores in prometaphase; (C) degradation of the protein at the end of mitosis (indicated by arrowhead). During interphase CENPF localizes to nucleoplasm (unmarked blastomeres of embryos in (A) and (C)). The embryo in (A) and the embryo in (C) were stained using specific mouse anti-CENPF antibody against N-terminus; the single blastomere in (B) was stained using rabbit anti-CENPF antibody against C-terminus. All embryos are early 16-cell stage embryos.

Feng *et al.* 2006). Most of the CENPF-depleted cells do not continue the cell-cycle progress (Holt *et al.* 2005, Yang *et al.* 2005) and undergo apoptosis (Yang *et al.* 2005). However, a minority of cells are able to progress through the cell cycle despite the premature mitotic exit with unaligned chromosomes (Holt *et al.* 2005). The progress of some of the cells is probably caused by insufficient function of the mitotic checkpoint, which is able to delay, but not arrest, the progress (Feng *et al.* 2006). From our immunofluorescence data it follows that the nuclei of CENPF dsRNA injected embryos are in many cases fragmented, or the number of nuclei is less than the number of blastomeres (Fig. 3C). This suggests that also in blastomeres the cell cycle progress is arrested. However, some of the blastomeres are able to develop further. Moreover, the results of different studies are not homogeneous as to the cell fate after CENPF silencing (Holt *et al.* 2005, Laoukili *et al.* 2005, Yang *et al.* 2005, Feng *et al.* 2006). Ma *et al.* (2006) suggest that this may be caused by different efficiencies of the mRNA silencing. We, however, agree with the hypothesis of Feng *et al.* (2006), who assumed that the variation in results might be caused by the usage of different cell lines. Since the embryonic cells are strongly forced to cell division, they are supposed to surmount the cell-cycle-arrest signals quite easily.

In conclusion, we showed that the introduction of CENPF-specific dsRNA into the zygote leads to mRNA and protein silencing in preimplantation development. The inhibition of CENPF mRNA results in considerable deterioration in developmental competence after achieving the 8c and arrest of the majority of embryos before reaching the 16c. These findings are in agreement

with data acquired on human somatic cells and indicate that after activation of embryonic genome transcription, CENPF is expressed and localized in the same way as in human somatic cells and that the expression of CENPF mRNA is necessary for proper course of preimplantation development.

Materials and Methods

IVF and embryo culture

Unless otherwise indicated, chemicals were purchased from Sigma (Sigma-Aldrich) and plastic from Nunclon (Nunc, Roskilde, Denmark).

Bovine embryos were obtained after *in vitro* maturation of oocytes and their subsequent fertilization and culture *in vitro*. Briefly, abattoir derived ovaries from cows and heifers were collected and transported in thermo containers in sterile saline at about 33 °C. The follicles with diameter between 5 and 10 mm were dissected with fine scissors and then punctured. The cumulus–oocyte complexes were evaluated and selected according to the morphology of cumulus and submitted to *in vitro* maturation in TCM 199 supplemented with 20 mM sodium pyruvate, 50 U/ml penicillin, 50 μg/ml streptomycin, 10% estrus cow serum (ECS) and gonadotropins (P.G. 600, 15 U/ml; Intervet, Boxmeer, Holland) without oil overlay in 4-well dishes under atmosphere of 5% CO₂–7% O₂–88% N₂ at 39 °C for 24 h.

For IVF, the cumulus–oocyte complexes were washed four times in PBS and once in fertilization medium (TALP) and transferred in groups of up to 40 into 4-well dishes containing 250 μl of TALP per well. The TALP medium contained 1.5 mg/ml BSA, 30 μg/ml heparin, 0.25 mM sodium pyruvate, 10 mM lactate and 20 μM penicillamine. Cumulus–oocyte complexes were then co-incubated with frozen–thawed wash

semen from one bull previously tested in the IVF system. Viable spermatozoa were washed in TALP and centrifuged at 100 *g* for 5 min. Spermatozoa were counted in a haemocytometer and diluted in the appropriate volume of TALP to give a concentration of 2×10^6 spermatozoa/ml. A 250 μ l aliquot of this suspension was added to each fertilization well to obtain a final concentration of 1×10^6 spermatozoa/ml. Plates were incubated for 20 h at 39 °C under an atmosphere composed of 5% CO₂–7% O₂–88% N₂.

At 20 h post fertilization (hpf) zygotes were denuded by gentle pipetting, and transferred to B2 Menezo medium supplemented with 10% ECS and cultured in an atmosphere of 5% CO₂–7% O₂–88% N₂ at maximum humidity (25 zygotes in 25 μ l of medium under mineral oil; COOK, Eight Mile Plains, Queensland, Australia). The dishes were examined at 32, 44, 56, 92 and 120 hpf and 2-cell, 4-cell, early 8-cell, late 8-cell embryo and morula were collected at each time point respectively.

The CHX treatment

To block the protein synthesis CHX (Sigma–Aldrich) was added to the culture medium at a final concentration of 10 μ g/ml 48 and 80 hpf respectively. After 24 h cultivation, the embryos were washed in PBS and fixed for immunofluorescence. In total, 84 embryos were included in the study in four independent experiments – 48 hpf: 27 CHX-treated embryos and 16 controls; 80 hpf: 22 CHX-treated embryos and 19 controls were immunofluorescently examined.

Synthesis of DNA template

The RNA for DNA template synthesis was isolated from bovine embryonic fibroblasts using RNeasy Mini Kit (Qiagen). The template was synthesized using primers 'CENPF dsRNA' (see Table 1). The identity of fibroblastic and embryonic sequence was verified by sequencing. These primers generated amplicons corresponding to the bovine cDNA sequences in GenBank (XM_612376) and were fused with the T7 promoter. The RT was performed at 55 °C using RETROscript (Ambion, Austin, TX, USA), primed with random decamers. The PCR reaction was performed using SuperTaq polymerase (Ambion).

The samples were heated at 95 °C for 3 min followed by 30 cycles of 94 °C 20 s, 50 °C 20 s and 72 °C 45 s. The final extension step was held for 5 min at 72 °C. The PCR product was purified using QIAquick PCR Purification Kit (Qiagen) and the identity was confirmed by sequencing.

Synthesis of dsRNA

The DNA template coupled with T7 promoter was *in vitro* transcribed using MEGAscript RNAi Kit (Ambion). An amount of 1 μ g of DNA template was used for each reaction. The reaction mixture was incubated for 5 h at 37 °C and the sense and antisense strands were transcribed in the same reaction. To anneal them, the sample was incubated at 75 °C for 5 min and then left to cool at room temperature. The residual DNA template and ssRNA were digested and the dsRNA was purified according to the manufacturer's instruction. One microlitre of RNA acquired by *in vitro* transcription and 1 μ l of final dsRNA were resolved by electrophoresis on 1.5% agarose gel to confirm the integrity of the dsRNA and efficiency of the annealing step.

Zygote microinjection

Good quality zygotes were injected 20 hpf at the stage of two pronuclei. dsRNAs were dissolved in RNase-free water to a final concentration of 800 ng/ μ l. Zygotes were microinjected with ~5 pl of the dsRNA using an MIS-5000 micromanipulator (Burleigh, Exfo Life Sciences, Mississauga, Ontario, Canada) and PM 2000B4 microinjector (MicroData Instrument, South Plainfield, NJ, USA). Pipettes for microinjection were made using P97 Pipette Puller (Sutter Instrument Company, Novato, CA, USA). Two control groups were established – the uninjected group and a group injected with GFP dsRNA. The microinjection medium was Whitten's medium supplemented with 10 mmol/l HEPES (pH 7.3).

In total, 839 embryos were included in the study in 12 independent injection sessions. Embryos were categorized into the following groups: 1) embryos injected with CENPF dsRNA (266 embryos), 2) embryos injected with GFP dsRNA (237 embryos), and 3) uninjected embryos (336 embryos).

Table 1 Details of primers used for quantitative RT-PCR and double-stranded RNA synthesis.

Primer	Sequences	Annealing temperature (°C)	Amplicon size (bp)
CENPF (XM_612376) dsRNA	5' AGGATCCTAATACGACTCACTATAGGGA-GAGGGGCTTCCAGAAGTTGTAAA 3' 5' ACTCGAGTAATACGACTCACTATAGGCA-GATGGACCCTACAGTTCTCGCT 3'	50	413
GFP dsRNA ^a (Anger <i>et al.</i> 2005)	5' AGGATCCTAATACGACTAATATAGGGA-GAATGGTGAGCAAGGGCGAGGA 3' 5' ACTCGAGTAATACGACTCACTATAGGGA-GAGCGGCCGCTTACTTGTACA 3'	55	712
CENPF (XM_612376) mRNA quantification	5' TTGTAAAGAAAGGGTTTGC 3' 5' CCAGCTGTTGGTTTGGAGG 3'	50	172
NPM1 (XM_001252818) mRNA quantification	5' ACAGCCAACGGTTTCTCTTG 3' 5' TTTCACCTCCTCCTCCTCT 3'	55	154
H2AFZ (NM_174809) mRNA quantification	5' AGGACGACTAGCCATGGACGTGTG 3' 5' CCACCACCAGCAATTGTAGCCTTG 3'	60	208

^aTranscribed from empty p-Bluescript-GFP vector; kindly donated by M Anger and P Šolc.

After microinjection, embryos were cultivated under the conditions mentioned above and collected at specific developmental stages (late 8c – day 3.5 post fertilization, late 16c – day 4.5 post fertilization). The number of embryos that reach each developmental stage was counted and the morphological state of each embryo was determined using phase-contrast technique.

Monitoring of mRNA degradation efficiency

The embryos were washed and lysed using FastLane Cell SYBR Green Kit (Qiagen). Single embryos were washed in DMEM without foetal bovine serum and supplemented with 2% (w/v) polyvinylalcohol (PVA), PBS supplemented with 2% (w/v) PVA and FCW buffer (a component of FastLane Cell SYBR Green Kit) and stored dry and deep-frozen at -80°C until used. Whole single embryos were lysed in $10\ \mu\text{l}$ of the mixture of Buffer FCPL and gDNA Wipeout Buffer 2 (both members of FastLane Cell RT-PCR kit; Qiagen) according to the manufacturer's instructions and the lysate was directly used for the RT-PCR. Quantitative RT-PCR was performed using One Step RT-PCR kit (Qiagen). The samples were incubated at 50°C for 30 min and heated at 95°C followed by 45 cycles of 94°C 20 s, 50°C 20 s and 72°C 30 s. The final extension step was held for 10 min at 72°C . The RT-PCR data were normalized to the number of blastomeres.

The experiments were carried out on Rotor-Gene 3000 (Corbett Research, Mortlake, New South Wales, Australia). Fluorescence data were acquired at 3°C below the melting temperature to distinguish the possible primer dimers. The qRT-PCR data were determined using serial dilutions; the standard curve was created by Internal Rotor-Gene software (Corbett Research, Mortlake, Australia). The starting amount of corresponding RNA in analysed samples was determined by appointing the Cts to the curve. Products were verified by melting analysis and gel electrophoresis on 1.5% agarose gel with ethidium bromide staining. The experiment was repeated four times.

Immunofluorescence

Embryos were fixed in 4% paraformaldehyde supplemented with 1% (v/v) Triton X-100 for 50 min at 4°C . Fixed embryos were processed immediately or stored in PBS up to 3 weeks at 4°C . After washing in PBS embryos were incubated in 1% (v/v) Triton X-100 for 15 min. All subsequent steps were done in PBS supplemented with BSA (0.25% for mouse anti-CENPF antibody against N-terminus – BD Biosciences, Erembodegem, Belgium; 0.4% for rabbit anti-CENPF antibody against C-terminus – Novus Biologicals, Littleton, CO, USA) and 0.05% (w/v) saponin (PBS/BSA/sap). Embryos were blocked with 2% (v/v) normal goat serum for 1 h and incubated with primary antibody in PBS/BSA/sap overnight at 4°C (mouse anti-CENPF antibody against N-terminus – 1:100; rabbit anti-CENPF antibody against C-terminus – 1:1000). After thorough washing the embryos were incubated with goat anti-mouse antibody conjugated with Alexa 594 (Invitrogen) or goat anti-rabbit antibody conjugated with FITC (Santa Cruz Biotechnology, Santa Cruz, CA, USA) or with Alexa 594 (Invitrogen) in PBS/BSA/sap for 1 h at room temperature in the dark.

The nuclei were stained and the embryos were mounted on glass slides using VECTASHIELD HardSet Mounting Medium with DAPI (Vector Laboratories, Peterborough, UK). The samples were examined with a confocal laser-scanning microscope Leica TCS SP (Leica Microsystems AG, Wetzlar, Germany). Controls of immunostaining specificity were carried out by omitting primary antibody or using another species-specific secondary antibody conjugate. The images were processed using the ImageJ software (NIH, Bethesda, MD, USA; <http://rsb.info.nih.gov/ij/>).

Statistical analyses

The data were analysed using SigmaStat 3.0 software (Jandel Scientific, San Rafael, CA, USA), the Student's *t*-test or Mann–Whitney Rank Sum tests were used. $P < 0.05$ was considered as significant.

Declaration of interest

The authors declare that there is no conflict of interest that would prejudice the impartiality of this scientific work.

Funding

The work was supported by the Grant Agency of the Czech Republic (No. 523/06/1226) and by the IRP IAPG (No. AVOZ50450515), T Toralová was supported also by the Grant Agency of the Czech Republic (No. 204/05/H023IV).

Acknowledgements

The authors would like to thank L Lišková, K Pivoňková, J Kaňková, M Kopčíková, O Šebesta, A Šašková, P Šolc and V Baran for their expert assistance during the experiments.

References

- Adjaye J, Herwig R, Brink TC, Herrmann D, Greber B, Sudheer S, Groth D, Carnwath JW, Lehrach H & Niemann H 2007 Conserved molecular portraits of bovine and human blastocysts as a consequence of the transition from maternal to embryonic control of gene expression. *Physiological Genomics* **31** 315–327.
- Anger M, Stein P & Schultz RM 2005 CDC6 requirement for spindle formation during maturation of mouse oocytes. *Biology of Reproduction* **72** 188–194.
- Ashe M, Pabon-Pena L, Dees E, Price KL & Bader D 2003 LEK is a potential inhibitor of pocket protein-mediated cellular processes. *Journal of Biological Chemistry* **279** 664–676.
- Bilodeau-Goesels S & Schultz GA 1997 Changes in ribosomal ribonucleic acid content within *in vitro*-produced bovine embryos. *Biology of Reproduction* **56** 1323–1329.
- Bolton VN, Oades PJ & Johnson MH 1984 The relationship between cleavage, DNA replication, and gene expression in the mouse 2-cell embryo. *Journal of Embryology and Experimental Morphology* **79** 139–163.
- Bomont P, Maddox P, Shah JV, Desai AB & Cleveland DW 2005 Unstable microtubule capture at kinetochores depleted of the centromere-associated protein CENPF. *EMBO Journal* **24** 3927–3939.
- Camous S, Kopečný V & Flechon JE 1986 Autoradiographic detection of the earliest stage of [^3H]-uridine incorporation into the cow embryo. *Biology of the Cell* **58** 195–200.

- Cheeseman IM, MacLeod I, Yates JR III, Oegema K & Desai A 2005 The CENP-F-like proteins HCP-1 and HCP-2 target CLASP to kinetochores to mediate chromosome segregation. *Current Biology* **5** 771–777.
- DeBaun MR, Niemitz EL & Feinberg AP 2003 Association of *in vitro* fertilization with Beckwith–Wiedemann syndrome and epigenetic alterations of LIT1 and H19. *American Journal of Human Genetics* **72** 156–160.
- Dees E, Robertson JB, Ashe M, Pabon-Pena L, Bader D & Goodwin RL 2005 LEK1 protein expression in normal and dysregulated cardiomyocyte mitosis. *Anatomical Record. Part A, Discoveries in Molecular, Cellular, and Evolutionary Biology* **286** 823–832.
- Ecker DJ, Stein P, Xu Z, Williams CJ, Kopf GS, Bilker WB, Abel T & Schultz RM 2004 Long-term effects of culture of preimplantation mouse embryos on behavior. *PNAS* **101** 1595–1600.
- Evans HJ, Edwards L & Goodwin RL 2007 Conserved C-terminal domains of mCenpf (LEK1) regulates subcellular localization and mitotic checkpoint delay. *Experimental Cell Research* **313** 2427–2437.
- Feng J, Huang H & Yen TJ 2006 CENPF is a novel microtubule-binding protein that is essential for kinetochores attachments and affects the duration of the mitotic delay. *Chromosoma* **115** 320–329.
- Goodwin RL, Pabón-Peña LM, Foster GC & Bader D 1999 The cloning and analysis of LEK1 identities variations in the LEK/centromere protein F/mitosin gene family. *Journal of Biological Chemistry* **274** 18597–18604.
- Hajeri VA, Stewart AM, Moore LL & Padilla PA 2008 Genetic analysis of the spindle checkpoint genes *san-1*, *mdf-2*, *bub-3* and the CENP-F homologues *hcp-1* and *hcp-2* in *Caenorhabditis elegans*. *Cell Division* **3** 6.
- Hales CN & Barker DJP 2001 The thrifty phenotype hypothesis. *British Medical Bulletin* **60** 5–20.
- Hamatani T, Carter MG, Sharov AA & Ko MSH 2004 Dynamics of global gene expression changes during mouse preimplantation development. *Developmental Cell* **6** 117–131.
- Holt SV, Vergnolle MA, Hussein D, Wozniak MJ, Allan VJ & Taylor SS 2005 Silencing Cenpf weakens centromeric cohesion, prevents chromosome alignment and activates the spindle checkpoint. *Journal of Cell Science* **118** 4889–4900.
- Hussein D & Taylor SS 2002 Farnesylation of Cenpf is required for G2/M progression and degradation after mitosis. *Journal of Cell Science* **115** 3403–3414.
- Iwamori N, Naito K, Sugiura K & Tojo H 2002 Preimplantation-embryo-specific cell cycle regulation is attributed to the low expression level of retinoblastoma protein. *FEBS Letters* **526** 119–123.
- Jakobsen AS, Avery B, Dieleman SJ, Knijn HM, Vos PLAM & Thomsen PD 2006 Transcription of ribosomal RNA genes is initiated in the third cell cycle of bovine embryos. *Molecular Reproduction and Development* **73** 196–205.
- Kanka J, Kepkova K & Nemcova L 2009 Gene expression during minor genome activation in pre-implantation bovine development. *Theriogenology* **72** 572–583.
- King WA, Niar A, Chartrain I, Betteridge KJ & Guay P 1988 Nucleolus organizer regions and nucleoli in preattachment bovine embryos. *Journal of Reproduction and Fertility* **82** 87–95.
- Kopečný V, Flechon JE, Camous S & Fulka J Jr 1989 Nucleologenesis and the onset of transcription in the eight-cell bovine embryo: fine-structural autoradiographic study. *Molecular Reproduction and Development* **1** 79–90.
- Kues WA, Sudheer S, Herrmann D, Carnwath JW, Havlicek V, Besenfelder U, Lehrach H, Adjaye J & Niemann H 2008 Genome-wide expression profiling reveals distinct clusters of transcriptional regulation during bovine preimplantation development *in vivo*. *PNAS* **105** 19768–19773.
- Laoukili J, Kooistra MR, Bras A, Kaw J, Kerkhoven RM, Morrison A, Clevers H & Medema RH 2005 FoxM1 is required for execution of the mitotic programme and chromosome stability. *Nature Cell Biology* **7** 126–136.
- Liao H, Winkfein RJ, Mack G, Rattner JB & Yen TJ 1995 CENPF is a protein of the nuclear matrix that assembles onto kinetochores at late G2 and is rapidly degraded after mitosis. *Journal of Cell Biology* **130** 507–518.
- Ma L, Zhao X & Zhu X 2006 Mitosin/CENP-F in mitosis, transcriptional control, and differentiation. *Journal of Biomedical Science* **13** 205–213.
- Memili E & First NL 2000 Zygotic and embryonic gene expression in cow: a review of timing and mechanisms of early gene expression as compared with other species. *Zygote* **8** 87–96.
- Misirlioglu M, Page GP, Sagirkaya H, Kaya A, Parrish JJ, First NL & Memili E 2006 Dynamics of global transcriptome in bovine matured oocytes and preimplantation embryos. *PNAS* **103** 18905–18910.
- Nganvongpanit K, Müller H, Rings F, Gilles M, Jennen D, Hölker M, Tholen E, Schellander K & Tesfaye D 2006a Targeted suppression of E-cadherin gene expression in bovine preimplantation embryo by RNA interference technology using double-stranded RNA. *Molecular Reproduction and Development* **73** 153–163.
- Nganvongpanit K, Müller H, Rings F, Hölker M, Jennen D, Tholen E, Havlicek V, Besenfelder U, Schellander K & Tesfaye D 2006b Selective degradation of maternal and embryonic transcripts in *in vitro* produced bovine oocytes and embryos using sequence specific double-stranded RNA. *Reproduction* **131** 861–874.
- Pavlok A, Kopečný V, Lucas-Hahn A & Niemann H 1993 Transcriptional activity and nuclear ultrastructure of 8-cell bovine embryos developed by *in vitro* maturation and fertilization of oocytes from different growth categories of antral follicles. *Molecular Reproduction and Development* **35** 233–243.
- Pouwels J, Kukkonen M, Lan W, Daum JR, Gorbisky GJ, Stukenberg T & Kallio MJ 2007 Shugoshin 1 plays a central role in kinetochore assembly and is required for kinetochore targeting of Plk1. *Cell Cycle* **6** 1579–1585.
- Redkar A, deRiel JK, Xu Y-S, Montgomery M, Patwardhan V & Litvin J 2002 Characterization of cardiac muscle factor 1 sequence motifs: retinoblastoma protein binding and nuclear localization. *Gene* **282** 53–64.
- Soukalis V, Reddy S, Pooley RD, Feng Y, Walsh CA & Bader DM 2005 Cytoplasmic LEK1 is a regulator of microtubule function through its interaction with LIS1 pathway. *PNAS* **102** 8549–8554.
- Telford NA, Watson AJ & Schultz GA 1990 Transition from maternal to embryonic control in early mammalian development: a comparison of several species. *Molecular Reproduction and Development* **26** 90–100.
- Vigneault C, Gravel C, Vallee M, McGraw S & Sirard MA 2009 Unveiling the bovine embryo transcriptome during the maternal to embryonic transition. *Reproduction* **137** 254–257.
- Wang QT, Piotrowska K, Ciemerych MA, Milenkovic L & Zernicka-Goetz M 2004 A genome-wide study of gene activity reveals developmental signalling pathways in the preimplantation mouse embryo. *Developmental Cell* **6** 133–144.
- Wei Y, Bader D & Litvin J 1996 Identification of a novel cardiac-specific transcript critical for cardiac myocyte differentiation. *Development* **122** 2779–2789.
- Yang Z, Guo J, Chen Q, Ding C, Du J & Zhu X 2005 Silencing mitosin induces misaligned chromosomes, premature chromosome decondensation before anaphase onset, and mitotic cell death. *Molecular and Cellular Biology* **25** 4062–4074.
- Zhou X, Wang R, Fan L, Li Y, Ma L, Yang Z, Yu W, Jing N & Zhu X 2005 Mitosin/CENPF as a negative regulator of activating transcription factor-4. *Journal of Biochemistry* **280** 13973–13977.
- Zhu X, Mancini MA, Chang K-H, Liu C-Y, Chen C-F, Shan B, Jones D, Yang-Feng TL & Lee W-H 1995 Characterization of a novel 350-kilodalton nuclear phosphoprotein that is specifically involved in mitotic-phase progression. *Molecular and Cellular Biology* **15** 5017–5029.

Received 8 June 2009

First decision 13 July 2009

Accepted 3 August 2009

Publication 2:

Role of UCHL1 in Anti-polyspermy Defense of Mammalian Eggs.

Susor A, Liskova L, **Toralova T**, Pavlok A, Pivonkova K, Karabinova P, Lopatarova M, Sutovsky P, Kubelka M.

Biol Reprod. 2010 Jun;82(6):1151-61. Epub 2010 Feb 17.; IF: 3.300

Role of Ubiquitin C-Terminal Hydrolase-L1 in Antipolyspermy Defense of Mammalian Oocytes¹

Andrej Susor,^{2,3} Lucie Liskova,³ Tereza Toralova,³ Antonin Pavlok,³ Katerina Pivonkova,³ Pavla Karabinova,³ Miloslava Lopatarova,⁵ Peter Sutovsky,⁴ and Michal Kubelka³

Institute of Animal Physiology and Genetics,³ Academy of Sciences of the Czech Republic, Libechev, Czech Republic
Division of Animal Sciences,⁴ Department of Obstetrics, Gynecology and Women's Health,
University of Missouri-Columbia, Columbia, Missouri
University of Veterinary and Pharmaceutical Sciences,⁵ Brno, Czech Republic

ABSTRACT

The ubiquitin-proteasome system regulates many cellular processes through rapid proteasomal degradation of ubiquitin-tagged proteins. Ubiquitin C-terminal hydrolase-L1 (UCHL1) is one of the most abundant proteins in mammalian oocytes. It has weak hydrolytic activity as a monomer and acts as a ubiquitin ligase in its dimeric or oligomeric form. Recently published data show that insufficiency in UCHL1 activity coincides with polyspermic fertilization; however, the mechanism by which UCHL1 contributes to this process remains unclear. Using UCHL1-specific inhibitors, we induced a high rate of polyspermy in bovine zygotes after *in vitro* fertilization. We also detected decreased levels in the monomeric ubiquitin and polyubiquitin pool. The presence of UCHL1 inhibitors in maturation medium enhanced formation of presumptive UCHL1 oligomers and subsequently increased abundance of K63-linked polyubiquitin chains in oocytes. We analyzed the dynamics of cortical granules (CGs) in UCHL1-inhibited oocytes; both migration of CGs toward the cortex during oocyte maturation and fertilization-induced extrusion of CGs were impaired. These alterations in CG dynamics coincided with high polyspermy incidence in *in vitro*-produced UCHL1-inhibited zygotes. These data indicate that antipolyspermy defense in bovine oocytes may rely on UCHL1-controlled functioning of CGs.

cortical granule, deubiquitinating, fertilization, in vitro fertilization, meiosis, oocyte, oocyte development, ovum, polyspermy, proteasome, ubiquitin, zygote

¹Major funding was provided by grant GACR 524/07/1087. P.K. and T.T. were supported by grant 204/09/H084; L.L. was supported by grant GACR 524/09/P435. This work was supported in part by National Research Initiative Competitive grant 2007-01319 from the USDA Cooperative State Research, Education and Extension Service to P.S. and by seed funding from the Food for the 21st Century Program of the University of Missouri-Columbia to P.S. This study was also supported by grant MSM 6215712403 and by Institutional Research Concept IAPG AV0Z50450515.

²Correspondence: Andrej Susor, Institute of Animal Physiology and Genetics, Academy of Sciences of the Czech Republic, 277 21 Libechev, Czech Republic. FAX: 420 315 639 510; e-mail: susor@iapg.cas.cz

Received: 22 September 2009.

First decision: 12 October 2009.

Accepted: 27 January 2010.

© 2010 by the Society for the Study of Reproduction, Inc.

This is an Open Access article, freely available through *Biology of Reproduction's* Authors' Choice option.

eISSN: 1529-7268 <http://www.biolreprod.org>

ISSN: 0006-3363

INTRODUCTION

The ubiquitin-proteasome system regulates many cellular processes via substrate-specific protein degradation [1–3] and protein stabilization [4]. Covalent conjugation of ubiquitin to its substrate proteins plays a crucial role in a wide variety of biological processes [5]. Posttranslational modification by ubiquitination can be reversed by deubiquitination, a mechanism that plays an important widely recognized role in regulation of ubiquitin-dependent pathways. The deubiquitinating enzymes (DUBs) have been implicated, for example, in cell growth, differentiation, oncogenesis, and development and in regulation of chromosome structure [6]. One such DUB, ubiquitin C-terminal hydrolase-L1 (UCHL1), is highly abundant in mammalian oocytes [7]. It is also expressed in neurons and in the testis [8, 9]; however, abnormal expression of UCHL1 is also found in many primary lung tumors [10, 11] and in colorectal cancer [12].

UCHL1 has relatively weak hydrolytic activity and catalyzes hydrolysis of C-terminal ubiquityl esters and amides *in vitro*; peptide-ubiquityl amides are preferred substrates of UCHL1 [13, 14]. This activity is thought to be critical for cytoplasmic protein degradation and for recycling free ubiquitin by cleaving ubiquitylated peptides that are products of proteasomal degradation of polyubiquitylated proteins [13, 14]. UCHL1 has also been shown to have ligase activity, which correlates with dimerization or oligomerization of the enzyme [15]. Crystallography findings support the idea that UCHL1 is a tightly regulated enzyme and suggest an enzymatic activation mediated by substrate binding [16]. UCHL1 in COS-7 cells is posttranslationally modified by monoubiquitin at lysine 157 (K157) near the active site [17]. Farnesylation of the C-terminus of membrane-associated UCHL1 has been demonstrated in neural cells [18], which may be important to UCHL1 association with organelle membranes and with the inner face of the plasma membrane in oocytes. It has been also suggested that UCHL1 plays an important role in apoptosis; UCHL1 directly interacts with and stabilizes the proapoptotic tumor suppressor protein TP53 through ubiquitination [19]. Accordingly, the lack of functional UCHL1 in the *gad* mutant mouse [20] results in the absence of a physiological apoptotic wave in the testis that is important for male fertility [21–23].

Of particular interest for the present study is the proposed role of UCHL1 in the prevention of abnormal polyspermic fertilization in mammals. Fertilization in mammals is characterized by formation of one male and one female pronucleus after incorporation of a single spermatozoon into an oocyte. Such a constellation of paternal and maternal chromatin leads to normal embryo development. However, fertilization by more than one spermatozoon, called polyspermy, causes aberrant

development and death of the embryo at an early stage of development [24, 25]. Active blocking of polyspermic fertilization is necessary to prevent incorporation of multiple spermatozoa into an oocyte. Mammalian oocytes utilize both extracellular zona pellucida (ZP)-mediated and plasma membrane-mediated blocking of polyspermy. Although little is known about plasma membrane blocking in mammals, fertilization results in ZP glycoprotein modifications caused by enzymes released after cortical granule (CG) extrusion [26]. Increased polyspermy incidence was reported during in vitro fertilization (IVF) of *gad* mutant mouse oocytes lacking functional UCHL1 [27] and in porcine zygotes treated with ubiquitin aldehyde (a specific inhibitor of UCHs) [28]; nevertheless, the mechanism by which UCHL1 and other related UCHs regulate polyspermy defense remains unclear.

MATERIALS AND METHODS

Oocyte Collection and Maturation In Vitro

Ovaries were obtained from a local slaughterhouse and transported to the laboratory in physiological saline at 20°C. They were briefly washed in 70% ethanol and then in physiological saline. Oocytes were obtained by aspiration of large antral follicles (>4 mm). Only oocytes surrounded by compact cumuli (cumulus-oocyte complexes [COCs]) were used for culture. The COCs were cultured in maturation medium [29] supplemented with 15% estrus cow serum (ECS) and 5 IU/ml of Suigonan PG-600 (Intervet International B.V.) at 38.5°C in an atmosphere of 5% CO₂ [29]. Samples were collected at 0 h (germinal vesicle stage [GV]), 24 h (metaphase II [MII]), and 20 h (1-cell zygote) after fertilization. At the end of culture, the cumulus cells were removed from oocytes by vortexing. Denuded oocytes were washed in PBS and stored at -80°C for immunoblotting experiments. Some oocytes and zygotes were evaluated for meiotic progression and fertilization by staining with 0.1 µg/ml of Hoechst 33258 (Sigma) and observed under an Olympus IX70 epifluorescence microscope.

Inhibition of UCHL1 in the Oocyte

To investigate the role of UCHL1 in the oocyte, the following specific inhibitors of UCHL1 were added to the medium at 20 µM concentration (unless stated otherwise) at the beginning of culture: C30 [30] (alternative designation LDN-57444 [662086; Merck]) and C16 [31] (kindly provided by Dr. Gregory D. Cuny, Harvard Center for Neurodegeneration and Repair, Brigham & Women's Hospital and Harvard Medical School, Boston, MA). C30 is a reversible, competitive, active site-directed isatin oxime with consistent preference for UCHL1 over UCHL3 by 28-fold. C16 is an uncompetitive inhibitor of UCHL1 that binds only to the Michaelis complex and not to free enzyme. Stock solutions of C16 and C30 were prepared in dimethyl sulfoxide (DMSO) (D2438; Sigma) and kept frozen at -20°C. Controls were treated with an equivalent amount of DMSO. Final working solutions of C16 and C30 were diluted immediately before usage. Meiotic progression was evaluated at 24 h after isolation (extrusion of first polar body [PB]). The COCs were washed thoroughly in fertilization medium (FM) before IVF.

In Vitro Fertilization

Frozen ejaculate from the same fertile bull (provided by the Czech Breeders Association), stored in sperm pellet form, was used in all experiments. Basic FM was used for sperm thawing, washing, and swim up [29]. Sperm pellets were plunged into 2 ml of FM warmed up to 39°C, centrifuged in conic tubes for 10 min at 250 × g, and washed twice in FM. After the second wash, sperm pellets were incubated for 10 min at 39°C and divided into two equal parts; each part was layered under 1 ml of FM in 8-ml tubes and then incubated for 10 min at 39°C for the swim-up procedure. The supernatants (2 × 0.7 ml) with motile spermatozoa were pooled and centrifuged. Spermatozoa were placed into each well of four-well Nunclon dishes (Thermo Fisher Scientific, Denmark) with 500 µl of FM supplemented with 1.5 mg/ml of crystallized bovine serum albumin (BSA), 0.25 mg/ml of D-penicillamin (Sigma), 2% fetal calf serum, and 5 IU/ml of heparin (Sigma). The final sperm concentration was 0.5 × 10⁶ sperm per milliliter of FM. Washed COCs were coincubated with spermatozoa for 20 h at 38.5°C in an atmosphere of 5% CO₂. No inhibitors were added to FM during IVF. The number of pronuclei and CG status were assessed at 20 h after fertilization as already described.

Parthenogenetic Activation

Bovine oocyte maturation and in vitro embryo culture were performed as described previously [32]. C30 inhibitor was dissolved in DMSO and added to maturation medium at 20 µM concentration; DMSO alone was added to control maturation medium. After 24 h of maturation, oocytes were stripped of cumulus cells by vortexing. Oocytes were activated according to an established method [33] with slight modifications. Briefly, oocytes were incubated in 5 µM ionomycin (Sigma) in Tyrode lactate-Hepes supplemented with 3 mg/ml of BSA for 5 min and subsequently in 2 mM 6-DMAP (Sigma) in EmbryoAssist medium (Medicult) supplemented with 15% ECS for 5 h. After activation, oocytes were transferred into pure EmbryoAssist medium with ECS. Embryo development was examined at 32, 44, 56, 92, 120, 156, and 180 h after activation, and the numbers of 2-cell, 4-cell, early 8-cell, and late 8-cell embryos and morulae and blastocysts were counted at each time point.

In Vitro mRNA Production for Microinjection

The pCMVFL3 vector with cDNA clone (OVR010079H10) containing the full-length porcine *UCHL1* sequence (GenBank accession number AK234541.1) was a gift from Professor Hirohide Uenishi (National Institute of Agrobiological Sciences, Tsukuba, Japan). The porcine-specific protein sequence (Q6SEG5) was aligned to the bovine protein sequence (ENSB-TAT00000006692) using BLAST analysis, and identity between both sequences was 96%. To generate the template for transcription, full-length porcine cDNA of *UCHL1* was cloned into the *SpeI* site (for N-terminal green fluorescent protein [GFP] tags) of the phageRNA (pRNA)-enhanced GFP (EGFP) or pRNA-empty vector containing a T3 promoter and *Xenopus* globin 5' untranslated region (UTR), 3' UTR, and Kozak sequences for high mRNA stability and efficient translation initiation [34]. *EGFP-UCHL1* mRNA and wild-type *UCHL1* mRNA for microinjection were produced by in vitro transcription of the linearized vector using mMMESSAGE mMACHINE T3 kit (1348; Ambion). After in vitro transcription, mRNAs were immediately polyadenylated using Poly(A) Tailing kit (AM1350; Ambion) for stabilization. They were purified using RNeasy Mini kit (74104; Qiagen). Identity of products was confirmed by sequencing. *EGFP* mRNA for control microinjection was transcribed from an empty pRNA-EGFP vector. The mRNAs were aliquoted (5 µl) at 500 ng of RNA per microliter and stored at -80°C until used for microinjection.

Oocyte Microinjection

Freshly isolated GV-stage oocytes were partly denuded from cumulus cells and cultured for 1 h in manipulation medium (MM) without hormones. Oocytes were microinjected with 5 pl of the mRNA solution using an MIS-5000 micromanipulator (Burleigh; Exfo Life Sciences) and a PM 2000B4 microinjector (MicroData Instrument). Pipettes for microinjection were prepared using a P97 Pipette Puller (Sutter Instrument Company). The microinjection medium was the MM (110 mM NaCl, 10 mM glucose, 8 mM Hepes, 5 mM KCl, 2 mM CaCl₂·H₂O, 0.5 mM KH₂PO₄, 0.4 mM MgSO₄·7H₂O, 0.1% NaHCO₃, 1 mg/ml of polyvinyl alcohol, 0.2 mg/ml of sodium pyruvate, and antibiotics). Oocytes were microinjected with *Uchl1* mRNA with dextran-fluorescein isothiocyanate (FITC) or with *EGFP-UCHL1* mRNA. Control oocytes were injected with dextran-FITC (1 mg/ml, 70 kDa; Sigma) (Supplemental Fig. S1 available at www.biolreprod.org). Following microinjection, oocytes were incubated in MM with PG-600. Only oocytes displaying EGFP fluorescence or dextran-FITC fluorescence were used for analysis. Oocytes were dry frozen at -80°C for immunoblotting or fixed in 4% paraformaldehyde (16005; Sigma) for immunofluorescence, in which case they were mounted in an antifade medium containing DNA stain 4',6'-diamidino-2-phenylindole (DAPI) and analyzed by confocal microscopy.

Immunoblotting of Oocyte Extracts

Unless stated otherwise, all reagents were obtained from Sigma. Exact numbers of oocytes (20, 50, or 100 oocytes per extract) were lysed in 3× Blue Loading Buffer (7722; Cell Signaling) with or without dithiothreitol (DTT) and then subjected to SDS-PAGE gel (12% or 15% acrylamide, 0.75-mm thick). To limit the amount of disulfide-bonded oligomers formed in cells, the thiol-blocking agent *N*-ethylmaleimide (NEM) was added to the cell lysis buffer [35, 36]. Proteins were transferred to Immobilon P membrane (Millipore Corporation) using a semidry blotting system (Whatman Biometra GmbH) for 30 min at 5 mA/cm². Blocking of the membrane was performed in 5% nonfat milk in Tris-buffered saline (TBS)-Tween buffer (TBS-T) (20 mM Tris, pH 7.4, 137 mM NaCl, and 0.5% Tween 20) for 1 h. After three washes for 10 min in TBS-T, the membrane was incubated overnight with the first antibody.

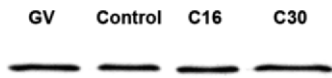


FIG. 1. The level of the monomeric form of UCHL1 does not change during oocyte maturation. Bovine oocytes were analyzed by immunoblotting (50 oocytes per lane). Protein lysates were prepared from GV-stage and MII-stage oocytes. Individual groups of MII oocytes were treated with UCHL1 inhibitor C16 or C30 or DMSO (vehicle solvent for inhibitors). A representative image from three independent experiments is shown.

All antibodies were diluted in 5% skim milk-TBS-T at 1:1000 dilution. UCHL1 was detected by mouse monoclonal antibody (58593; Santa Cruz Biochemicals) or by goat polyclonal antibody (5937; Chemicon). Antiubiquitin antibodies included mouse monoclonal antimionubiquitin (0508; Sigma), mouse antipolyubiquitin (K⁶³ linkage specific, PW0600; Biomol), and mouse antipolyubiquitin (58595; Santa Cruz Biochemicals). Washed membranes were incubated with appropriate horseradish peroxidase-conjugated secondary anti-IgG antibodies (1:10,000 dilution; Jackson ImmunoResearch) in 5% nonfat milk-TBS-T for 1 h at room temperature. Protein bands were visualized by an ECL-PLUS detection system (GE Healthcare) according to the manufacturer's instructions. All Western blot experiments described in *Results* were performed at least two times, and representative images are shown in the figures. Band intensities were measured using ImageJ software (National Institutes of Health). Data were normalized to the number of oocytes (equal number of oocytes per line in each sample). The control was considered 100%.

Immunocytochemistry

For immunofluorescence microscopy, denuded and ZP-free oocytes (dezoned in 0.25% pronase) were washed in PBS, fixed for 60 min at 4°C in 4% paraformaldehyde in PBS, and again washed in PBS. Oocytes were permeabilized with 1% Triton X-100 for 20 min, washed and blocked for 2 h in 2% BSA in PBS, and incubated with primary antibody overnight at 4°C. All primary and secondary antibodies were diluted in 0.2% BSA in PBS. Anti-UCHL1 antibody (5937; Chemicon) was used at 1:500 dilution; antiubiquitin antibodies were used as already described. Oocytes were incubated with appropriate secondary antibodies (Alexa Fluor 488 and 543; Invitrogen) for 60 min at room temperature. As a control, oocytes were incubated with secondary antibody only. *Lens culinaris* agglutinin (LCA rhodamine, 1042; Vector Laboratories) was used as a marker of CGs [37]. F-actin was stained with 1 mg/ml of Phalloidin-Alexa Fluor 568 (12380; Molecular Probes). Oocytes and zygotes were mounted in mounting medium with DAPI (Vectashield; Vector Laboratories). To prevent deformities, 100- μ m coverslip spacers (Zweckform) were used. Samples were examined under a Leica SP2 inverted confocal microscope equipped with an Acousto-Optical Beam Splitter (Leica Microsystems). Fluorescence intensities were measured using ImageJ software.

Statistical Analysis

Data were analyzed using SigmaStat 3.0 software (Jandel Scientific). *z*-Test was used for analysis of differences in proportions of characteristics of interest within groups. Student *t*-test or Mann-Whitney rank sum test was used for analysis of densitometric measurements. $P < 0.05$ was considered significant.

RESULTS

Protein Levels of UCHL1 Are Stable During Oocyte Maturation

An immunoblotting approach was used to detect expression of UCHL1 in bovine oocytes; the specific band of approximately 27 kDa (monomer form) was recognized and did not significantly change during oocyte maturation. We used two UCHL1-specific inhibitors, C16 and C30, to disrupt UCHL1 activity [30, 31]. Oocytes were treated with both inhibitors for 24 h at a concentration of 20 μ M. We observed no difference in UCHL1 (27-kDa form) expression levels between GV- and MII-stage oocytes or any differences between control oocytes and oocytes treated with specific UCHL1 inhibitors ($P > 0.05$) (Fig. 1). Meiotic progression was not impaired in the presence of UCHL1 inhibitors (data not shown).

In summary, we observed stable levels of the monomeric form of UCHL1 during oocyte maturation. Inhibition of hydrolytic activity of UCHL1 did not block meiotic progression of bovine oocytes.

Subcellular Localization of UCHL1 in Bovine Oocytes

To study localization of UCHL1 in bovine oocytes, we used two different approaches. We microinjected oocytes with in vitro-synthesized UCHL1 mRNA fused with EGFP (*EGFP-UCHL1*). This UCHL1 mRNA was based on the porcine UCHL1 sequence, which is highly homologous to the bovine sequence (98% amino acid sequence homology [see *Materials and Methods*]). Two different concentrations (125 or 250 ng/ μ l) of in vitro-synthesized mRNA were used. At 1 h after microinjection of 125 ng/ μ l of *EGFP-UCHL1* mRNA into GV-stage oocytes, the majority of EGFP signal was predominantly detected in cortical and subcortical regions (Fig. 2A). Low-level signal was visible throughout the cytoplasm and GV nucleoplasm (Fig. 2A). However, at the MII stage, EGFP-UCHL1 localized exclusively to the subcortical region (Fig. 2B). In contrast, oocytes injected with 250 ng/ μ l of *EGFP-UCHL1* mRNA were unable to progress beyond the MI stage of meiosis. EGFP-UCHL1 fluorescent signal in such mRNA-injected oocytes was detected in the oocyte cortex, subcortically, and in the perivitelline space (PVS). The differential interference contrast (DIC) images showed colocalization of this PVS signal with small droplets or vesicles (Fig. 2, E and F, arrows).

The specificity of localization of EGFP-UCHL1 was confirmed in control experiments using *EGFP* mRNA alone (125 or 250 ng/ μ l). EGFP signal was visible throughout the cytoplasm and was absent from the nucleus (Fig. 2, C and D).

These results were further confirmed by immunocytochemistry using specific anti-UCHL1 antibody (Fig. 3, A and B). Immunolocalization of UCHL1 agreed with EGFP-UCHL1 localization in microinjection experiments. The antibody labeled cortical and subcortical regions in GV-stage and MII-stage oocytes; in GV oocytes, fluorescent signal was also detected in the nucleus (Fig. 3A). Localization of native UCHL1 was unaffected in oocytes treated with C16 and C30 inhibitors (data not shown).

Inhibition of UCHL1 Causes Polyspermy During Bovine IVF

UCHL1 protein has been implicated in antipolyspermy defense in vitro in both mouse [27] and pig [28]. To explore the mechanistic basis for these observations, we studied the effects of downregulation of oocyte UCHL1 on bovine IVF. To investigate the role of UCHL1 during meiotic maturation of bovine oocytes, we treated oocytes with UCHL1-specific membrane-permeant inhibitors C16 and C30.

We did not use the RNA interference method, as UCHL1 expression is stable during oocyte maturation and its turnover is low (Supplemental Fig. S2). Because these inhibitors are highly specific [30, 31], we were able to use them at a relatively low concentration of 20 μ M. Higher concentration of UCHL1-specific inhibitors (100 μ M) did not block meiotic progression in bovine oocytes; however, 30% of MII-stage oocytes extruded all their chromosomes in the form of two PBs (Supplemental Fig. S3).

We then examined fertilization rates and occurrence of polyspermy after IVF in oocytes treated for the whole oocyte maturation period of 24 h with specific UCHL1 inhibitors (C16 and C30) and in control oocytes matured without inhibitors (with DMSO as a vehicle control). In the majority of zygotes

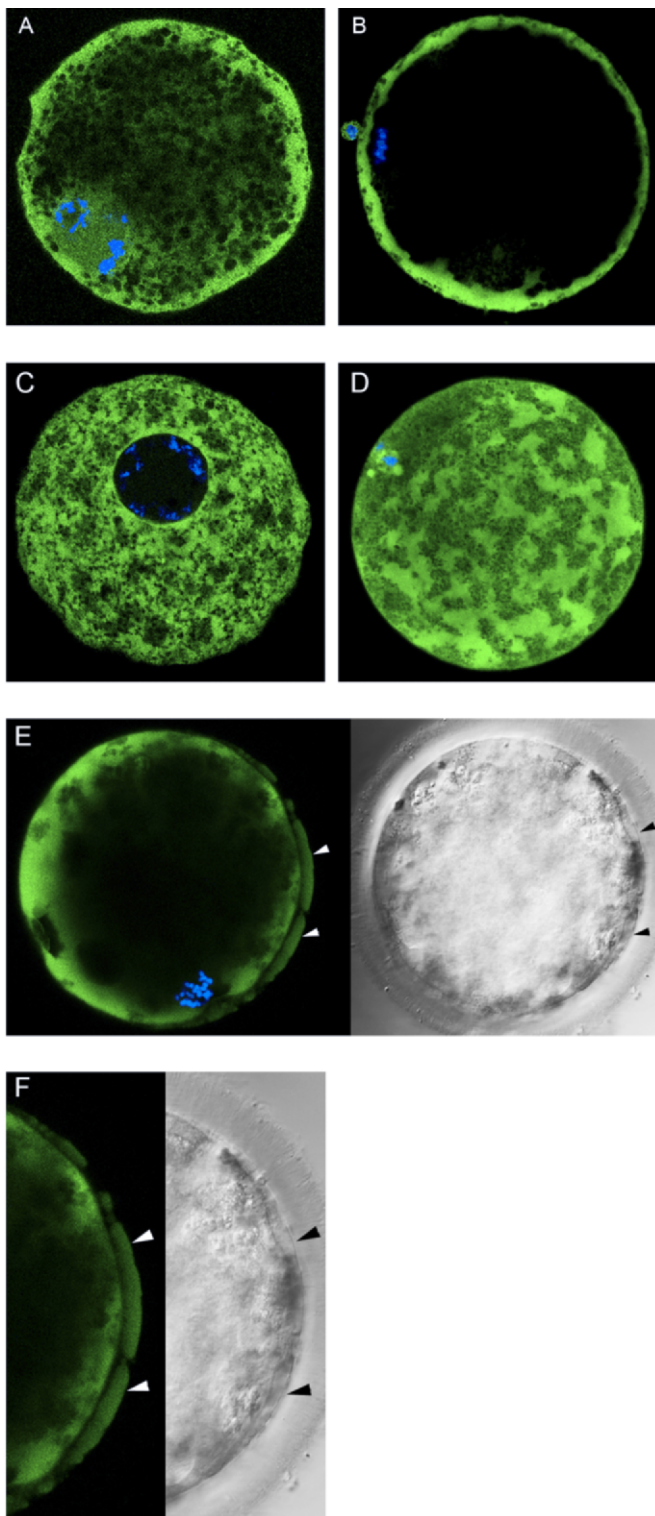


FIG. 2. Localization of GFP-tagged UCHL1 in bovine oocytes. **A–D**) Representative confocal images of bovine oocytes microinjected with 125 ng/ μ l of *UCHL1* mRNA. **A**) At 1 h after microinjection of mRNA, EGFP-UCHL1 protein is localized predominantly in the subcortical region, with low signal in the cytoplasm and some accumulation in the oocyte nucleus and GV (10 of 11 oocytes examined had the described phenotype). **B**) At 24 h after microinjection, oocytes reached MII, and EGFP-UCHL1 fluorescence was predominantly visible in the oocyte cortex (14 of 14 examined). **C**) As a negative control for EGFP-UCHL1, *EGFP* mRNA (125 ng/ μ l) was used, resulting in even distribution of EGFP throughout the ooplasm and complete exclusion from the nucleus at 1 h after microinjection (23 of 23 examined). **D**) Microinjected control oocytes with *EGFP* mRNA (125 ng/ μ l) at 24 h after microinjection (18 of 18

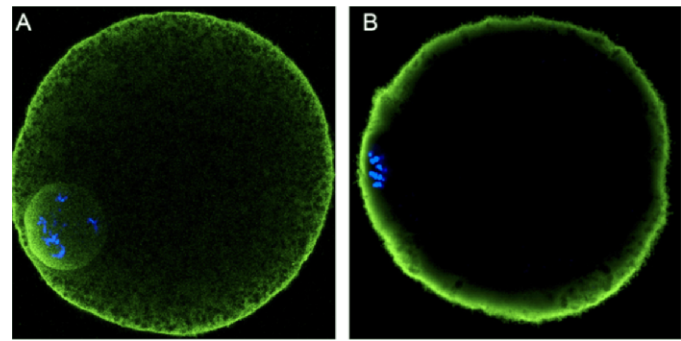


FIG. 3. Localization of native UCHL1. Polyclonal antibody against UCHL1 detects subcortical and nuclear accumulation of endogenous UCHL1 in a GV-stage oocyte (**A**) (22 of 22 examined) and an MII-stage oocyte (**B**) (19 of 19 examined). Green indicates UCHL1; blue, DAPI for DNA staining. Original magnification $\times 300$.

that originated from oocytes treated with UCHL1 inhibitors, more than two pronuclei were found at 20 h after IVF (60% in the C16-treated group and 66% in the C30-treated group) (Fig. 4 and Table 1). When oocytes were stained for chromatin or DNA, the predominant pattern was the presence of three pronuclei in inhibitor-treated oocytes, suggestive of dispermic fertilization. In contrast, only 10% of dispermic or polyspermic zygotes were detected in vehicle control (DMSO [$P < 0.001$]), while the overall fertilization rate was not significantly different between treatments. These results suggest that, although inhibition of UCHL1 through meiosis does not impair nuclear maturation, the efficiency of antipolyspermy defense is reduced; thus, UCHL1 activity during in vitro maturation of bovine oocytes affects the rate of sperm penetration or incorporation during fertilization of MII oocytes.

Because developmental competence of embryos is impaired in polyspermy [38], we examined developmental competence of UCHL1 inhibitor-treated oocytes. We performed parthenogenic activation of oocytes treated with C30 ($n = 59$) and DMSO ($n = 44$). No significant difference was found in developmental competence of parthenotes produced from oocytes cultivated in 20 μ M C30 compared with the control group ($P > 0.05$ for each developmental stage examined) (Fig. 5).

Failure of CG Translocation During Meiotic Maturation in UCHL1-Inhibited Oocytes

The foregoing results suggested that inhibition of UCHL1 aggravates polyspermy in vitro. We next sought to determine whether downregulation of UCHL1 function inhibits the landmark mechanism necessary for blocking polyspermy (i.e., CG maturation and CG extrusion or exocytosis). We focused on distribution changes of CGs in MII oocytes. In GV-stage oocytes, CGs form clusters; as oocytes progress through meiosis, CG clusters dissociate, and CGs invade the cortical region, forming a thin layer [37, 39]. We stained CGs with rhodamine-labeled LCA; for classification of CG distribution, we adopted the previously established terms of *oocyte-like*

← examined). **E**) Oocytes microinjected with 250 ng/ μ l of *EGFP-UCHL1* mRNA and arrested in MI; arrows indicate EGFP-UCHL1 fluorescence in the PVS. This fluorescence colocalizes with PVS membrane vesicles in the DIC image (10 of 10 examined). **F**) Detailed image of **E**. Green indicates EGFP-UCHL1 or EGFP; blue, DAPI used for DNA staining. Original magnification $\times 300$ (**A–E**) and $\times 350$ (**F**).

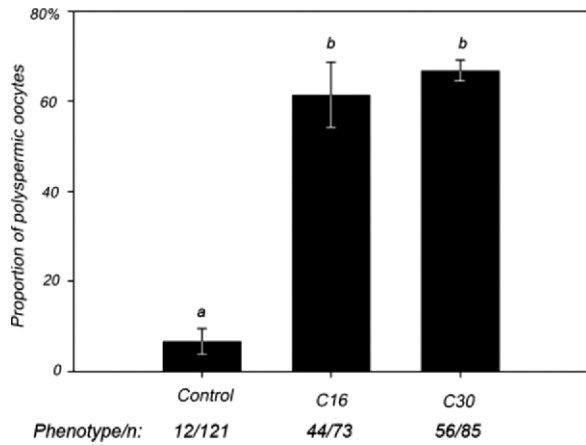


FIG. 4. Incidence of polyspermy in UCHL1 inhibitor-treated oocytes. Formation of supernumerary male pronuclei occurs in zygotes obtained by IVF of oocytes matured in the presence of UCHL1 inhibitor C16 or C30. Values from three independent replicates are shown. Different lowercase letters indicate statistical significance ($P < 0.001$).

pattern (typical of GV stage), *intermediate* pattern, and *egg-like* pattern (typical of MII stage) [37].

Migration of CGs was indeed altered in oocytes treated with UCHL1 inhibitors C16 and C30 (Fig. 6, C and D). A majority of MII oocytes or eggs treated with inhibitors during in vitro maturation displayed an oocyte-like CG localization pattern similar to that of GV-stage oocytes (Fig. 6A). Karyokinesis or meiotic progression was not altered (data not shown). In control groups treated with DMSO, CGs relocated uniformly to the cortical area of the oocyte, displaying an egg-like pattern at MII (Fig. 6B). Data on CG translocation are summarized in Figure 7 and Supplemental Table S1.

In GV-stage oocytes injected with 125 ng/μl of *EGFP-UCLH1* mRNA, redistribution of CGs was not impaired (Fig. 6E). At the 250 ng/μl concentration, *EGFP-UCLH1* mRNA blocked redistribution of CGs during oocyte maturation (Fig. 6F).

Inspired by these observations, we investigated if high polyspermy observed in inhibitor-treated zygotes coincided with impaired GC extrusion. Oocytes were matured in the presence of 20 μM C16 or C30, washed thoroughly, and fertilized using a standard IVF protocol without inhibitors. We observed high retention of CGs in inhibitor-matured zygotes (Fig. 8, B and C) but not in control zygotes at 20 h after fertilization (Fig. 8A). Data on CG extrusion are summarized in Figure 9 and Supplemental Table S2. Figure 10 shows the positive correlation between polyspermy ratio and CG extrusion at 20 h after IVF. Migration of CGs is a cytoskeleton-dependent process in which F-actin plays the major role [40, 41]. When we stained F-actin with Phalloidin-Alexa Fluor 568, we found greater abundance of transzonal projections (TZPs) in oocytes treated during in vitro maturation

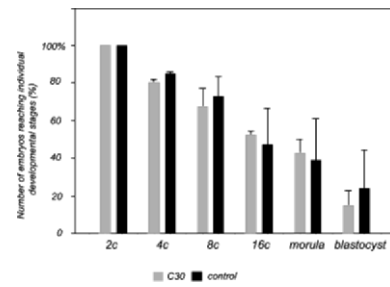


FIG. 5. Developmental competence of embryos after parthenogenetic activation. The numbers of embryos reaching individual developmental stages are shown on the y-axis. The number of 2-cell-stage (2c) embryos is considered 100%. The proportion of oocytes that do not develop beyond the 1-cell stage was not significantly different in C30-treated (38%) vs. control (34%) oocytes. Developmental competence was examined in two independent experiments; bars represent the mean ± SEM.

with C16 and C30 (Supplemental Fig. S4). The retraction or depolymerization of F-actin-rich TZPs is a hallmark of oocyte maturation, and their retention beyond the GV breakdown stage is indicative of cytoskeletal dysfunction.

Treatment of Oocytes with Specific UCHL1 Inhibitors Reduces Monoubiquitin Levels and Increases Protein Ubiquitination

UCHL1 maintains the cytoplasmic pool of unconjugated monoubiquitin by recycling polyubiquitin chains. Consequently, we monitored free monoubiquitin levels and polyubiquitin in oocytes treated with C30 and C16. The average free monoubiquitin level decreased by 50% to 70% compared with controls (Fig. 11B). Conversely, formation of polyubiquitin chains and ubiquitination of proteins were increased 4 to 5 times in MII-stage oocytes treated with inhibitors compared with GV-stage oocytes and DMSO-treated MII oocytes (Fig. 11A). Overexpression of UCHL1 in oocytes injected with 125 ng/μl of *EGFP-UCLH1* mRNA at the GV stage resulted in 2- to 4-fold increase of free ubiquitin (monoubiquitin) at 24 h after microinjection (Fig. 11C). In contrast, we detected no change in ubiquitination of proteins after microinjection (data not shown). Results were similar for both types of mRNA injected (*EGFP-UCLH1* and nontagged *UCHL1*) (Supplemental Fig. S1).

Taken together, these results demonstrate that UCHL1 promotes disassembly of polyubiquitin chains during meiotic maturation. Conversely, UCHL1 regulates formation of polyubiquitin chains in bovine oocytes.

Presumptive Oligomeric Forms of UCHL1 Increase in the Presence of UCHL1 Inhibitors

Increased formation of polyubiquitin chains and protein ubiquitination observed in the presence of UCHL1 inhibitors

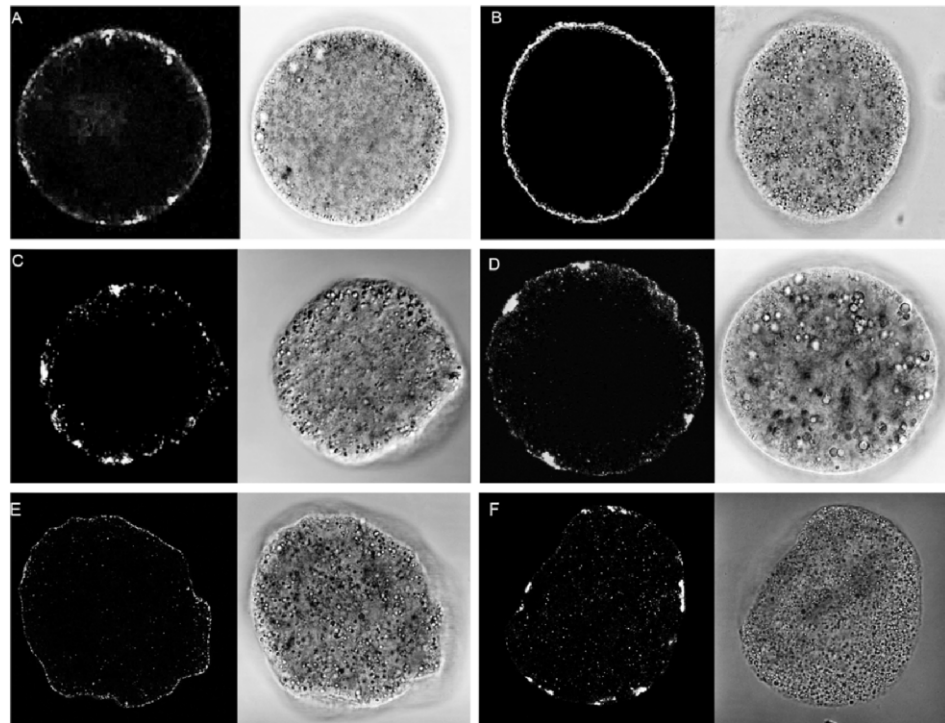
TABLE 1. Polyspermy incidence in one-cell bovine zygotes 20 h post IVF.*

Treatment	Fertilization status			Total n
	Normal fertilized (%)	Polyspermic (%)	Nonfertilized (%)	
DMSO (control)	96 (79) ^a	12 (10) ^a	13 (11) ^a	121
C16 (20 μM)	14 (19) ^b	44 (60) ^b	15 (21) ^a	73
C30 (20 μM)	17 (20) ^b	56 (66) ^b	12 (14) ^a	85

* Number of pronuclei was counted in zygotes obtained by IVF of oocytes matured in the presence of UCHL1 inhibitors; data are from three independent experiments.

^{a,b} Values with different superscript letters indicate statistical significance ($P < 0.001$).

FIG. 6. Downregulation of UCHL1 affects migration or cortical translocation of CGs during oocyte maturation. **A–D**) Representative confocal images show GV-stage oocytes fixed immediately after isolation (**A**). **B**) Normal cortical migration of CGs (egg like) in an MII oocyte treated with DMSO. **C and D**) The CG distribution pattern in oocytes cultured in the presence of UCHL1 inhibitor C16 or C30 is similar to that of GV-stage (oocyte like) oocytes. **E and F**) Egg-like CG status in oocytes microinjected with 125 ng/ μ l of *EGFP-UCHL1* mRNA (**E**) and oocyte-like CG distribution following treatment with 250 ng/ μ l of *EGFP-UCHL1* mRNA concentration (**F**). Images are representative of three independent replicates. A summary of CG distribution for all groups is given in Supplemental Table S1. Original magnification $\times 175$.



could account for increased ubiquitin ligase activity of dimeric and oligomeric forms of UCHL1 [15, 42]. By immunoblotting analysis, we identified several higher-mass UCHL1 bands at approximately 37 kDa (Supplemental Fig. S5) and in the range of 50–150 kDa (Fig. 12A). Expression of UCHL1 monomer did not change during meiotic maturation of bovine oocytes. Also, the 37-kDa UCHL1 band, presumably the monoubiquitinated form of UCHL1 [17], did not change significantly during oocyte maturation (Supplemental Fig. S5). However, the content of presumptive UCHL1 oligomers (75–150 kDa) increased 6-fold in oocytes treated with C16 or C30 inhibitors (Fig. 12A).

Treatment of control and inhibitor-exposed oocyte lysates with 40 mM DTT (disulfide bond-reducing agent) and 4 mM NEM (alkylating reagent) was used to determine whether the presumptive UCHL1 oligomers could be linked by disulfide bonds. In the presence of DTT, both 50- and 75-kDa UCHL1

species were visible (Fig. 12A), likely corresponding to the presumptive dimer and oligomer of UCHL1, respectively. Without DTT, UCHL1 bands were observed at 50, 75, 100, and 150 kDa (Fig. 12B). These masses could correspond to multimerization of 27-kDa UCHL1, forming dimers, tetramers, and hexamers. The lack of presumptive oligomers within the range of 100–150 kDa in the presence of DTT strengthens the hypothesis that presumptive oligomers are cross-linked by disulfide bonds. In contrast, 50- and 75-kDa oligomers were not sensitive to DTT treatment. Finally, data shown in Figure 12 suggest increased formation of presumptive UCHL1 oligomers in the presence of inhibitors C16 and C30 during the *in vitro* maturation period.

Inhibition of UCHL1 Increases Formation of K63-Linked Multiubiquitin Chains

Polyubiquitin chains are linked through the C-terminal G76 residue of one ubiquitin molecule bound covalently to one of seven internal lysine residues (K6, K11, K27, K29, K33, K48, or K63) of another ubiquitin molecule [43–46]. In most cases, all molecules within an isopeptide polyubiquitin chain are linked at the same internal lysine position. Consequently, polyubiquitin chains can be distinguished based on the internal linkage site (e.g., K48 or K63 chains). In dimeric or oligomeric form, UCHL1 functions as a ubiquitin ligase that promotes formation of K63-linked polyubiquitin chains [15, 47]. To determine if this is the case in bovine oocytes, we performed immunocytochemical analysis of matured oocytes with mouse monoclonal antibody specific to K63-linked polyubiquitin chains. We found increased fluorescent signal in the cytoplasm for K63-linked ubiquitin antibody in oocytes treated with UCHL1 inhibitor C30 (Fig. 13B) compared with control oocytes treated with DMSO (Fig. 13A). Densitometric evaluation of these oocyte groups clearly showed higher fluorescence intensity (6.96 and 6.19, respectively) in C16- and C30-treated oocytes compared with 0.56 in the control group. These data support our hypothesis that inhibition of hydrolase

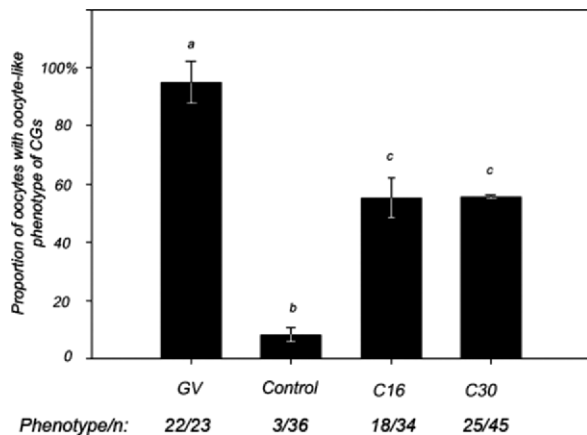


FIG. 7. Proportion of oocytes with the oocyte-like pattern of CG distribution in control and UCHL1 inhibitor-treated groups. Bars represent the mean \pm SEM. Values from three independent experiments are given. Different lowercase letters indicate statistical significance ($P < 0.001$).

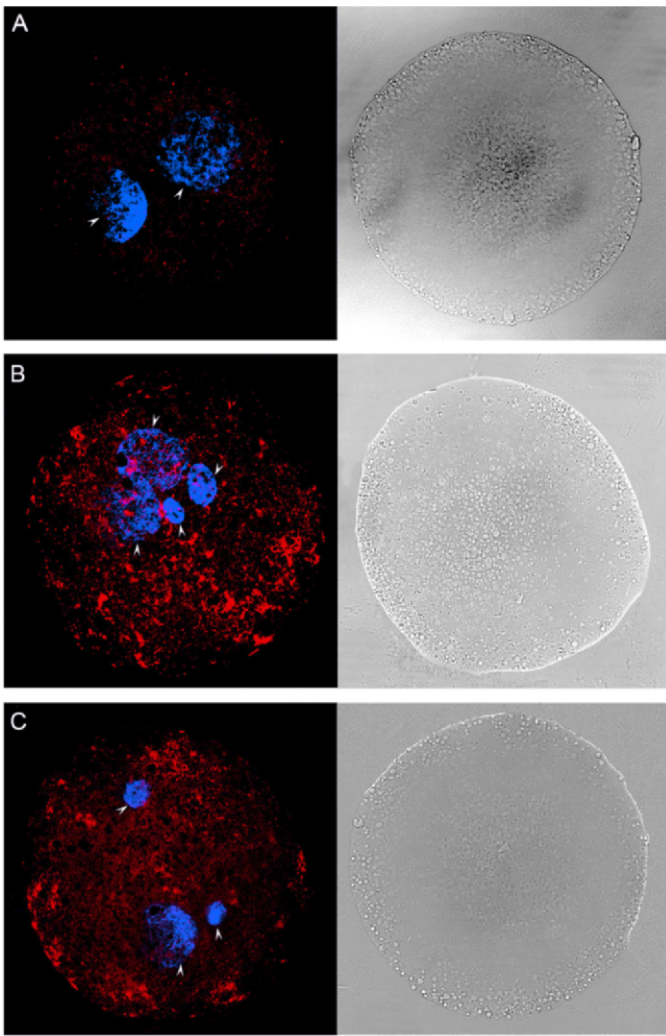


FIG. 8. Exocytosis of CGs in zygotes obtained by IVF of oocytes matured with UCHL1 inhibitor C16 or C30. Confocal images of zygotes at 20 h after IVF were acquired with identical settings for all treatments. **A)** Low fluorescence intensity of the LCA-rhodamine conjugate in a 1-cell zygote raised from oocytes matured in the presence of DMSO vehicle. **B and C)** Zygotes developed from oocytes matured with UCHL1 inhibitor C16 and C30, respectively. Images are representative of three independent experiments. The CG status in 1-cell zygotes for all groups is summarized in Supplemental Table S2. Original magnification $\times 230$.

activity of UCHL1 stimulates ligase activity of this enzyme in bovine oocytes, resulting in increased protein stabilization or modification through K63-linked polyubiquitination.

DISCUSSION

UCHL1 is one of the most abundant proteins in mammalian oocytes [7, 48]. In the present study, we demonstrate that UCHL1 is involved in regulation of the fertilization process in bovine oocytes, most likely by controlling migration of CGs to the oocyte cortex during oocyte maturation. Such observations are consistent with the aforescribed cortical and subcortical localization of UCHL1.

Treatment with specific inhibitors of UCHL1 activity leads to altered CG translocation during oocyte maturation and to increased polyspermy during bovine IVF. Our data show significant differences in polyspermy rates among oocytes in which UCHL1 was inhibited during in vitro maturation. Similar results were obtained using two inhibitors with

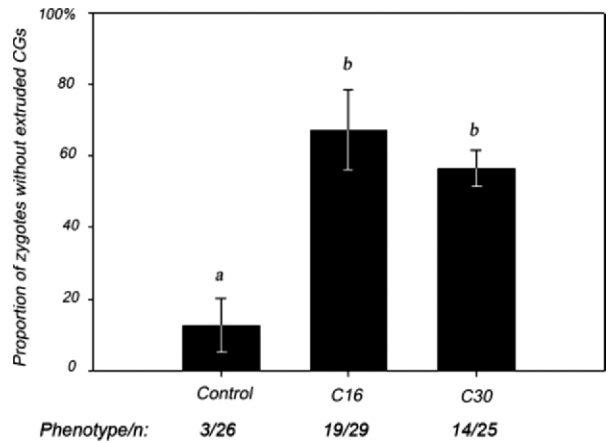


FIG. 9. Absence of CG exocytosis in 1-cell zygotes obtained by IVF of oocytes matured with UCHL1 inhibitor C16 or C30. Oocytes were vehicle treated (DMSO) or exposed to 20 μ M C16 or C30 for 24 h. Bars represent the mean \pm SEM. Values are from three independent experiments. Different lowercase letters indicate statistical significance ($P < 0.001$). The CG status in 1-cell zygotes for all groups is summarized in Supplemental Table S2.

different mechanisms of action, proving specific inhibition of UCHL1. Moreover, developmental competence was unaffected in parthenogenetic embryos that originated from inhibitor-treated oocytes. The higher rate of oocyte penetration by spermatozoa in such treated oocytes is in agreement with results from IVF of *gad* mice [27]. In *gad* mice, the modified *gad* allele encodes a truncated UCHL1 protein lacking a 42-amino acid segment containing a catalytic residue [13]. The *gad* mice have reduced fertility, with fewer pups per litter [27, 49]. High polyspermy was also reported by Yi et al. [28] in porcine oocytes fertilized in the presence of ubiquitin aldehyde, a specific nonpermeant inhibitor of UCH family enzymes.

Using immunocytochemical staining, we showed subcortical localization of native UCHL1 in bovine oocytes during maturation. Similar results were obtained when *EGFP-UCHL1* mRNA was expressed in oocytes. Cortical or subcortical localization of this protein was previously described in mouse and pig [27, 28]. In neural cells, two forms of UCHL1 are known, a soluble form and a membrane-anchored form, the

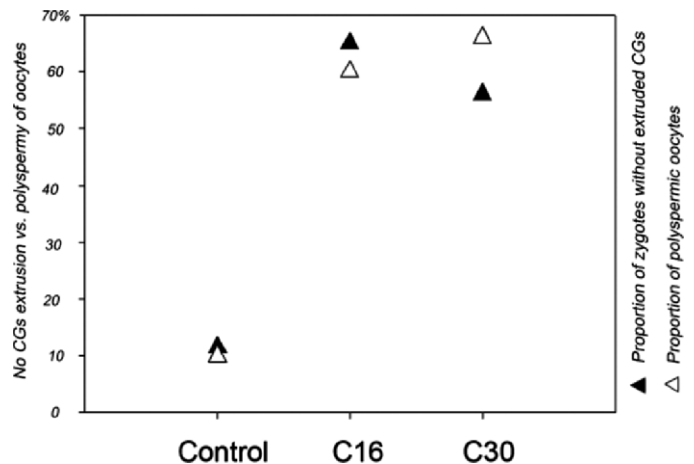


FIG. 10. Coincidence of polyspermy and failed CG extrusion in bovine zygotes treated with inhibitors of UCHL1. Analysis of data was obtained from experiments monitoring the number of oocyte-incorporated spermatozoa (see Fig. 4) and CG exocytosis at 20 h after IVF (see Fig. 8). Coefficient of determination $R^2 = 0.9275$.

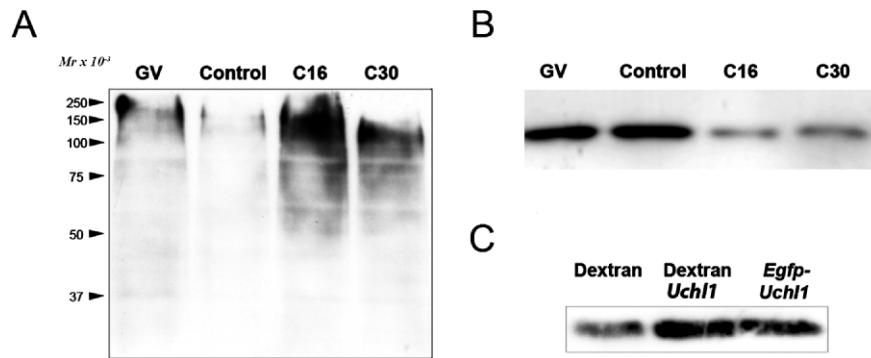


FIG. 11. Monoubiquitin and polyubiquitin levels in oocytes treated with UCHL1 inhibitors and after overexpression of UCHL1. UCHL1 was inhibited using 20 μ M C16 or C30 during the in vitro maturation period (24 h). Control oocytes were cultured with inhibitor vehicle or solvent (DMSO) for the same period. **A**) In the presence of C16 or C30, chemiluminescence signal for ubiquitin is detected at a higher molecular mass in immunoblots; image is representative of two independent replicates. **B**) The monoubiquitin pool is decreased in C16- or C30-treated MII oocytes compared with control MII- and GV-stage oocytes; image is representative of three independent replicates. **C**) Microinjection of 125 ng/ μ l of *UCHL1* or *EGFP-UCHL1* mRNA increased the monoubiquitin pool in injected oocytes compared with control oocytes microinjected with dextran; image is representative of two independent replicates.

latter being farnesylated [18]. Farnesylation is a consensus signal for protein anchoring to a membrane. Previously, we reported three different isoforms of monomeric UCHL1 using two-dimensional gel electrophoresis [7]. These data suggest that oocytes carry posttranslationally modified UCHL1 forms that could coincide with differential localization of UCHL1 in the oocyte, including nuclear, subcortical, and membrane-bound forms. We detected fluorescent signal in the nucleus of GV-stage oocytes (Figs. 2A and 3A), which suggests that indigenous UCHL1 may also have an intranuclear function, as observed in somatic cells [50].

Differential localization of UCHL1 might regulate distinct pools of ubiquitin in an oocyte. Metaphase-anaphase transition during meiosis and mitosis depends on ubiquitination and proteasomal degradation of cyclin B, brought about by the ubiquitin ligase within the anaphase-promoting complex (APC) [51, 52]. Successful nuclear progression through meiosis in bovine oocytes treated with C16 and C30 inhibitors may be explained by the fact that the monoubiquitin pool, which is required for APC activity, is probably not completely depleted in the inhibitor-treated oocytes. Accordingly, meiotic progres-

sion is not impaired in the *gad* mouse [27]. Furthermore, other UCH family members present in the ooplasm (such as UCHL3) could compensate for the shortage of UCHL1 activity in both cases. Inhibition of UCHL1 in GV-stage pig oocytes seems to have a more dramatic effect compared with that in bovine oocytes; it leads to only a slight decrease in free ubiquitin but causes an early meiotic arrest at the MI stage [7]. Greater sensitivity of porcine oocytes to inhibition of UCHL1 could explain this observation.

Our experiments clearly show that UCHL1 is the mediator of monoubiquitin regeneration in oocytes. Overexpression of UCHL1 by mRNA microinjection significantly increased the ooplasmic monoubiquitin pool (Fig. 11C); however, no changes in polyubiquitination of proteins were seen in injected oocytes, as was also the case in inhibitor-treated oocytes (data not shown). Although the lower concentration of exogenous *UCHL1* mRNA did not have an effect on meiosis, 2-fold overexpression of UCHL1 impaired nuclear and cytoplasmic oocyte maturation. Impaired redistribution of CGs in these oocytes clearly shows that high expression of UCHL1 led oocytes to meiotic incompetence. Nuclear and cytoplasmic maturation are interconnected events [53]. Furthermore, a 2-fold increase in the concentration of microinjected mRNA led to inhibition of meiosis at the MI stage and coincided with the presence of UCHL1-containing vesicles in the PVS (Fig. 2, E and F). This might suggest that massive overexpression of

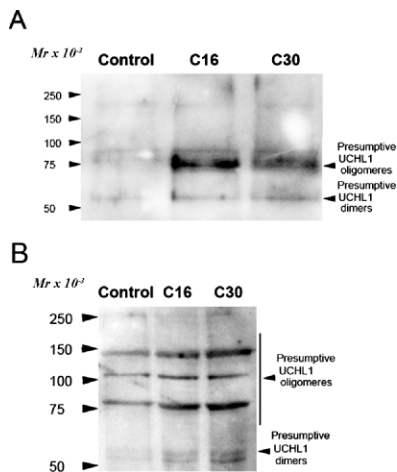


FIG. 12. Formation of presumptive UCHL1 oligomers in the presence of UCHL1 inhibitor C16 or C30. **A**) UCHL1 oligomers migrate predominantly at the 75-kDa level in the presence of the disulfide bond-reducing agent DTT. **B**) UCHL1 oligomers migrate at higher molecular mass when DTT is omitted from the oocyte lysis buffer. Images representative of two independent experiments are shown.

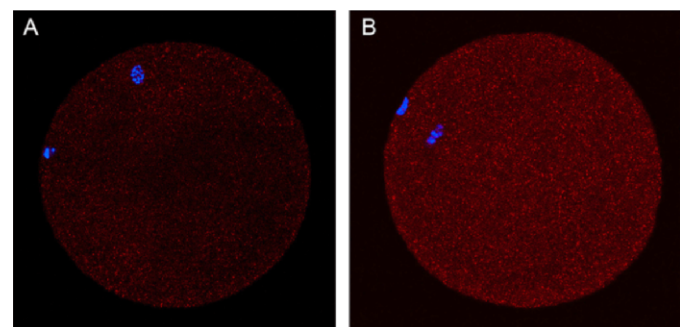


FIG. 13. Inhibition of UCHL1 stimulates formation of K63-linked polyubiquitin chains. **A**) Oocytes treated with DMSO only (0 of 10 examined). **B**) Immunocytochemical analysis shows higher fluorescence intensity of K63-linked ubiquitin chains in oocytes matured for 24 h in the presence of UCHL1 inhibitor (9 of 12 examined). Images were recorded with identical acquisition settings. Original magnification \times 300.

UCHL1 can cause cell damage or even cell death, as reported in primary spermatocytes in transgenic mice overexpressing UCHL1 in testes [22] and in breast cancer cells [54]. Alternatively, UCHL1 could be responsible for stabilization of the oocyte plasma membrane.

Immunoblots showed increased formation of putative UCHL1 oligomers in oocytes treated with C16 or C30. Liu et al. [15] demonstrated that UCHL1 has two separate enzymatic functions; in the monomeric form, it has weak hydrolytic activity toward polyubiquitin chains, whereas in the oligomeric state it functions as a ubiquitin ligase that stabilizes proteins through K63-linked polyubiquitination [42]. This dual enzymatic function could explain regulation of ubiquitin levels in oocytes, whereby specific UCHL1 inhibitors reduce the monoubiquitin pool, leading to increased content of polyubiquitin chains and ubiquitinated proteins. Using immunocytochemistry, we demonstrated increased K63-linked polyubiquitination in UCHL1 inhibitor-treated oocytes, which is known to stabilize proteins [55]. Based on these results, we hypothesize that increased K63-linked polyubiquitination may lead to impaired reorganization of cortical cytoskeleton and consequently to altered migration of CGs.

Our data suggest that activity of the ubiquitin-proteasome pathway, altered by a reduced monoubiquitin pool and by increased ubiquitination of proteins in oocytes with downregulated UCHL1, was responsible for high polyspermy rates in bovine zygotes. Mechanisms controlling sperm-oocyte interactions during fertilization are ubiquitin-proteasome dependent [56–59]. Exocytosis of CGs in mammalian oocytes is required to produce ZP-associated blocking of polyspermy [26, 60], which is one of the most important factors affecting embryonic developmental competence [61]. It has been observed that CGs migrate to the periphery of the oocyte during maturation [37, 39]. The oocyte maturation-associated generation of CG asymmetry and the clustering of CGs in the oocyte cortex correlate with acquisition of exocytotic competence (i.e., the ability of CGs to undergo exocytosis in response to increased intracellular calcium concentration induced by the fertilizing spermatozoon) [62]. Inhibition of UCHL1 impairs cytoplasmic maturation by altering migration of CGs, which occurs during oocyte progression through meiosis [37]. Migration of CGs relies on oocyte microfilament cytoskeleton [40, 41]. While CGs in control oocytes migrated to the cortex, CGs in oocytes treated with UCHL1 inhibitors remained in the position similar to that of GV-stage oocytes; thus, CG exocytosis was impaired in the inhibitor-treated oocytes (following IVF). We rarely observed CG exocytosis at 20 h after IVF in 1-cell zygotes that were treated with C16 or C30 during oocyte maturation, which further supports the proposed relationship between CG distribution and exocytosis. Therefore, high polyspermy rates in IVF zygotes originating from inhibitor-treated oocytes are likely due to insufficient polyspermy blocking.

Very little is known about the role that ubiquitin and proteasomes play in cytoskeletal dynamics. Most evidence is from somatic cells. Csizmadia et al. [63] reported that the proteasome inhibitor EPI (experimental proteasome inhibitor) induced reorganization and relocation of nonubiquitinated actin microfilaments and microtubules. Ubiquitination of the Lys118 residue of actin imparts one or more conformations that may be involved in regulation of muscle contractile activity [64]. Porcine COCs treated with proteasomal inhibitor MG132 had substantially increased total G- and F-actin, and this treatment inhibited the microfilament-driven process of cumulus expansion [65]. Downregulation of UCHL1 in podocytes altered podocyte morphology and localization of the F-actin component α -actinin-4 [66]. Similarly, we showed that F-actin

containing TZPs, normally disappearing early during oocyte maturation, was much more abundant in oocytes when UCHL1 was inhibited; this suggests that TZPs and their depolymerization may affect CG migration or at the very least are reflective of microfilament dynamics in the maturing oocyte cortex. It has also been reported that downregulation of UCHL1 induces changes in somatic cell morphology that might be driven by cytoskeletal dynamics [30]. The DUB CYK-3 (*Caenorhabditis elegans* UCH, an orthologue of mammalian USP32) has specificity for cleaving ubiquitin from linear fusion proteins. In CYK-3-deficient *C. elegans* zygotes, actin-dependent events are hindered [67]. Those zygotes fail to undergo first embryonic cleavage; however, they form an F-actin ring at the presumptive cleavage site. Notably, we observed extrusion of the entire oocyte DNA content in the form of two PBs in oocytes treated with 100 μ M C30 for 24 h. Mtango et al. [68] observed anomalous second PB extrusion in mouse oocytes injected with the UCH inhibitor ubiquitin aldehyde. Azoury et al. [69] suggested that the PB extrusion phenotype is dependent on actin filaments, which is in agreement with our results showing that UCHL1 is involved in cytoskeleton-driven CG reorganization.

Our results suggest that impaired function of UCHL1 correlates with failure of CG migration to the oocyte cortex and thus leads to insufficient antipolyspermy defense. Therefore, polyspermy observed in bovine oocytes treated with UCHL1 inhibitors, or in those oocytes that overexpressed UCHL1, is likely due to insufficient ZP-mediated polyspermy blocking in response to the lack of CG exocytosis after IVF, which is presumably induced by enhanced ligase activity of UCHL1. It is unclear how the ubiquitin-proteasome pathway is involved in regulation of cytoskeletal dynamics, which controls redistribution of CGs. Further study of UCHL1 ubiquitination may provide clues to physiological functions of this enzyme in cytoskeleton and broaden our understanding of CG dynamics. Overall, the finding that UCHL1 indirectly regulates CG redistribution during meiotic maturation of mammalian oocytes leads us to hypothesize that abnormal distribution of CGs causes high polyspermy rates under in vitro conditions. Further analysis of how UCHL1 and the ubiquitin-proteasome pathway in general promote redistribution of CGs during meiosis will be fertile ground for future studies.

ACKNOWLEDGMENTS

The authors are indebted to Dr. Hana Kovarova for helpful comments about the manuscript; to Patricia Jandurova, Lenka Travnickova, and Stepan Hladky for technical assistance; and to Ms. Kathy Craighead for manuscript editing. C16 and C30 inhibitors for this study were kindly provided by Dr. Gregory D. Cuny, Harvard Center for Neurodegeneration and Repair, Brigham & Women's Hospital and Harvard Medical School, Boston, MA. The pCMVFL3 vector with cDNA clone was kindly provided by Professor Hirohide Uenishi, National Institute of Agrobiological Sciences, Tsukuba, Japan.

REFERENCES

1. Etlinger JD, Gu M, Li X, Weitman D, Rieder RF. Protease/inhibitor mechanisms involved in ATP-dependent proteolysis. *Revis Biol Celular* 1989; 20:197–216.
2. Muller S, Schwartz LM. Ubiquitin in homeostasis, development and disease. *Bioessays* 1995; 17:677–684.
3. Sutovsky P. Ubiquitin-dependent proteolysis in mammalian spermatogenesis, fertilization, and sperm quality control: killing three birds with one stone. *Microsc Res Tech* 2003; 61:88–102.
4. Kaiser P, Huang L. Global approaches to understanding ubiquitination. *Genome Biol* 2005; 6:e233.
5. Hershko A, Ciechanover A, Varshavsky A. Basic Medical Research Award: the ubiquitin system. *Nat Med* 2000; 6:1073–1081.

6. Chung CH, Baek SH. Deubiquitinating enzymes: their diversity and emerging roles. *Biochem Biophys Res Commun* 1999; 266:633–640.
7. Susor A, Ellederova Z, Jelinkova L, Halada P, Kavan D, Kubelka M, Kovarova H. Proteomic analysis of porcine oocytes during in vitro maturation reveals essential role for the ubiquitin C-terminal hydrolase-L1. *Reproduction* 2007; 134:559–568.
8. Gong B, Leznik E. The role of ubiquitin C-terminal hydrolase L1 in neurodegenerative disorders. *Drug News Perspect* 2007; 20:365–370.
9. Kwon J, Wang YL, Setsuie R, Sekiguchi S, Sakurai M, Sato Y, Lee WW, Ishii Y, Kyuwa S, Noda M, Wada K, Yoshikawa Y. Developmental regulation of ubiquitin C-terminal hydrolase isozyme expression during spermatogenesis in mice. *Biol Reprod* 2004; 71:515–521.
10. Hibi K, Liu Q, Beaudry GA, Madden SL, Westra WH, Wehage SL, Yang SC, Heitmiller RF, Bertelsen AH, Sidransky D, Jen J. Serial analysis of gene expression in non-small cell lung cancer. *Cancer Res* 1998; 58:5690–5694.
11. Sasaki H, Yukiue H, Moriyama S, Kobayashi Y, Nakashima Y, Kaji M, Fukai I, Kiriyaama M, Yamakawa Y, Fujii Y. Expression of the protein gene product 9.5, PGP9.5, is correlated with T-status in non-small cell lung cancer. *Jpn J Clin Oncol* 2001; 31:532–535.
12. Yamazaki T, Hibi K, Takase T, Tezel E, Nakayama H, Kasai Y, Ito K, Akiyama S, Nagasaka T, Nakao A. PGP9.5 as a marker for invasive colorectal cancer. *Clin Cancer Res* 2002; 8:192–195.
13. Larsen CN, Price JS, Wilkinson KD. Substrate binding and catalysis by ubiquitin C-terminal hydrolases: identification of two active site residues. *Biochemistry* 1996; 35:6735–6744.
14. Larsen CN, Krantz BA, Wilkinson KD. Substrate specificity of deubiquitinating enzymes: ubiquitin C-terminal hydrolases. *Biochemistry* 1998; 37:3358–3368.
15. Liu Y, Fallon L, Lashuel HA, Liu Z, Lansbury PT Jr. The UCH-L1 gene encodes two opposing enzymatic activities that affect α -synuclein degradation and Parkinson's disease susceptibility. *Cell* 2002; 111:209–218.
16. Das C, Hoang QQ, Kreinbring CA, Luchansky SJ, Meray RK, Ray SS, Lansbury PT, Ringe D, Petsko GA. Structural basis for conformational plasticity of the Parkinson's disease-associated ubiquitin hydrolase UCHL1. *Proc Natl Acad Sci U S A* 2006; 103:4675–4680.
17. Meray RK, Lansbury PT Jr. Reversible monoubiquitination regulates the Parkinson disease-associated ubiquitin hydrolase UCH-L1. *J Biol Chem* 2007; 282:10567–10575.
18. Liu Z, Meray RK, Grammatopoulos TN, Fredenburg RA, Cookson MR, Liu Y, Logan T, Lansbury PT Jr. Membrane-associated farnesylated UCH-L1 promotes alpha-synuclein neurotoxicity and is a therapeutic target for Parkinson's disease. *Proc Natl Acad Sci U S A* 2009; 106:4635–4640.
19. Yu J, Tao Q, Cheung KF, Jin H, Poon FF, Wang X, Li H, Cheng YY, Röcken C, Ebert MP, Chan AT, Sung JJ. Epigenetic identification of ubiquitin carboxyl-terminal hydrolase L1 as a functional tumor suppressor and biomarker for hepatocellular carcinoma and other digestive tumors. *Hepatology* 2008; 48:508–518.
20. Saigoh K, Wang YL, Suh JG, Yamanishi T, Sakai Y, Kiyosawa H, Harada T, Ichihara N, Wakana S, Kikuchi T, Wada K. Intragenic deletion in the gene encoding ubiquitin carboxy-terminal hydrolase in gad mice. *Nat Genet* 1999; 23:47–51.
21. Kwon J, Mochida K, Wang YL, Sekiguchi S, Sankai T, Aoki S, Ogura A, Yoshikawa Y, Wada K. Ubiquitin C-terminal hydrolase L-1 is essential for the early apoptotic wave of germinal cells and for sperm quality control during spermatogenesis. *Biol Reprod* 2005; 73:29–35.
22. Wang YL, Liu W, Sun YJ, Kwon J, Setsuie R, Osaka H, Noda M, Aoki S, Yoshikawa Y, Wada K. Overexpression of ubiquitin carboxyl-terminal hydrolase L1 arrests spermatogenesis in transgenic mice. *Mol Reprod Dev* 2006; 73:40–49.
23. Kwon J, Wang YL, Setsuie R, Sekiguchi S, Sato Y, Sakurai M, Noda M, Aoki S, Yoshikawa Y, Wada K. Two closely related ubiquitin C-terminal hydrolase isozymes function as reciprocal modulators of germ cell apoptosis in cryptorchid testis. *Am J Pathol* 2004; 165:1367–1374.
24. Hunter RH. Sperm-egg interactions in the pig: monospermy, extensive polyspermy, and the formation of chromatin aggregates. *J Anat* 1976; 122:43–59.
25. Hunter RH. Oviduct function in pigs, with particular reference to the pathological condition of polyspermy. *Mol Reprod Dev* 1991; 29:385–391.
26. Ducibella T. The cortical reaction and development of activation competence in mammalian oocytes. *Hum Reprod Update* 1996; 2:29–42.
27. Sekiguchi S, Kwon J, Yoshida E, Hamasaki H, Ichinose S, Hideshima M, Kuraoka M, Takahashi A, Ishii Y, Kyuwa S, Wada K, Yoshikawa Y. Localization of ubiquitin C-terminal hydrolase L1 in mouse ova and its function in the plasma membrane to block polyspermy. *Am J Pathol* 2006; 169:1722–1729.
28. Yi YJ, Manandhar G, Sutovsky M, Li R, Jonáková V, Oko R, Park CS, Prather RS, Sutovsky P. Ubiquitin C-terminal hydrolase-activity is involved in sperm acrosomal function and anti-polyspermy defense during porcine fertilization. *Biol Reprod* 2007; 77:780–793.
29. Pavlok A, Lapathitis G, Cech S, Kubelka M, Lopatárová M, Holý L, Klíma J, Motlík J, Havlíček V. Simulation of intrafollicular conditions prevents GVBD in bovine oocytes: a better alternative to affect their developmental capacity after two-step culture. *Mol Reprod Dev* 2005; 71:197–208.
30. Liu Y, Lashuel HA, Choi S, Xing X, Case A, Ni J, Yeh LA, Cuny GD, Stein RL, Lansbury PT Jr. Discovery of inhibitors that elucidate the role of UCH-L1 activity in the H1299 lung cancer cell line. *Chem Biol* 2003; 10:837–846.
31. Mermerian AH, Case A, Stein RL, Cuny GD. Structure-activity relationship, kinetic mechanism, and selectivity for a new class of ubiquitin C-terminal hydrolase-L1 (UCH-L1) inhibitors. *Bioorg Med Chem Lett* 2007; 17:3729–3732.
32. Pavlok A, Lucas-Hahn A, Niemann H. Fertilization and developmental competence of bovine oocytes derived from different categories of antral follicles. *Mol Reprod Dev* 1992; 31:63–67.
33. Susko-Parrish JL, Leibfried-Rutledge ML, Northey DL, Schutzkus V, First NL. Inhibition of protein kinases after an induced calcium transient causes transition of bovine oocytes to embryonic cycles without meiotic completion. *Dev Biol* 1994; 166:729–739.
34. McGuinness BE, Anger M, Kouznetsova A, Gil-Bernabé AM, Helmhart W, Kudo NR, Wuensche A, Taylor S, Hoog C, Novak B, Nasmyth K. Regulation of APC/C activity in oocytes by a Bub1-dependent spindle assembly checkpoint. *Curr Biol* 2009; 19:369–380.
35. Carleton M, Brown DT. The formation of intramolecular disulfide bridges is required for induction of the Sindbis virus mutant ts23 phenotype. *J Virol* 1997; 71:7696–7703.
36. Opstelten DJ, Wallin M, Garoff H. Moloney murine leukemia virus envelope protein subunits, gp70 and Pr15E, form a stable disulfide linked complex. *J Virol* 1998; 72:6537–6545.
37. Connors A, Kanatsu-Shinohara M, Schultz RM, Kopf RS. Involvement of the cytoskeleton in the movement of cortical granules during oocyte maturation, and cortical granule anchoring in mouse eggs. *Dev Biol* 1998; 200:103–115.
38. Santos P, Chaveiro A, Simões N, Moreira da Silva F. Bovine oocyte quality in relation to ultrastructural characteristics of zona pellucida, polyspermic penetration and developmental competence. *Reprod Domest Anim* 2008; 43:685–689.
39. Wang WH, Sun QY, Hosoe M, Shioya Y, Day BN. Quantified analysis of cortical granule distribution and exocytosis of porcine oocytes during meiotic maturation and activation. *Biol Reprod* 1997; 56:1376–1382.
40. Sun QY, Lai L, Park KW, Kühholzer B, Prather RS, Schatten H. Dynamic events are differently mediated by microfilaments, microtubules, and mitogen-activated protein kinase during porcine oocyte maturation and fertilization in vitro. *Biol Reprod* 2001; 64:879–889.
41. Sun QY, Schatten H. Regulation of dynamic events by microfilaments during oocyte maturation and fertilization. *Reproduction* 2006; 31:193–205.
42. Doss-Pepe EW, Chen L, Madura K. Alpha-synuclein and parkin contribute to the assembly of ubiquitin lysine 63-linked multiubiquitin chains. *J Biol Chem* 2005; 280:16619–16624.
43. Johnson ES, Ma PC, Ota IM, Varshavsky A. A proteolytic pathway that recognizes ubiquitin as a degradation signal. *J Biol Chem* 1995; 270:17442–17456.
44. Hershko A, Ciechanover A. The ubiquitin system. *Annu Rev Biochem* 1998; 67:425–479.
45. Peng J, Schwartz D, Elias JE, Thoreen CC, Cheng D, Marsischky G, Roelofs J, Finley D, Gygi SP. A proteomics approach to understanding protein ubiquitination. *Nat Biotechnol* 2003; 21:921–926.
46. Kim HT, Kim KP, Lledias F, Kisselev AF, Scaglione KM, Skowrya D, Gygi SP, Goldberg AL. Certain pairs of ubiquitin-conjugating enzymes (E2s) and ubiquitin-protein ligases (E3s) synthesize nondegradable forked ubiquitin chains containing all possible isopeptide linkages. *J Biol Chem* 2007; 282:17375–17386.
47. Setsuie R, Wada K. The functions of UCH-L1 and its relation to neurodegenerative diseases. *Neurochem Int* 2007; 51:105–111.
48. Massicotte L, Coenen K, Mourof M, Sirard MA. Maternal housekeeping proteins translated during bovine oocyte maturation and early embryo development. *Proteomics* 2006; 6:3811–3820.
49. Yamazaki K, Wakasugi N, Sakakibara A, Tomita T. Reduced fertility in fragile axonal dystrophy (gad) mice. *Jikken Dobutsu* 1988; 37:195–199.

50. Caballero OL, Resto V, Patturajan M, Meerzaman D, Guo MZ, Engles J, Yochem R, Ratovitski E, Sidransky D, Jen J. Interaction and colocalization of PGP9.5 with JAB1 and p27(Kip1). *Oncogene* 2002; 21:3003–3010.
51. Hershko A. Mechanisms and regulation of the degradation of cyclin B. *Philos Trans R Soc Lond B Biol Sci* 1999; 354:1571–1576.
52. Morgan DO. Regulation of the APC and the exit from mitosis. *Nat Cell Biol* 1999; 2:47–53.
53. Ferreira EM, Vireque AA, Adona PR, Meirelles FV, Ferriani RA, Navarro PA. Cytoplasmic maturation of bovine oocytes: structural and biochemical modifications and acquisition of developmental competence. *Theriogenology* 2009; 71:836–848.
54. Wang WJ, Li QQ, Xu JD, Cao XX, Li HX, Tang F, Chen Q, Yang JM, Xu ZD, Liu XP. Over-expression of ubiquitin carboxy terminal hydrolase-L1 induces apoptosis in breast cancer cells. *Int J Oncol* 2008; 33:1037–1045.
55. Hofmann RM, Pickart CM. In vitro assembly and recognition of Lys-63 polyubiquitin chains. *J Biol Chem* 2001; 276:27936–27943.
56. Sakai N, Sawada MT, Sawada H. Non-traditional roles of ubiquitin-proteasome system in fertilization and gametogenesis. *Int J Biochem Cell Biol* 2004; 36:776–784.
57. Sun QY, Fuchimoto D, Nagai T. Regulatory roles of ubiquitin-proteasome pathway in pig oocyte meiotic maturation and fertilization. *Theriogenology* 2004; 62:245–255.
58. Sutovsky P, Manandhar G, McCauley TC, Caamaño JN, Sutovsky M, Thompson WE, Day BN. Proteasomal interference prevents zona pellucida penetration and fertilization in mammals. *Biol Reprod* 2004; 71:1625–1637.
59. Yi YJ, Manandhar G, Oko RJ, Breed WG, Sutovsky P. Mechanism of sperm-zona pellucida penetration during mammalian fertilization: 26S proteasome as a candidate egg coat lysin. *Soc Reprod Fertil Suppl* 2007; 63:385–408.
60. Hoodbhoy T, Talbot P. Mammalian cortical granules: contents, fate, and function. *Mol Reprod Dev* 1994; 39:439–448.
61. Bembenek JN, Richie CT, Squirell JM, Campbell JM, Eliceiri KW, Poteryaev D, Spang A, Golden A, White JG. Cortical granule exocytosis in *C. elegans* is regulated by cell cycle components including separase. *Development* 2007; 134:3837–3848.
62. Ducibella T, Kurasawa S, Duffy P, Kopf GS, Schultz RM. Regulation of the polyspermy block in the mouse egg: maturation-dependent differences in cortical granule exocytosis and zona pellucida modifications induced by inositol 1,4,5-trisphosphate and an activator of protein kinase C. *Biol Reprod* 1993; 48:1251–1257.
63. Csizmadia V, Raczynski A, Csizmadia E, Fedyk ER, Rottman J, Alden CL. Effect of an experimental proteasome inhibitor on the cytoskeleton, cytosolic protein turnover, and induction in the neuronal cells in vitro. *Neurotoxicology* 2008; 2:232–243.
64. Burgess S, Walker M, Knight PJ, Sparrow J, Schmitz S, Offer G, Bullard B, Leonard K, Holt J, Trinick J. Structural studies of arthrin: monoubiquitinated actin. *J Mol Biol* 2004; 341:1161–1173.
65. Yi YJ, Nagyova E, Manandhar G, Procházka R, Sutovsky M, Park CS, Sutovsky P. Proteolytic activity of the 26S proteasome is required for the meiotic resumption, germinal vesicle breakdown, and cumulus expansion of porcine cumulus-oocyte complexes matured in vitro. *Biol Reprod* 2008; 78:115–126.
66. Meyer-Schwesinger C, Meyer TN, Munster S, Klug P, Saleem M, Helmchen U, Stahl RAK. A new role for the neuronal ubiquitin C-terminal hydrolase-L1 (UCH-L1) in podocyte process formation and podocyte injury in human glomerulopathies. *J Pathol* 2009; 217:452–464.
67. Kaitna S, Schnabel H, Schnabel R, Hyman AA, Glotzer M. A ubiquitin C-terminal hydrolase is required to maintain osmotic balance and execute actin-dependent processes in the early *C. elegans* embryo. *J Cell Sci* 2002; 115:2293–2302.
68. Mtango NR, Sutovsky M, Zhong Z, Vandervoort K, Latham KE, Sutovsky P. Roles of de-ubiquitinating enzymes UCHL1 and UCHL3 in oocyte maturation, fertilization, and zygotic development. In: Abstracts of the 42nd Annual Meeting of the Society for the Study of Reproduction, July 18–22, 2009, Pittsburgh, Pennsylvania. *Biol Reprod* 2009; 81(Suppl): Abstract 329.
69. Azoury J, Verlhac MH, Dumont J. Actin filaments: key players in the control of asymmetric divisions in mouse oocytes. *Biol Cell* 2009; 10:69–76.

Publication 3:

Transcriptomic analysis of *in vivo* and *in vitro* produced bovine embryos revealed a developmental change in cullin 1 expression during maternal-to embryonic transition.

Vodickova Kepkova K, Vodicka P, **Toralova T**, Lopatarova M, Cech S, Dolezel R, Havlicek V, Besenfelder U, Kuzmany A, Sirard M-A, Laurincik J, Kanka J.
Theriogenology. 2011 Jun;75(9):1582-95. Epub 2011 Mar 15.; IF: 2.073

Transcriptomic analysis of *in vivo* and *in vitro* produced bovine embryos revealed a developmental change in cullin 1 expression during maternal-to-embryonic transition

K. Vodickova Kepkova^{a,e,*}, P. Vodicka^a, T. Toralova^a, M. Lopatarova^b, S. Cech^b, R. Dolezel^b, V. Havlicek^c, U. Besenfelder^c, A. Kuzmany^c, M.-A. Sirard^d, J. Laurincik^e, J. Kanka^a

^a Institute of Animal Physiology and Genetics, The Academy of Sciences of the Czech Republic, v.v.i., Rumburská 89, 277 21 Libechev, Czech Republic

^b Veterinary and Pharmaceutical University, Faculty of Veterinary Medicine, Palackeho 1-3, 612 42 Brno, Czech Republic

^c Reproduction centre—Wieselburg, University of Veterinary Medicine, Vienna, Austria

^d Centre de Recherche en Biologie de la Reproduction, Département des Sciences Animales, Université Laval, Sainte-Foy, Québec, Canada G1K 7P4

^e Constantine the Philosopher University, Faculty of Natural Sciences, Trieda A. Hlinku, SK-949 74 Nitra, Slovak Republic

Received 29 October 2010; received in revised form 12 December 2010; accepted 19 December 2010

Abstract

Pre-implantation embryos derived by *in vitro* fertilization differ in their developmental potential from embryos obtained *in vivo*. In order to characterize changes in gene expression profiles caused by *in vitro* culture environment, we employed microarray constructed from bovine oocyte and preimplantation embryo-specific cDNAs (BlueChip, Université Laval, Québec). The analysis revealed changes in the level of 134 transcripts between *in vitro* derived (cultured in COOK BVC/BVB media) and *in vivo* derived 4-cell stage embryos and 97 transcripts were differentially expressed between 8-cell stage *in vitro* and *in vivo* embryos. The expression profiles of 7 selected transcripts (*BUB3*, *CUL1*, *FBL*, *NOLCI*, *PCAF*, *GABPA* and *CNOT4*) were studied in detail. We have identified a switch from Cullin 1-like transcript variant 1 to Cullin 1 transcript variant 3 (UniGene IDs **BT.36789** and **BT.6490**, respectively) expressions around the time of bovine major gene activation (8-cell stage). New fibrillar protein was detected by immunofluorescence already in early 8-cell stage and this detection correlated with increased level of fibrillar mRNA. The qRT-PCR analysis revealed significant differences in the level of *BUB3*, *NOLCI*, *PCAF*, *GABPA* and *CNOT4* gene transcripts between *in vivo* derived (IVD) and *in vitro* produced (IVP) embryos in late 8-cell stage. The combination of these genes represents a suitable tool for addressing questions concerning normal IVD embryo development and can be potentially useful as a marker of embryo quality in future attempts to optimize *in vitro* culture conditions.
© 2011 Elsevier Inc. All rights reserved.

Keywords: Preimplantation embryo; *In vivo* derived; Microarray; Real-time RT-PCR; Cullin 1; Fibrillar

1. Introduction

In vitro produced (IVP) bovine embryos represent a valuable resource for embryology research and recently also for routine embryo transfer, but IVP process still

suffers from low efficiency (< 40% IVP embryos reaching blastocyst stage). Factors contributing to this problem include oocyte quality, conditions of *in vitro* oocyte maturation and embryo culture conditions [1]. To address these problems, several groups have studied the influence of different media compositions and culture conditions on the developmental competence of *in vitro* cultured bovine oocytes [2,3,4]. Others have con-

* Corresponding author. Tel.: +420 315 639 566; Fax: +420 315 639 510.

E-mail address: kepkova@iapg.cas.cz (K.V. Kepkova).

centrated on embryonic preimplantation development period where maternal-to-embryonic transition (MET) takes place. This shift from utilization of maternally produced and stored transcripts to mRNAs produced by newly activated embryonic genome occurs at a species-specific time-point [5]. In the bovine embryos, a minor gene activation was reported to start between 1–4-cell stage [6], while major gene activation takes place at 8–16-cell stage [7]. Attempts were made to compare changes in abundance of specific transcripts during this developmental period and to relate them to the quality of IVP and *in vivo* derived (IVD) bovine embryos. It was shown that stress response genes are up-regulated during *in vitro* development while metabolism related genes are down-regulated compared to *in vivo* derived embryos [8]. For some markers (SOX, G6PD) changes were detected before MET, suggesting possible influence of *in vitro* culture on the rate of maternal mRNA stocks polyadenylation or depletion/degradation. The disadvantage of similar quantitative RT-PCR (qRT-PCR) based studies is the fact that the levels of only a few preselected transcripts could be studied. Alternative strategies allowing for wider transcriptome coverage include screening of stage specific EST libraries [9] or use of microarrays [10,11]. The previously cited studies compared IVD embryos or oocytes with IVP embryos at the blastocyst stage which occurs several days after MET at the 8-cell stage [10,11]. A study by Vigneault et al. [12] showed that many transcripts are newly expressed already in the 6-cell and early 8-cell stage bovine embryos. Thus we have utilized custom bovine embryo-specific microarray (BlueChip) [13] to characterize transcriptome changes between IVP and IVD bovine embryos at the time of minor and major embryonic genome activation (4-cell stage and 8-cell stage, respectively). Based on a list of candidate genes identified by microarray, we have studied the expression levels of selected transcripts during *in vitro* culture of preimplantation embryos in different culture media.

2. Materials and methods

2.1. Isolation of bovine oocytes, *in vitro* fertilization and embryo culture

Bovine embryos were obtained after *in vitro* maturation of oocytes and their subsequent fertilization and culture *in vitro* [14]. Antral follicles with diameter between 4 and 10 mm were dissected with fine scissors and then punctured. The cumulus-oocyte complexes were evaluated and selected according to the morphology of cumulus and submitted to *in vitro* maturation in

tissue culture medium (TCM) 199 supplemented with 20 mM sodium pyruvate, 50 U/ml penicillin, 50 µg/ml streptomycin, 10% estrus cow serum (ECS) and gonadotropins (P.G. 600, 15 U/ml, Intervet, Boxmeer, The Netherlands) without oil overlay in 4-well dishes under atmosphere of 5% CO₂–7% O₂–88% N₂ at 39 °C for 24 h.

For *in vitro* fertilization (IVF), cumulus-oocyte complexes were washed four times in PBS and once in fertilization medium, then transferred in groups of up to 40 into four-well dishes (Nunc) containing 250 µl of fertilization medium [14] per well. Viable spermatozoa were washed in fertilization medium and pelleted by centrifugation at 100 × g for 5 min. Spermatozoa were counted in a haemocytometer and diluted in the appropriate volume of fertilization medium to give a concentration of 2 × 10⁶ spermatozoa/ml. A 250 µl aliquot of this suspension was added to each fertilization well to obtain a final concentration of 1 × 10⁶ spermatozoa/ml. Plates were incubated for approximately 20 h at 39 °C in an atmosphere composed of 5% CO₂–7% O₂–88% N₂.

At approximately 20 h post fertilization (hpf) presumptive zygotes were denuded by gentle pipetting and divided into two groups. The first group were transferred to Bovine Vitro Cleave medium (BVC, COOK, Eight Mile Plains, Australia) and the second group were transferred to Menezo B2 medium (Sevapharma, Prague, Czech Republic). All zygotes were cultured in an atmosphere of 5% CO₂–7% O₂–88% N₂ at maximum humidity (25 zygotes in 25 µl of medium under mineral oil). At 100 hpf the BVC medium was replaced by Bovine Vitro Blast medium (BVB, COOK) and both groups of embryos were cultured to the hatched blastocyst stage. The dishes were examined at 32, 44, 60, 92, 120, 156 and 180 hpf, and 2-cell, 4-cell, early 8-cell, late 8-cell embryo, morula, blastocysts and hatched blastocysts were collected at each respective time point.

2.2. Recovery of embryos at different developmental stages from bovine oviducts

Hormonal treatment of donor animals and embryo collection were performed according to [15]. Briefly, a total of 24 heifers (crossbreed Czech Motley and Holstein) were pre-synchronized by administration of prostaglandin F_{2α} analogue (cloprostenol 500 µg i.m., Oestrophan[®] 0.25 mg/ml Bioveta, Czech Republic) twice within 11 days. Two days after each of the PGF_{2α} treatments the animals received GnRH analogue (leclirelin 50 µg i.m., Supergestran[®], Nordic Pharma, Czech

Republic). Ultrasound-guided transvaginal aspirations of the dominant follicles were performed on day 9 of estrus cycle. Forty two hours later the animals received the first of eight consecutive FSH-injections (in total 450 UI of FSH at 12 h intervals in decreasing doses, Pluset®, Calier S.A., Spain). Two PGF2 α treatments were performed 60 and 72 h after the initial FSH-treatment. Finally, 48 h after the first PGF2 α treatment, ovulation was induced by giving hCG (2500 UI i.v., Pregnyl® 1500, Organon, Netherlands) simultaneously with the artificial insemination (AI) using one straw of frozen semen from a bull of proven fertility. Embryos at 2-cell, 4-cell and late 8-cell stage were recovered by oviductal flushing using a minimally invasive endoscopic approach 1–4 days after artificial insemination [16]. The developmental stage as well as the morphological integrity of the recovered embryos was assessed according to IETS guidelines [17]. Embryos of the same developmental stage assessed excellent and good were pooled in groups of ten embryos, washed in PBS, frozen in a minimum amount of medium in siliconized 0.6 ml cups and stored at -80°C . All animal treatments were approved by the Central Committee for Animal Protection, Ministry of Agriculture of the Czech Republic, Prague (project of experiments No. 37/2006) and fully conformed to the Czech Animal Protection Law (No. 246/92).

2.3. Suppression subtractive hybridization and cDNA array preparation

PolyA+ mRNA from pools of 25 *in vitro* matured metaphase II oocytes or 50 4-cell stage and 8-cell stage *in vitro* produced embryos after culture in COOK BVC/BVB medium was extracted by a Dynabeads mRNA DIRECT Micro Kit (Dyna, Oslo, Norway) according to the manufacturer's instructions.

The extracted mRNA was converted into cDNA and amplified using Super Smart cDNA synthesis kit (BD Biosciences Clontech, Palo Alto, CA) and subtraction immediately followed using PCR Select cDNA Subtraction Kit (BD Biosciences Clontech, Palo Alto, CA) according to the manufacturer's instructions. *In vitro* produced 4-cell stage embryos were subtracted from IVP 8-cell stage embryos, IVP 8-cell stage embryos from IVP 4-cell stage embryos and *in vitro* matured MII stage oocytes from IVP 4-cell stage embryos. Selected subtracted cDNAs were sent to the Centre de Recherche en Biologie de la Reproduction, Département de Sciences Animales, Université Laval, where they were used for microarray preparation.

BlueChip, V3 array contains 3,136 sequences spot-

ted in triplicates (9,408 spots in total, including controls). All experimental sequences were derived from cDNA libraries generated by the set of SSHs with bovine oocytes, preimplantation embryos and somatic tissues: GV oocytes subtracting somatic tissues, GV oocytes subtracting day 8 blastocysts, day 8 blastocyst subtracting GV oocytes, day 8 blastocyst subtracting somatic tissues (SSH libraries present on the original BlueChip array as described in [13]), 4-cell stage embryos subtracting MII oocytes, 4-cell stage embryos subtracting 8-cell stage embryos, 8-cell stage embryos subtracting 4-cell stage embryos (3 libraries generated in our laboratory, as described above), 8-cell stage embryos subtracting α amanitin treated 8-cell stage embryos, early cleaving 2-cell stage embryos subtracting late cleaving embryos, 6 h *in vitro* matured oocytes subtracting GV oocytes, 6 h *in vivo* matured oocytes subtracting 6 h *in vitro* matured oocytes and 6 h post-LH *in vivo* oocytes subtracting 2 h pre-LH *in vivo* oocytes. Samples coming from the SpotReport Alien cDNA Array Validation System (Stratagene, La Jolla, CA), Alien 1 (540 spots) and Alien 2 (540 spots) and other samples, namely blank (96 spots), GFP (4 spots), GFP1 (378 spots), GFP1 (6 spots), GFP1/16 (6 spots), GFP1/8 (6 spots), GFP L (6 spots) and H2O/DMSO (384 spots), negative (6 spots), plant (540 spots) were included in the array as negative controls. These spots can be used for the determination of background hybridization during statistical analysis. Housekeeping genes, namely tubulin (12 spots), ubiquitin (12 spots), and actin (12 spots) were added as positive controls.

2.4. RNA extraction and aRNA preparation

One biological replicate represented by a pool of 20 embryos was prepared for each stage studied (8-cell stage IVD and IVP, 4-cell stage IVD and IVP embryos) and three technical replicates including dye-swap were performed for each comparison.

Poly (A)+ mRNA was extracted from pools of 20 *in vivo* or *in vitro* (after culture in COOK BVC/BVB medium) produced 4-cell and 8-cell stage embryos, using a Dynabeads mRNA DIRECT Micro Kit (Dyna, Oslo, Norway) according to the manufacturer's instructions.

Amplified RNA (aRNA) was prepared with a two-round amplification protocol using Amino Allyl MessageAmp™II aRNA Amplification kit (Ambion, Austin, TX). In subsequent labelling reaction, 5 μg of aRNA were conjugated with either Alexa Fluor 555 or Alexa Fluor 647 dyes (Invitrogen, Carlsbad, CA).

2.5. Array hybridization, scanning and data analysis

Labelled probes (2 μg of each Alexa Fluor 555 and 647 conjugated aRNA) were mixed together and denatured for 5 min at 90 °C. Denatured probes were mixed with 45 μl of SlideHyb™ Glass Array Hybridization Buffer #1 (Ambion, Austin, TX) preheated to 68 °C and incubated on the array for 18 h at 50 °C in a humidified chamber. Slides were washed twice with 2 \times SSC-0.5% SDS for 15 min at 55 °C, twice with 0.5 \times SSC-0.5% SDS for 15 min at 55 °C and dried by centrifugation at room temperature for 5 min at 1200g. Images were scanned using GeneTAC UC4 microarray scanner (Genomic Solutions, Ann Arbor, MI) and analyzed using TIGR Spotfinder software 3.1.1 (TM4 software suit, [18]). After within-slide lowess (locally weighted scatterplot smoothing) and between-slide scale normalization [19] in TIGR Midas 2.19, the data were sorted in Excel (Microsoft, Redmond, WA), and only the features with signal present in all three within-array replicates were selected, averaged and used for further analysis of differential expression in significance analysis of microarrays software (SAM version 3.02, Stanford University; <http://www-stat.stanford.edu/~tibs/SAM/>) [20]. Using one class response type, parameter delta was adjusted so that median number of false positives among differentially expressed genes was <1. This resulted in 134 genes identified as differentially expressed between 4-cell stage IVD and IVP embryos, with FDR of 0.56% and 97 genes identified as differentially expressed between 8-cell stage IVD and IVP embryos, with FDR of 0.63%. Interologous Interaction Database (I2D; an on-line database of known and predicted mammalian and eukaryotic protein-protein interactions, [21]) was used to search for possible protein-protein interaction partners for proteins identified as regulated in our microarray study. Version 1.80 of I2D, including 254,361 source interactions and 238,288 predicted interactions (<http://ophid.utoronto.ca/ophidv2.201/ppi.jsp>) was used for interaction search with human selected as target organism. Protein-protein interaction network was visualized using NAViGaTOR (Network Analysis, Visualization & Graphing TORonto) 2.1.13 software (<http://ophid.utoronto.ca/navigator>). In protein-protein interaction networks, nodes represent proteins and edges between nodes represent physical interactions between the proteins. NAViGaTOR allows nodes to be color-coded according to Gene Ontology (GO—a controlled vocabulary describing properties of genes) terms. “View groups of approximate cliques” analysis tool was used on the resulting network to

identify sets of nodes that are highly interconnected (cliques).

2.6. Quantitative RT-PCR analysis of gene expression

Poly (A)+ mRNA was extracted from the pools of 20 oocytes and embryos in each stage of development, using a Dynabeads mRNA DIRECT Micro Kit (Dyna, Oslo, Norway) according to the manufacturer’s instructions. Before isolation 1 pg of the Luciferase mRNA (Promega, Madison, WI) per oocyte/embryo was added as an external standard.

Levels of specific mRNAs (selected genes and primer sequences designed using Beacon Designer7 are listed in Table 1) were measured by real-time RT-PCR. mRNA equivalent of 0.5 embryo was amplified by a One-step RT-PCR kit (Qiagen, Hilden, Germany) with real-time detection using SybrGreenI fluorescent dye on a Rotor Gene 3000 instrument (Corbett Research, Mortlake, Australia). The reaction mix contained QIAGEN OneStep RT-PCR Buffer (1 \times), dNTP Mix (400 μM of each), forward and reverse primers (both 400 μM), SybrGreenI (1:50.000 of 1000 \times stock solution, Invitrogen, Carlsbad, CA), RNase inhibitor (Promega, Madison, WI), RT-PCR Enzyme Mix (1 μl) and template RNA. The real-time RT-PCR reactions were prepared in duplicates, with oocytes and embryos on the one reaction, and reactions were repeated three times.

Reaction conditions were: reverse transcription at 50 °C for 30 min, initial activation at 95 °C for 15 min, cycling: denaturation at 94 °C for 20 sec, annealing at a temperature specific for each set of primers (see Table 1) for 20 sec, extension at 72 °C for 30 sec. Products were verified by melting analysis and gel electrophoresis on 1.5% agarose gel with ethidium bromide staining.

The relative concentration of templates in different samples was determined using comparative analysis software (Corbett Research, Mortlake, Australia). The results for individual target genes were normalized according to the relative concentration of the external standard. Ratios of the target gene concentration to the Luciferase mRNA concentration were estimated in each sample.

Data are presented in as mean \pm SEM. The mean \pm SEM was obtained from three independent real-time RT-PCRs from three different batches of embryos. The significance of differences between stages 8-cell *in vitro* and 8-cell *in vivo* was evaluated using a t-test (Kyplot v2.0 beta15, KyensLab Incorporated, Tokyo, Japan).

Table 1
Primer sequences and PCR conditions used to evaluate expression of selected genes in bovine embryos by qRT-PCR.

Official symbol (Gene)	GenBank ID	Primer sequence (5'→3')	Amplicon size (bp)	Annealing temperature (°C)
<i>BUB3</i>	XM_879565	Forward CAGGGTTATGTATTAAGTTCTATC Reverse TCTGTGACACTTGAAGGC	102	50
<i>CUL1</i>	XM_875152	Forward CTGAAGTTCTATACTCAACAATG Reverse ACAATCTCTCCAAGTCACC	162	50
<i>NOLC1</i>	XM_590941 NM_001075608	Forward GAGCGAGCCAATCAGGTTCC Reverse AGAGTTGACTTGGACAGAGATG	114	55
<i>FBL</i>	XM_581057	Forward AAGCGGACCAACATTATTC Reverse GCATTCAGGGCTACAATC	134	50
<i>PCAF</i>	XM_613744	Forward ATATACTCTGCCCACTGATAATG Reverse CAAGACAGGTAAGGTGTATGATG	179	55
<i>GABPA</i>	AF057717	Forward TGA CTGATATAACCTCACTACAC Reverse ATCTCATTCACTGTGTTCTTGG	166	55
<i>CNOT4</i>	NM_001035432	Forward ACTCGTTCAGTGGTCTCTC Reverse GGTCTTCCTTTGCGTCAG	199	55

BUB3 (Budding uninhibited by benzimidazoles), *CUL1* (Cullin 1), *NOLC1* (Nucleolar and coiled-body phosphoprotein 1, nucleolar phosphoprotein p130–NOPP140), *FBL* (Fibrillarin), *PCAF* (p300/CBP-associated factor), *GABPA* (GA-binding protein transcription factor, alpha subunit), *CNOT4* (CCR4–NOT transcription complex, subunit 4).

2.7. Sequencing

A fragment of the Cullin 1 gene, amplified by PCR with the use of primers listed in Table 1, was purified using a GenElute PCR Clean-Up Kit (Sigma–Aldrich, Prague, Czech Republic). Sequencing reaction was performed with one of the amplification primers (3.2 pmol, forward primer) and 10 ng/100 bp of purified PCR fragment, using BigDye® Terminator v3.1 Cycle Sequencing Kit (Applied Biosystems, Prague, Czech Republic). Sequence readout was performed on the 3100-Avant Genetic Analyzer (Applied Biosystems, Prague, Czech Republic). Analysis and alignment of resulting sequences was performed in BioEdit 7.0.9.1 and ClustalX 2.0.12 software.

2.8. Analysis of *CUL1* gene structure

Exalign [22] web interface (<http://159.149.109.9/exalign/>) was used to compare exonic structure of bovine cullin 1 gene (UniGene **BT.6490**) with the whole set of human, mouse, rat and cow gene structures in a BLAST-like way (“database search” mode), looking for the genes with the most similar structure to the one of the query gene. Bovine cullin 1 mRNA RefSeq ID **XM_876699** and cullin 1-like RefSeq ID **XM_589507** were used as input with following advanced options: Include XM genes: yes; Display top 3 results; Only results with Blast hit: yes.

2.9. Immunostaining

Embryos were fixed in 4% paraformaldehyde supplemented with 1% TritonX-100 50 min. at 4 °C. Fixed

embryos were processed immediately or stored in PBS up to 3 weeks at 4 °C. After washing in PBS, the embryos were incubated in 0.75% TritonX-100 for 15 min. All subsequent steps were done in PBS supplemented with 0.25% BSA and 0.05% saponin (PBS/BSA/sap). Embryos were blocked with 2% normal goat serum for 1 h and incubated with primary antibody (rabbit polyclonal anti-Cullin 1–Abcam, Cambridge, UK or mouse monoclonal anti-Fibrillarin–Cytoskeleton, Denver, CO) 1:100 in PBS/BSA/sap overnight at 4 °C. After thorough washing the embryos were incubated with goat anti-mouse antibody conjugated with Alexa 594 (Invitrogen, Carlsbad, CA) 1:800 in PBS/BSA/sap or with anti-rabbit fluorescein conjugated antibody 1:350 in PBS/BSA/sap (Santa Cruz biotechnology, Heidelberg, Germany) for 1 h at room temperature darkling. Controls of immunostaining specificity were carried out by omitting primary antibody or using another species specific secondary antibody conjugate. The nuclei were stained and the embryos were mounted on glass slides using VECTASHIELD HardSet Mounting Medium with DAPI (Vector Laboratories, Peterborough, UK). Fluorescence was detected on Leica TCS SP2 laser-scanning confocal microscope (Leica, Mannheim, Germany).

3. Results and discussion

3.1. Suppression subtractive hybridization

Suppression subtractive hybridization (SSH) is a powerful technology for identification of genes that are

differentially regulated between two samples. SSH was used to analyze transcription activation during preimplantation development of rabbit and bovine embryos [23]. We have used SSH to prepare three bovine cDNA libraries enriched for transcripts differentially regulated during preimplantation development. Selected cDNAs (Supplementary File 1, labelled in green) representing novel clones, not present on previous version of the bovine oocyte and preimplantation embryo specific BlueChip microarray [13] were included in BlueChip version 3 array design.

3.2. Microarray and protein-protein interaction network modelling

Due to the small amount of RNA in one embryo and the limited source of IVD embryos, pooling was used to average biological variation and to obtain sufficient starting amount of RNA for amplification. As only one biological replicate represented by a pool of 20 embryos was available for each stage studied, our selection of differentially expressed genes is based on statistical analysis of technical replicates. By this methodology, it is possible to identify genes differentially expressed in the sample particularly studied (e.g. differences between the one particular group of 4-cell stage IVD embryos and the other particular group of 4-cell stage IVP embryos) but not to generalize obtained results to other samples. However, in this case the true independent biological unit should be one embryo or group of embryos from one particular donor and thus the pool of 20 embryos, originated from several donors should represent sufficient sample to warrant biologically meaningful results and to generate the useful list of candidate genes for further study. Significance analysis of microarrays (SAM) [20] software was used to identify differentially expressed genes. We have identified 81 candidate genes as more abundant and 53 candidate genes as less abundant in 4-cell stage IVP compared to IVD embryos. Another 47 candidate genes more abundant and 50 candidate genes less abundant in 8-cell stage IVP compared to IVD embryos were identified. Complete microarray data including raw data are deposited in Gene Expression Omnibus (GEO), Accession No. **GSE24714**; selected candidate genes are listed in Supplementary File 2.

Where possible, Protein/Swiss-Prot accession numbers of human orthologs to candidate genes identified as differentially regulated by microarray approach were found (Supplementary File 2) and introduced into Interologous Interaction Database (I2D) [21] in order to explore possible interaction partners and to construct

protein-protein interaction network (Supplementary File 3) that enables the graphical visualization of possible functional relationships among molecules (Supplementary File 4, simplified network view in Fig. 1). Four groups of highly interconnected nodes (cliques) were identified in the resulting network by an automated computational algorithm. The first identified cluster contained 5 proteins corresponding to the genes found to be differentially regulated in IVP and IVD embryos: Fibrillarin (FBL), Eukaryotic translation initiation factor 4E (EIF4E), 60S ribosomal protein L5 (RPL5), 60S ribosomal protein L8 (RPL8) and 60S acidic ribosomal protein P0 (RPLP0) (Fig. 1, dark blue lines). The second cluster consisted of three proteins, all corresponding to the genes identified as differentially regulated in IVD vs IVP embryos: Cullin 1 (CUL1), S-phase kinase-associated protein 1A (SKP1A) and Catenin beta-1 (CTNNB1) (Fig. 1, dark red lines). The third cluster contained 2 proteins corresponding to the genes identified as differentially regulated in IVD vs IVP embryos: CCR4-NOT transcription complex subunit 4 (CNOT4) and UHRF2 E3 ubiquitin-protein ligase (UHRF2) and four other interacting proteins (Fig. 1, green lines). From these 3 clusters, we have selected *FBL*, *CUL1* and *CNOT4* genes for further study. The last cluster contained 2 proteins corresponding to the genes identified as differentially regulated in IVD vs IVP embryos: SUV39H2 Histone-lysine N-methyltransferase (SUV39H2) and SMG1 Serine/threonine-protein kinase (SMG1) and two other interacting proteins (Fig. 1, light blue lines); no gene from this cluster was selected for further study. Instead, we have selected 4 other transcripts from the list of candidate genes (BUB3, NOLC1, PCAF and GABPA), based on their reported or presumptive role in embryonic development and studied their expression by qRT-PCR.

3.3. Expression of selected transcripts in IVP and IVD embryos

For selected transcripts, we have first evaluated if differential expression between IVP and IVD embryos observed on microarray will be confirmed by qRT-PCR. Then we analyzed the expression pattern of selected transcripts during *in vitro* culture from MII oocyte stage until blastocyst stage. We used two different sources of media for embryo culture, commercially available COOK BVC/BVB and Menezo B2 [24]. The design of COOK media resides on the switch from pyruvate metabolite to glucose during post-compaction period. Menezo B2 represents the most complex medium used for cultivation from zygote till blastocyst stage.

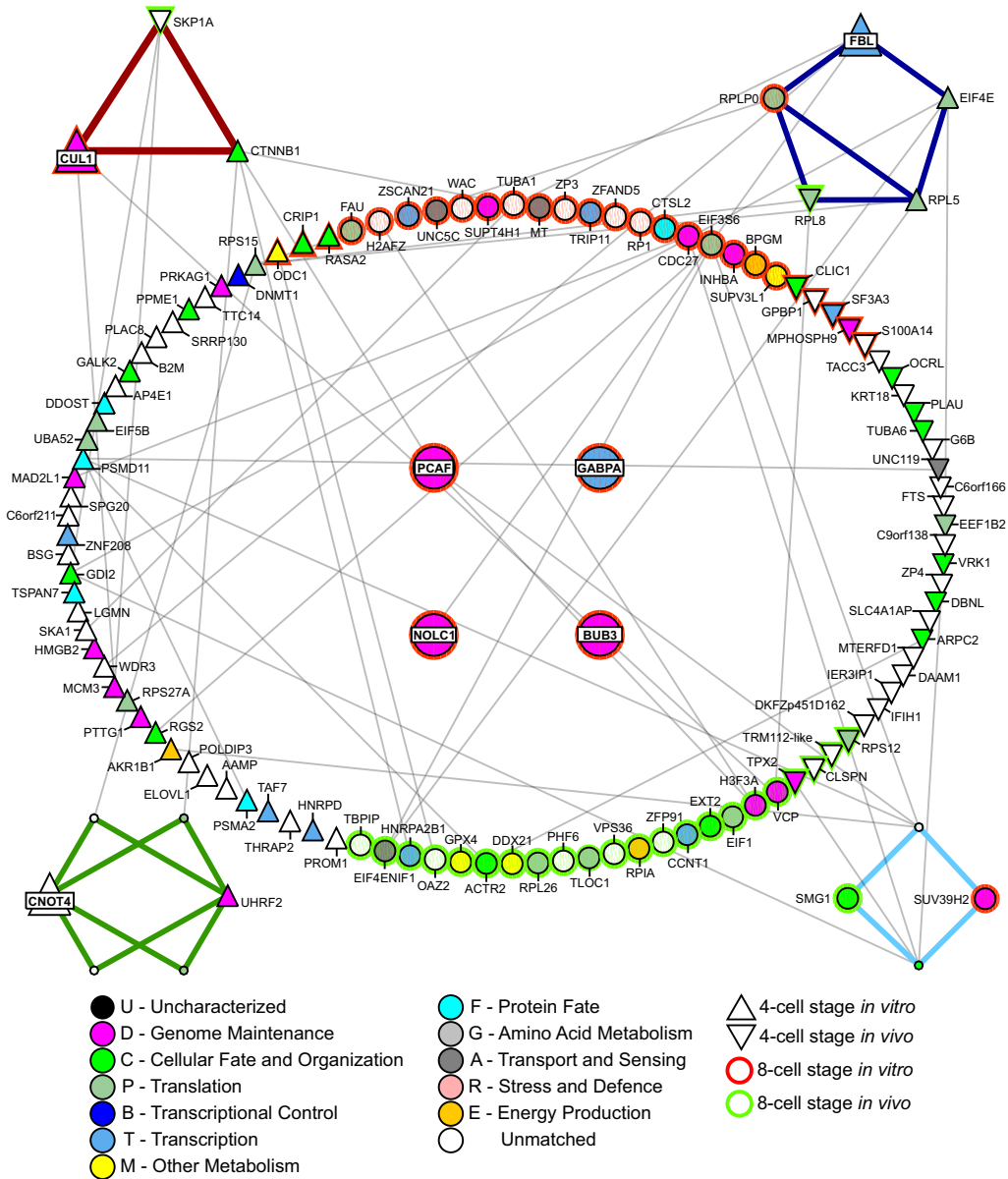


Fig. 1. Simplified view of the network of possible protein-protein interactions, generated by querying I2D database for candidate genes identified on microarray as differentially regulated between IVD and IVP embryos. Nodes representing candidate gene protein orthologs are shown as circles and triangles with protein name next to node and genes selected for qRT-PCR verification are highlighted by increased node size with label centred over the node. Colour of nodes represents Gene Ontology function. Four clusters of highly interconnected nodes (cliques) identified within the network are highlighted by coloured edges, biggest group (sorted by max. degree) containing FBL in dark blue, second biggest group containing CUL1 in red, the third group containing CNOT4 in green and last group in light blue.

3.3.1. Expression of cullin 1 and cullin 1-like in bovine preimplantation embryo

Cullin 1-like (*CUL1*) transcript was more abundant at both 4-cell stage and 8-cell stage IVP embryos in our microarray study. There are five major categories of cullins in metazoan (*CUL1* through *CUL5*) and an additional vertebrate specific class containing *CUL7* and

Parkin-like cytoplasmic protein (*PARC*) [25]. *CUL1* forms ubiquitin ligase complexes SCF, which consist of three invariable components, Skp1, *CUL1* (*Cdc53* in yeast) and Rbx1, and a variable component F-box protein. SCF complexes mediate ubiquitination of proteins involved in cell-cycle progression, mainly during G1/S phase transition, and are also involved in regulation of

centrosome duplication [26,27]. *Cull1* null mice embryos die around E5.5–E7.5 before the onset of gastrulation, showing signs of cyclin E dysregulation [28,29]. Attempts to derive *Cull1*^{-/-} embryonic stem cells were unsuccessful, consistent with an essential role for Cull1 in proliferation of early embryonic cell types [29]. In RT-PCR for *CUL1* transcript, we have detected two products with the same length (data not shown) but different melting points (Fig. 2A), with the first product present from MII oocytes till early 8-cell stage embryos and the second product from late 8-cell stage embryos till blastocyst stage. The search of the Entrez Gene

DNA database revealed that cullin 1-like and cullin 1 represent two different genes from cullin family (UniGene IDs **BT.36789**, resp. **BT.6490**), both on chromosome 4 but located in two different regions. Sequencing of amplified fragments confirmed the identity of the first fragment with *Bos taurus* cullin 1-like, transcript variant 1 mRNA (GeneBank ID **XM_589507.3**, 97–99% similarity from MII till 4-cell stage, 88% similarity for early 8-cell stage embryos) and the identity of the second fragment with *Bos taurus* cullin 1, transcript variant 3 mRNA (GeneBank ID **XM_876699**, 87% similarity for late 8-cell stage, 95–98% similarity from

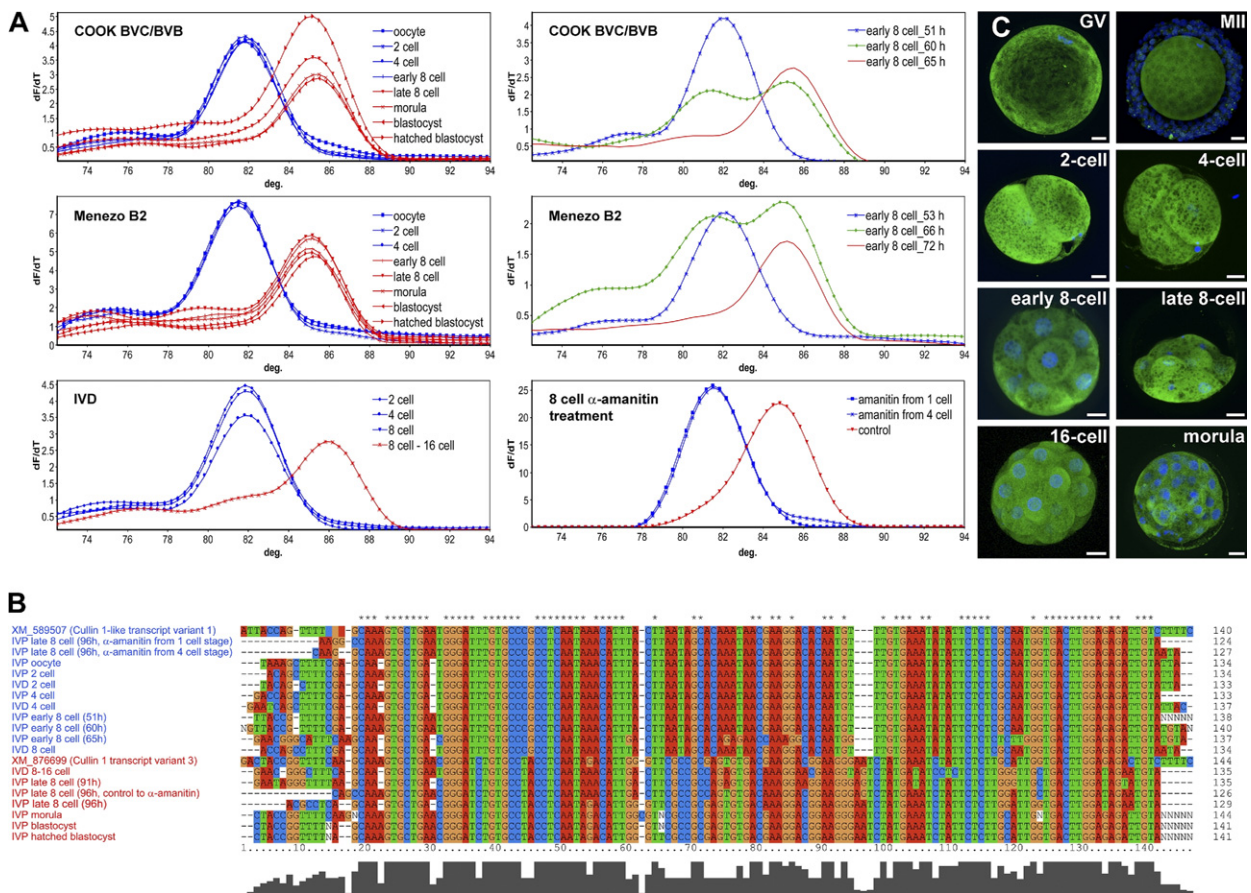


Fig. 2. Switch from expression of *CUL1*-like transcript variant 1 to *CUL1* transcript variant 3 during preimplantation embryo development. A) Melting curves show the presence of two different products obtained by RT-PCR (primers designed against *CUL1* transcript variant 2, cDNA present on microarray) from IVP (COOK BVC/BVB and Menezo B2 culture systems) and IVD embryos (left column). More detailed study showed an earlier switch in transcript variants in COOK BVC/BVB culture system (around 60 hpf) compared to Menezo B2 medium (around 66 hpf). When α -amanitin was added to the culture medium at a final concentration of 100 μ g/ml (from late 1- to 8-cell stage or from 4- to 8-cell stage), only the product with lower melting temperature was detected in late 8-cell stage embryos, while product with higher melting temperature was detected in control late 8-cell stage embryos (right column). B) Sequencing of RT-PCR products. Sequences detected in IVP MII oocytes, 2-cell, 4-cell, early 8-cell and α -amanitin treated late 8-cell stage IVP embryos and 2-cell stage, 4-cell stage and 8-cell stage IVD embryos cluster together with *CUL1*-like transcript variant 1, while sequences detected in IVP late 8-cell stage embryos, morulas, blastocysts and hatched blastocysts and 8-16-cell stage IVD embryos cluster together with *CUL1* transcript variant 3. C) Immunofluorescence staining of *CUL1* in IVP oocytes and embryos shows protein presence throughout preimplantation development. All scale bars represent 20 μ m.

morula till hatched blastocyst) (Fig. 2B). To confirm the observed switch in these gene variants, we cultured IVP bovine embryos from 1-cell or 4-cell up to late 8-cell stage in the presence of α -amanitin, inhibitor of transcription by RNA polymerase II. Only low levels of cullin 1-like mRNA and no cullin 1 mRNA were detected in α -amanitin treated late 8-cell stage embryos, while cullin 1 mRNA was detected in control 8-cell stage embryos (Fig. 2A). CUL1 protein as detected by immunofluorescence staining was present throughout the whole period of preimplantation development, with diffuse cytoplasmic localization (Fig. 2C) which is consistent with its function in protein ubiquitination and subsequent degradation [28,29]. Marin's [30] study of diversification of the cullin family in eukaryotes identified bovine cullin 1-like (RefSeq ID XM_589507) as orthologous to cullin 1 in other animal species. We have used Exalign tool [22] to compare exon-intron structure of both bovine *CUL1* genes to the genes in human, mouse and rat. This comparison showed that cullin 1 (BT.6490) shares the same structure (Supplementary File 5) with the human, mouse and rat cullin 1 genes and seems to be their true ortholog, while intronless cullin 1-like (BT.36789) probably emerged by duplication within the bovine genome. It remains to be solved whether both genes have similar function or not. Currently, there are 5 ESTs associated with cullin 1-like (BT.36789) in UniGene database, four of them belonging to the 2-cell IVP bovine embryo EST library (dbEST 15406) and one belonging to the bovine oocyte cDNA SSH library (dbEST 17330) [27]. Another 84 ESTs, representing many different tissues, including brain, liver, intestine, skin and muscle are associated with cullin 1 (BT.6490), corresponding to its ubiquitous expression and indispensable function in other species. Hwang et al. [31] detected by real-time RT-PCR with primers specific to cullin 1, transcript variant 3 mRNA expression of cullin 1 in bovine IVP morula, blastocyst and hatched blastocyst, but not in the 2-cell to 16-cell stage embryos. Together with our results, all this suggests that cullin 1-like, transcript variant 1 mRNA represents maternal transcript, which is gradually degraded after fertilization and cullin 1 transcript variant 3 represents new embryonic mRNA synthesized from 8-cell stage on. Similar developmental change has already been described in protein translation initiation factor *eIF-1A* gene during mouse embryonic genome activation [32]. The fact that a switch in transcript variants occurs around 8-cell stage, where major gene activation takes place and *CUL1* importance for cell cycle regulation, warrants its further investigation.

3.3.2. Expression of *FBL* transcript and localization of *FBL* protein in bovine IVP preimplantation embryo

Fibrillarin (*FBL*) was found to be more abundant in IVP than in IVD 4-cell stage embryos. *FBL* is localized to the fibrillar centres (FCs) and the dense fibrillar component (DFC) of nucleolus, where it is involved in primary rRNA transcript processing. Svarcova et al. [33] have shown recently that de-novo fibrillarin mRNA synthesis is required for re-formation of the functional nucleolus during the major genome activation period in cattle embryos. Previously, fibrillarin protein was first detected by immunofluorescence at late 8-cell stage in IVP bovine embryos, but was absent in embryos cultured in the presence of α -amanitin. In our study, qRT-PCR showed very low *FBL* mRNA level up to 4-cell stage, by early 8-cell stage levels of *FBL* transcript started to increase in both culture media, but this increase was much more pronounced in Menezes B2 medium as compared with Cook BVC/BVB medium (Fig. 4A). We have also studied *FBL* protein level and localization by immunofluorescence in *in vitro* matured oocytes and IVP embryos. Clear signal for *FBL* was detected in the GV stage oocyte nucleolus (Fig. 3, GV, arrowhead). From MII stage oocytes till 4-cell stage IVP embryos, *FBL* was undetectable. Contrary to the findings of [33], we have detected the first *FBL* signal with pattern typical for newly forming nucleoli in early 8-cell stage IVP embryos in our culture conditions (Fig. 3, early 8-cell, arrowheads). This is similar to the results obtained in bovine embryos derived *in vivo* [34].

3.3.3. Expression profiling of *NOLC1*, *BUB3*, *PCAF*, *GABPA* and *CNOT4* during bovine preimplantation development

Transcript for other nucleolar protein, Nucleolar phosphoprotein p130, nucleolar and coiled-body phosphoprotein 1 (*NOLC1*, Nopp140) was found to be more abundant in IVP than in IVD 8-cell stage embryos in our microarray study. Phosphoprotein *NOLC1* shuttles between nucleolus, cytoplasm and coiled bodies [35] and serves as chaperone for small nucleolar ribonucleoprotein particle (snoRNP) complexes. *NOLC1* also functions as a transcription factor for RNA polymerase II [36] and interacts with casein kinase 2 [37] and RNA polymerase I [38]. The latter *NOLC1* function suggests that it can be also involved in nucleologenesis during embryonic development and in maintenance of nucleolus integrity [39]. In this study, qRT-PCR profile of *NOLC1* transcript in IVP oocytes and embryos showed low transcript levels in 2-cell stage and 4-cell stage

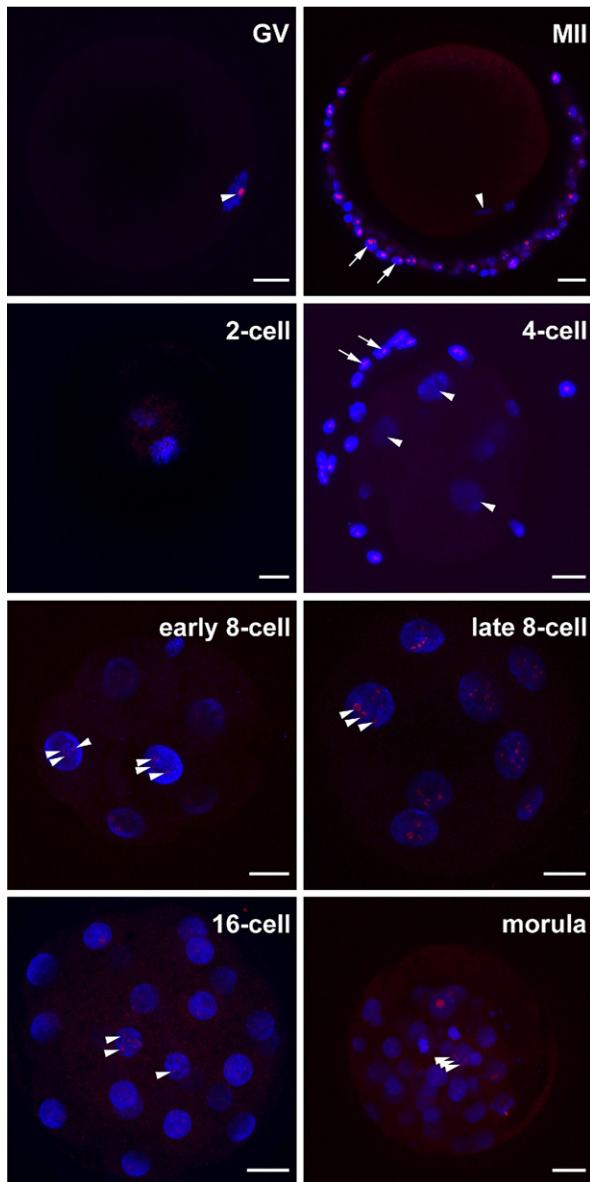


Fig. 3. Fibrillarin protein localization in bovine oocytes and IVP embryos. GV) FBL signal was detected in nucleolus of GV stage oocyte (arrowhead); MII) while clear signal could be detected in nucleoli of cumulus cells (arrows), no localized FBL signal was detected in MII stage oocyte (arrowhead shows metaphase II chromosomes); 2-cell) no localized FBL signal was detected; 4-cell) no FBL signal was present in nuclei of embryo (arrowheads), while clear signal could be detected in nucleoli of cumulus cells (arrows); early 8-cell) faint but clearly localized FBL signal was detected in nuclei of early 8-cell stage embryo, showing formation of new nucleoli (arrowheads); late 8-cell, 16-cell, morula) stronger localized FBL signal was detected (arrowheads). All scale bars represent 20 μm .

embryos and increasing transcript levels from early 8-cell stage till blastocyst. In both *in vitro* culture conditions, *NOLCI* transcript levels were higher at both

4-cell stage and 8-cell stage than in IVD embryos, confirming results from microarrays (Fig. 4B).

Spindle checkpoint component BUB3 is essential for establishment of microtubule-kinetochore attachment during mitosis [40] and its deletion on mouse model results in early embryonic lethality around day E6.5–E7.4 accompanied by an accumulation of mitotic errors [41]. *BUB3* transcript was identified in two microarray studies as up-regulated in bovine and human oocytes [11,42], underlining its importance for correct preimplantation embryo cell cycle progression. We have identified *BUB3* transcript as more abundant in 8-cell stage IVP embryos, which may indicate requirements for tighter checkpoint controls in non-optimal *in vitro* conditions. qRT-PCR profiling of *BUB3* level during *in vitro* development showed a slow decrease in transcript levels from oocytes to early 8-cell stage and then increase in morula and blastocyst stage in both *in vitro* culture conditions (Fig. 4C).

The p130/CBP associated-factor (PCAF) is a protein with intrinsic histone acetylase activity [43], which participates in transcriptional activation by interaction with transcription factors and by chromatin remodeling. While null mutation of *PCAF* is not lethal, probably because of the compensating effect of closely related *PCAF-B/GCN5* protein [44], composite *PCAF/GCN5* mutants show even earlier embryonic lethality than *GCN5* mutation alone, confirming the role of *PCAF* in regulation of early embryonic transcription. In our microarray experiment, *PCAF* transcript was more abundant in 8-cell stage IVP embryos and qRT-PCR profile confirmed this result, showing very low transcript levels up to 4-cell stage, with small increase in early 8-cell stage followed by steeper increase from late 8-cell to blastocyst stage and decrease in hatched blastocyst stage (Fig. 4D).

DNA binding protein GABPA is a component of ETS transcription complex GABP (also known as NRF-2 in humans). This transcription factor is essential for regulation of expression of mitochondrial respiration chain genes and its deletion results in embryo lethality at preimplantation stage [45]. Kinoshita et al. [46] showed that *Gabpa* is involved also in regulation of Oct4 level in the mouse embryonic stem cell lines, probably by down-regulation of Oct4 repressors. As Oct4 is necessary for self-renewal of embryonic stem cells *in vitro* and formation of inner cell mass *in vivo*, this *Gabpa* function also explains the early lethality of null phenotype. Again we have found *GABPA* to be more abundant in 8-cell stage IVP embryos relative to their IVD counterparts. The expression profiling of IVP

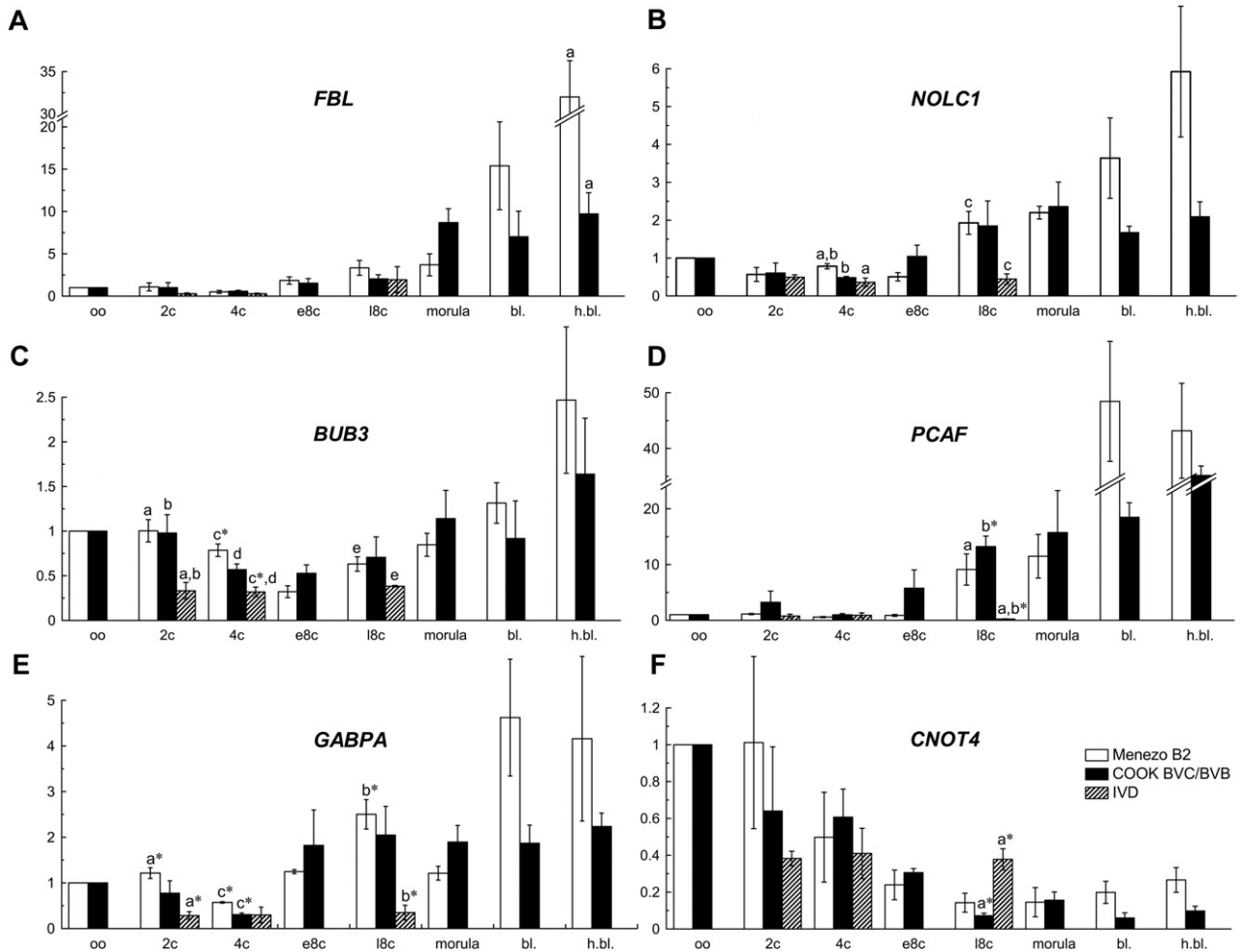


Fig. 4. Relative abundance of *FBL*, *NOLC1*, *BUB3*, *PCAF*, *GABPA* and *CNOT4* mRNAs in bovine IVP (oo, MII oocyte; 2c, 2-cell; 4c, 4-cell; e8c, early 8-cell; l8c, late 8-cell stage; bl., blastocyst; h. bl., hatched blastocyst) and IVD embryos (2c, 2-cell; 4c, 4-cell; l8c, late 8-cell stage) was estimated by one-step RT-PCR with real time detection. The results were normalized according to the relative concentration of the external standard (Luciferase mRNA, 1 pg per oocyte/embryo) and represent mean \pm SD from 3 independent qRT-PCR experiments (3 different pools of oocytes/embryos). *–c Same superscripts above the columns indicate significant differences ($P < 0.05$), asterisks indicate significance at $P < 0.01$.

embryos by qRT-PCR showed moderate *GABPA* transcript levels from MII oocytes to 4-cell stage embryos, with significantly increased level from early 8-cell stage to blastocyst (Fig. 4E). This is consistent with the requirement of this transcription factor for OCT4 level regulation at the time of blastocyst formation.

CNOT4 protein is a component of a CCR4-NOT multifunctional complex. CCR4-NOT is composed of at least 9 identified subunits and is involved in the regulation of transcription by controlling the distribution of TFIID transcription factor across promoters [47], RNA deadenylation and both cytoplasmic [48] and nuclear RNA degradation [49], transcription coupled DNA repair [50] and protein ubiquitination [51].

CNOT4 is an E3 ubiquitin ligase, capable of direct interactions with UbcH6, UbcH9 and UbcH5B E2 ubiquitin conjugating enzymes [51]. The first known substrate of CNOT4 ubiquitin ligase activity was an EGD/NAC [52], nascent polypeptide-associated complex, functioning as a chaperone for newly synthesized proteins and also as transcriptional coactivator. CNOT4 also directly regulates by ubiquitination the protein level of both yeast and human histone demethylase Jhd2 (resp. JARID1C) and in this way it globally regulates transcription [53]. There is currently little information about the involvement of CCR4-NOT complex and CNOT4 subunit particularly in the early mammalian development, but its many different functions and

conservation of its expression throughout eukaryotes suggest its importance. In our study, *CNOT4* transcript levels were constantly decreasing from 2-cell stage embryos till morula stage and slightly increasing thereafter. *CNOT4* was identified as a transcript more abundant in the IVP than in IVD 4-cell stage embryos on microarray, but this difference was not confirmed by qRT-PCR, while at the late 8-cell stage we have detected significantly more transcript in IVD embryos, compared to IVP (Fig. 4F).

We used two different culture media (Menezes B2, COOK) for in vitro culture. The differences in gene expression were minimal between embryos cultured in Menezes B2 or COOK during development from the 2-cell to morula stage. Embryos cultured in Menezes B2 medium exhibited a higher level of mRNA in all investigated genes at blastocyst and hatched blastocyst. This difference was not significant in majority of investigated genes because of high variability of the mRNA level in blastocyst and hatched blastocyst stages. Most probably, embryos in Menezes B2 medium developed faster in the blastocyst stage and resulted higher number of cells in individual blastocysts exhibited a higher level of mRNA. From this point of view, Menezes B2 medium is superior to COOK medium for the production of bovine blastocysts.

4. Conclusions

In summary, using microarray analysis and protein-protein interaction modelling, *CUL1*, *FBL* and *CNOT4* genes were chosen for subsequent particular analysis. The transcription variant 1 of Cullin 1-like mRNA was present from MII oocyte till early 8-cell stage, the transcription variant 3 of Cullin 1 became prevalent from late 8-cell stage onward. Cullin 1-like, transcript variant 1 mRNA represents maternal transcript, which is gradually degraded after fertilization and Cullin 1 transcript variant 3 represents new embryonic mRNA synthesized from 8-cell stage on. The molecular basis for this change in Cullin gene expression during bovine embryonic genome activation is not known.

New fibrillarin protein was detected by immunofluorescence already in early 8-cell stage, and its detection correlated with increased level of fibrillarin RNA.

The qRT-PCR analysis revealed significant differences in the level of *BUB3*, *NOLC1*, *PCAF*, *GABPA* and *CNOT4* gene transcripts between IVD and IVP embryos in late 8-cell stage. The complex of these genes represents a suitable tool for answering questions

concerning normal IVD embryos development and optimization of IVP embryo culture conditions.

Appendix. Supplementary data

Supplementary data associated with this article can be found, in the online version, at [doi:10.1016/j.theriogenology.2010.12.019](https://doi.org/10.1016/j.theriogenology.2010.12.019).

Acknowledgments

The authors thank I. Dufort, J. Kankova, M. Kopcikova and V. Pech for their skilful technical assistance, the Laboratory of Confocal and Fluorescence Microscopy, Faculty of Science, Charles University, Prague for technical assistance with confocal imaging and Institute of Microbiology, AS CR, v.v.i, Prague for using their GeneTAC UC4 Microarray Scanner. This study was supported by the Institutional Research Concepts IAPG No. AV0Z50450515, IMIC No. AV0Z50200510, Grant No. 1M0538, GACR project No. 523/09/1035, GACR project No. 204/09/H084, MSM 6215712403, CLONET project MRTN-CT-2006-035468, DFG and VEGA 1/0012/10.

References

- [1] Lonergan P, Fair T. In vitro-produced bovine embryos: dealing with the warts. *Theriogenology* 2008;69:17–22.
- [2] Mourot M, Dufort I, Gravel C, Algriany O, Dieleman S, Sirard MA. The influence of follicle size, FSH-enriched maturation medium, and early cleavage on bovine oocyte maternal mRNA levels. *Mol Reprod Dev* 2006;73:1367–79.
- [3] Russell DF, Baqir S, Bordignon J, Betts DH. The impact of oocyte maturation media on early bovine embryonic development. *Mol Reprod Dev* 2006;73:1255–70.
- [4] Watson AJ, De Sousa P, Caveney A, Barcroft LC, Natale D, Urquhart J, Westhusin ME. Impact of bovine oocyte maturation media on oocyte transcript levels, blastocyst development, cell number, and apoptosis. *Biol Reprod* 2000;62:355–64.
- [5] Telford NA, Watson AJ, Schultz GA. Transition from maternal to embryonic control in early mammalian development: a comparison of several species. *Mol Reprod Dev* 1990;26:90–100.
- [6] Memili E, First NL. Control of gene expression at the onset of bovine embryonic development. *Biol Reprod* 1999;61:1198–207.
- [7] Memili E, Dominko T, First NL. Onset of transcription in bovine oocytes and preimplantation embryos. *Mol Reprod Dev* 1998;51:36–41.
- [8] Gutierrez-Adan A, Rizos D, Fair T, Moreira PN, Pintado B, de la Fuente J, Boland MP, Lonergan P. Effect of speed of development on mRNA expression pattern in early bovine embryos cultured in vivo or in vitro. *Mol Reprod Dev* 2004;68:441–8.
- [9] McHughes CE, Springer GK, Spate LD, Li R, Woods R, Green MP, Korte SW, Murphy CN, Green JA, Prather RS. Identification and quantification of differentially represented transcripts in in vitro and in vivo derived preimplantation bovine embryos. *Mol Reprod Dev* 2009;76:48–60.

- [10] Corcoran D, Fair T, Park S, Rizos D, Patel OV, Smith GW, Coussens PM, Ireland JJ, Boland MP, Evans AC, Lonergan P. Suppressed expression of genes involved in transcription and translation in *in vitro* compared with *in vivo* cultured bovine embryos. *Reproduction* 2006;131:651–60.
- [11] Adjaye J, Herwig R, Brink TC, Herrmann D, Greber B, Sudheer S, Groth D, Carnwath JW, Lehrach H, Niemann H. Conserved molecular portraits of bovine and human blastocysts as a consequence of the transition from maternal to embryonic control of gene expression. *Physiol Genomics* 2007;31:315–27.
- [12] Vigneault C, Gravel C, Vallee M, McGraw S, Sirard MA. Unveiling the bovine embryo transcriptome during the maternal to embryonic transition. *Reproduction* 2009;137:245–57.
- [13] Sirard MA, Dufort I, Vallee M, Massicotte L, Gravel C, Reghenas H, Watson AJ, King WA, Robert C. Potential and limitations of bovine-specific arrays for the analysis of mRNA levels in early development: preliminary analysis using a bovine embryonic array. *Reprod Fertil Dev* 2005;17:47–57.
- [14] Pavlok A, Lucas-Hahn A, Niemann H. Fertilization and developmental competence of bovine oocytes derived from different categories of antral follicles. *Mol Reprod Dev* 1992;31:63–7.
- [15] Kues WA, Sudheer S, Herrmann D, Carnwath JW, Havlicek V, Besenfelder U, Lehrach H, Adjaye J, Niemann H. Genome-wide expression profiling reveals distinct clusters of transcriptional regulation during bovine preimplantation development *in vivo*. *Proc Natl Acad Sci USA* 2008;105:19768–73.
- [16] Besenfelder U, Havlicek V, Mosslacher G, Brem G. Collection of tubal stage bovine embryos by means of endoscopy. A technique report. *Theriogenology* 2001;55:837–45.
- [17] Robertson I, Nelson R. E., Certification and identification of the embryo. In: *Manual of the International Embryo Transfer Society: a procedural guide and general information for the use of embryo transfer technology emphasizing sanitary procedures*, 3rd ed.; 1998, p. 103–116.
- [18] Saeed AI, Sharov V, White J, Li J, Liang W, Bhagabati N, Braisted J, Klapa M, Currier T, Thiagarajan M, Sturn A, Snuffin M, Rezantsev A, Popov D, Ryltsov A, Kostukovich E, Borisovskiy I, Liu Z, Vinsavich A, Trush V, Quackenbush J. TM4: a free, open-source system for microarray data management and analysis. *Biotechniques* 2003;34:374–8.
- [19] Yang YH, Dudoit S, Luu P, Lin DM, Peng V, Ngai J, Speed TP. Normalization for cDNA microarray data: a robust composite method addressing single and multiple slide systematic variation. *Nucleic Acids Res* 2002;30:e15.
- [20] Tusher VG, Tibshirani R, Chu G. Significance analysis of microarrays applied to the ionizing radiation response. *Proc Natl Acad Sci USA* 2001;98:5116–21.
- [21] Brown KR, Jurisica I. Online predicted human interaction database. *Bioinformatics* 2005;21:2076–82.
- [22] Pavesi G, Zambelli F, Caggese C, Pesole G. Exalign: a new method for comparative analysis of exon-intron gene structures. *Nucleic Acids Res* 2008;36:e47.
- [23] Bui LC, Leandri RD, Renard JP, Duranthon V. SSH adequacy to preimplantation mammalian development: scarce specific transcripts cloning despite irregular normalisation. *BMC Genomics* 2005;6:155.
- [24] Staessen C, Janssenswillen C, De Clerck E, Van Steirteghem A. Controlled comparison of commercial media for human *in vitro* fertilization: Menezo B2 medium versus Medi-Cult universal and BM1 medium. *Hum Reprod* 1998;13:2548–54.
- [25] Bosu DR, Kipreos ET. Cullin-RING ubiquitin ligases: global regulation and activation cycles. *Cell Div* 2008;3:7.
- [26] Freed E, Lacey KR, Huie P, Lyapina SA, Deshaies RJ, Stearns T, Jackson PK. Components of an SCF ubiquitin ligase localize to the centrosome and regulate the centrosome duplication cycle. *Genes Dev* 1999;13:2242–57.
- [27] Penetier S, Uzbekova S, Guyader-Joly C, Humblot P, Mermilod P, Dalbies-Tran R. Genes preferentially expressed in bovine oocytes revealed by subtractive and suppressive hybridization. *Biol Reprod* 2005;73:713–20.
- [28] Dealy MJ, Nguyen KV, Lo J, Gstaiger M, Krek W, Elson D, Arbeit J, Kipreos ET, Johnson RS. Loss of Cull1 results in early embryonic lethality and dysregulation of cyclin E. *Nat Genet* 1999;23:245–8.
- [29] Wang Y, Penfold S, Tang X, Hattori N, Riley P, Harper JW, Cross JC, Tyers M. Deletion of the Cull1 gene in mice causes arrest in early embryogenesis and accumulation of cyclin E. *Curr Biol* 1999;9:1191–4.
- [30] Marin I. Diversification of the cullin family. *BMC Evol Biol* 2009;9:267.
- [31] Hwang KC, Cui XS, Park SP, Shin MR, Park SY, Kim EY, Kim NH. Identification of differentially regulated genes in bovine blastocysts using an annealing control primer system. *Mol Reprod Dev* 2004;69:43–51.
- [32] Davis W Jr, Schultz RM. Developmental change in TATA-box utilization during preimplantation mouse development. *Dev Biol* 2000;218:275–83.
- [33] Svarcova O, Laurincik J, Avery B, Mlynec M, Niemann H, Maddox-Hyttel P. Nucleolar development and allocation of key nucleolar proteins require *de novo* transcription in bovine embryos. *Mol Reprod Dev* 2007;74:1428–35.
- [34] Laurincik J, Schmoll F, Mahabir E, Schneider H, Stojkovic M, Zakhartchenko V, Prella K, Hendrixen PJ, Voss PL, Moeszlacher GG, Avery B, Dieleman SJ, Besenfelder U, Muller M, Ochs RL, Wolf E, Schellander K, Maddox-Hyttel P. Nucleolar proteins and ultrastructure in bovine *in vivo* developed, *in vitro* produced, and parthenogenetic cleavage-stage embryos. *Mol Reprod Dev* 2003;65:73–85.
- [35] Isaac C, Yang Y, Meier UT. Nopp140 functions as a molecular link between the nucleolus and the coiled bodies. *J Cell Biol* 1998;142:319–29.
- [36] Miao LH, Chang CJ, Tsai WH, Lee SC. Identification and characterization of a nucleolar phosphoprotein, Nopp140, as a transcription factor. *Mol Cell Biol* 1997;17:230–9.
- [37] Li D, Meier UT, Dobrowolska G, Krebs EG. Specific interaction between casein kinase 2 and the nucleolar protein Nopp140. *J Biol Chem* 1997;272:3773–9.
- [38] Chen HK, Pai CY, Huang JY, Yeh NH. Human Nopp140, which interacts with RNA polymerase I: implications for rRNA gene transcription and nucleolar structural organization. *Mol Cell Biol* 1999;19:8536–46.
- [39] Baran V, Brochard V, Renard JP, Flechon JE. Nopp 140 involvement in nucleologenesis of mouse preimplantation embryos. *Mol Reprod Dev* 2001;59:277–84.
- [40] Logarinho E, Resende T, Torres C, Bousbaa H. The human spindle assembly checkpoint protein Bub3 is required for the establishment of efficient kinetochore-microtubule attachments. *Mol Biol Cell* 2008;19:1798–813.
- [41] Kalitsis P, Earle E, Fowler KJ, Choo KH. Bub3 gene disruption in mice reveals essential mitotic spindle checkpoint function during early embryogenesis. *Genes Dev* 2000;14:2277–82.
- [42] Gasca S, Pellestor F, Assou S, Loup V, Anahory T, Dechaud H, De Vos J, Hamamah S. Identifying new human oocyte marker

- genes: a microarray approach. *Reprod Biomed Online* 2007;14:175–83.
- [43] Yang XJ, Ogryzko VV, Nishikawa J, Howard BH, Nakatani Y. A p300/CBP-associated factor that competes with the adenoviral oncoprotein E1A. *Nature* 1996;382:319–24.
- [44] Yamauchi T, Yamauchi J, Kuwata T, Tamura T, Yamashita T, Bae N, Westphal H, Ozato K, Nakatani Y. Distinct but overlapping roles of histone acetylase PCAF and of the closely related PCAF-B/GCN5 in mouse embryogenesis. *Proc Natl Acad Sci USA* 2000;97:11303–6.
- [45] Risteovski S, O’Leary DA, Thornell AP, Owen MJ, Kola I, Hertzog PJ. The ETS transcription factor GABPalph α is essential for early embryogenesis. *Mol Cell Biol* 2004;24:5844–9.
- [46] Kinoshita K, Ura H, Akagi T, Usuda M, Koide H, Yokota T. GABPalph α regulates Oct-3/4 expression in mouse embryonic stem cells. *Biochem Biophys Res Commun* 2007;353:686–91.
- [47] Lenssen E, James N, Pedruzzi I, Dubouloz F, Cameroni E, Bisig R, Maillet L, Werner M, Roosen J, Petrovic K, Winderickx J, Collart MA, De Virgilio C. The Ccr4-Not complex independently controls both Msn2-dependent transcriptional activation—via a newly identified Glc7/Bud14 type I protein phosphatase module—and TFIID promoter distribution. *Mol Cell Biol* 2005;25:488–98.
- [48] Tucker M, Valencia-Sanchez MA, Staples RR, Chen J, Denis CL, Parker R. The transcription factor associated Ccr4 and Caf1 proteins are components of the major cytoplasmic mRNA deadenylase in *Saccharomyces cerevisiae*. *Cell* 2001;104:377–86.
- [49] Azzouz N, Panasenko OO, Colau G, Collart MA. The CCR4-NOT complex physically and functionally interacts with TRAMP and the nuclear exosome. *PLoS One* 2009;4:e6760.
- [50] Gaillard H, Tous C, Botet J, Gonzalez-Aguilera C, Quintero MJ, Viladevall L, Garcia-Rubio ML, Rodriguez-Gil A, Marin A, Arino J, Revuelta JL, Chavez S, Aguilera A. Genome-wide analysis of factors affecting transcription elongation and DNA repair: a new role for PAF and Ccr4-not in transcription-coupled repair. *PLoS Genet* 2009;5:e1000364.
- [51] Albert TK, Hanzawa H, Legtenberg YI, de Ruwe MJ, van den Heuvel FA, Collart MA, Boelens R, Timmers HT. Identification of a ubiquitin-protein ligase subunit within the CCR4-NOT transcription repressor complex. *EMBO J* 2002;21:355–64.
- [52] Panasenko O, Landrieux E, Feuermann M, Finka A, Paquet N, Collart MA. The yeast Ccr4-Not complex controls ubiquitination of the nascent-associated polypeptide (NAC-EGD) complex. *J Biol Chem* 2006;281:31389–98.
- [53] Mersman DP, Du HN, Fingerman IM, South PF, Briggs SD. Polyubiquitination of the demethylase Jhd2 controls histone methylation and gene expression. *Genes Dev* 2009;23:951–62.

Publication 4:

Bovine preimplantation embryos with silenced nucleophosmin mRNA are able to develop until the blastocyst stage due to preservation of sufficient protein amount.

Toralova T, Benesova V, Vodickova Kepkova K, Vodicka P, Susor A, Kanka J.

Submitted to Biology of Reproduction

Bovine preimplantation embryos with silenced nucleophosmin mRNA are able to develop until the blastocyst stage due to preservation of sufficient protein amount

Tereza Toralová¹, Veronika Benešová^{1,2}, Kateřina Vodičková Kepková¹, Petr Vodička¹, Andrej Šušor³, Jiří Kaňka^{1,4}

¹ Institute of Animal Physiology and Genetics v.v.i. Academy of Sciences of the Czech Republic, Department of Reproductive and Developmental Biology, Rumburská 89, 277 21 Liběchov, Czech Republic

² Charles University in Prague, Faculty of Science, Albertov 6, 128 43 Prague, Czech Republic

³ Center for Reproductive Sciences, Department of Obstetrics, Gynecology and Reproductive Sciences, University of California, San Francisco, CA 94143-0556, USA.

Short title: Maternal nucleophosmin is stored until blastocyst

Summary sentence: Maternal nucleophosmin is stored throughout the whole preimplantation development, even though the transcription of nucleophosmin from embryonic genome starts at late 8-cell stage.

Keywords: preimplantation development, nucleophosmin/Npm1/b23, nucleolus, maternal protein, embryonic genome activation

Grant support: Major funding was provided by GACR 523/09/1035. TT was supported also by GACR 204/09/H084. VB and TT were supported by GAUK 43-251133.

⁴ **Corresponding author:** Jiří Kaňka, Institute of Animal Physiology and Genetics v.v.i. Academy of Sciences of the Czech Republic, Department of Reproductive and Developmental Biology, Rumburská 89, 277 21 Liběchov, Czech Republic

E-mail: kanka@iapg.cas.cz

Abstract

This study was conducted to investigate the effect of silencing nucleophosmin on the development of in vitro produced bovine embryos. Nucleophosmin is an abundant multifunctional nucleolar phosphoprotein that participates for example in ribosome biogenesis or centrosome duplication control. We showed that although the transcription of embryonic nucleophosmin started already at late 8-cell stage, the maternal protein was stored throughout the whole preimplantation development and was sufficient for the progression to the blastocyst stage. At the beginning of embryogenesis, the translation occurs on maternally-derived ribosomes, the functionally active nucleoli emerge during the fourth cell cycle in bovines. We found that nucleophosmin localization reflected the nucleolar formation during bovine preimplantation development. The protein was detectable from the beginning of embryonic development. Before embryonic genome activation, it was dispersed throughout the nucleoplasm. The typical nucleolar localization emerged with the formation of active nucleoli. At the blastocyst stage, nucleophosmin tended to localize especially to the trophectoderm. To see for how long is maternal nucleophosmin preserved we silenced the nucleophosmin mRNA using RNA interference approach. Although a large portion of nucleophosmin was degraded in embryos with silenced nucleophosmin mRNA (decrease by 86.8%), an amount sufficient for normal development was preserved and we detected only a temporal delay in nucleophosmin relocalization to nucleoli. Moreover, we observed no nuclear-shape or cytoskeleton defects previously found in somatic cells and only a slight decrease in embryonic developmental competence. Thus, our results show that the preserved amount of maternal nucleophosmin is sufficient for preimplantation development of bovine embryo.

Introduction

The preimplantation development of mammals still hides many secrets, especially regarding gene expression. After fertilization, the embryonic genome is gradually activated, starting with minor genome activation, presumably initiated at 2-4-cell stage in bovines and followed by major genome activation at late 8-cell stage [1, 2]. Although the role of many transcripts during early embryogenesis was revealed [3, 4, 5, 6] and many potentially important genes were identified [7], [8, 9] the role of plenty of others is still far from clear.

Nucleophosmin (NPM1; B23; numatrin; NO38) is an abundant multifunctional phosphoprotein, whose most important roles are rRNA processing, ribosome biogenesis and centrosome duplication control [10, 11, 12, 13]. Moreover, nucleophosmin acts as a histone chaperone and thus is involved in controlling chromatin transcription [14]. Much like many other proteins engaged in ribosome biogenesis, nucleophosmin shuttles between nucleolus and cytoplasm or non-nucleoli region of the nucleus [10, 15, 16, 17] and participates in protein transport, for example of p120 [16]; Rex protein [18]; Rev protein [19] or nucleolin [20].

At the beginning of mammalian embryogenesis all the mRNAs and plenty of the proteins used by the embryo come from reserves that were generated during oocyte maturation. Nucleophosmin seems to originate from maternal reserves at least until the 8-cell stage when it starts to transfer to the developing nucleolus in bovine preimplantation embryo [21].

During the first three cycles electron-dense spherical masses of tightly packed fibrils, called nucleolar precursor bodies (NPBs), are present in the embryonic nucleus. Ribosomal RNA synthesis is inactive during this period. Transformation of the NPBs into fibrillo-granular nucleoli at the time of major genome activation represents the formation of typical rRNA synthesizing nucleolus [22, 23, 24, 25]. It has been proposed that nucleophosmin together with nucleolin functions in assembly of preribosomal particles [26]. Nucleophosmin inheres in the peripheral portion of the dense fibrillar component and the granular component of nucleolus [27] that emerges at the end of fourth cell cycle in cattle [22, 23, 24, 28]. Although it seems that maternal nucleophosmin is stored even after the embryonic genome activation (EGA), it is not able to transfer to the evolving nucleoli in α -amanitin treated embryos and remains dispersed in the nucleoplasm [21, 29].

Silencing of nucleophosmin in somatic cells causes disorganization of nuclear and nucleolar structures with formation of micronuclei, delays mitosis, suspends DNA synthesis and induces activation of p53 [30, 31]. Moreover, many of the *Npm1*^{-/-} cells hold multiple centrosomes or are multinucleated [32]. The role of nucleophosmin in cell proliferation is still far from clear. Nucleophosmin is generally overexpressed in proliferating cells, but on the other hand, it is important for the maintenance of genome stability and acts as proliferative suppressor [32]. The *Npm1*^{-/-} mouse embryos implant into the endometrium without any detectable defect, nevertheless they die during the ongoing development [32, 33].

Here we show that though in bovine preimplantation embryos the amount of maternal protein continuously decreases, the remaining extent is sufficient for normal preimplantation development of embryos with silenced nucleophosmin mRNA.

Materials and Methods

In vitro fertilization and embryo culture

Unless otherwise indicated, the chemicals were purchased from Sigma (Sigma-Aldrich, St. Louis, MO) and plastic from Nunclon (Nunc, Roskilde, Denmark).

Bovine embryos were obtained after in vitro maturation of oocytes and their subsequent fertilization and in vitro culture. Briefly, abattoir derived ovaries from cows and heifers were collected and transported in thermocontainers in sterile saline at about 33°C. The follicles with diameter between 5 and 10 mm were dissected with fine scissors and then punctured. The cumulus-oocyte complexes were evaluated and selected according to the morphology of cumulus and submitted to in vitro maturation in TCM 199 (Earle's salt) supplemented with 20 mM sodium pyruvate, 50 U/ml penicillin, 50 µg/ml streptomycin, 10% estrus cow serum (ECS) and gonadotropins (P.G. 600, 15 U/ml, Intervet, Boxmeer, Holland) without paraffin overlay in four-well dishes under humidified atmosphere for 24 h at 39°C with 5% CO₂.

For in vitro fertilization (IVF), the cumulus oocyte complexes were washed four times in phosphate buffer saline (PBS) and once in fertilization medium Tyrode's albumin lactate pyruvate (TALP) and transferred in groups of up to 30 into four-well dishes containing 250 µl of TALP per well. The TALP medium contained 1.5 mg/ml bovine serum albumin (BSA), 30 µg/ml heparin, 0.25 mM sodium pyruvate, 10 mM lactate and 20 µM

penicillamine. Cumulus–oocyte complexes were then co-incubated with frozen-thawed wash semen from one bull previously tested in the IVF system. Viable spermatozoa were washed in TALP and centrifuged at 100x g for 5 min. Spermatozoa were counted in a haemocytometer and diluted in the appropriate volume of TALP to give a concentration of 2×10^6 spermatozoa/ml. A 250 μ l aliquot of this suspension was added to each fertilization well to obtain a final concentration of 1×10^6 spermatozoa/ml. Plates were incubated under humidified atmosphere with 5% CO₂ for 20 h at 39 °C.

Following fertilization, presumed zygotes were denuded by gentle pipetting, and transferred to EmbryoAssist medium (Origio, Jyllinge, Denmark) supplemented with 10% ECS and cultured in humidified atmosphere of 5% CO₂ - 5% O₂ - 90% N₂ (25 zygotes in 25 μ l of medium under liquid paraffin; Origio). At morula stage the EmbryoAssist medium was replaced by BlastAssist medium and embryos cultivated till hatched blastocyst. The dishes were examined at 24 h post isolation and 32, 44, 56, 92, 104, 120, 156 and 180 hours post fertilization (hpf), and MII oocytes and 2-cell, 4- cell, early 8-cell, late 8-cell embryos, 16-cell embryos, morula, blastocysts and hatched blastocysts were collected at each time point respectively.

Quantification of mRNA expression in individual developmental stages

Poly (A)+ mRNA was extracted from the pools of 20 oocytes and embryos in each stage of development, using a Dynabeads mRNA DIRECT Micro Kit (Invitrogen Dynal AS, Oslo, Norway) according to the manufacturer's instructions. Before isolation, 1 pg of the Luciferase mRNA (Promega, Madison, WI) per oocyte/embryo was added as an external standard. Primer sequences were designed using Beacon Designer 7 from bovine nucleophosmin gene sequence (GenBank accession number NM_001035441). The expression of specific mRNA was measured by quantitative RT-PCR. mRNA equivalent of 1 embryo was amplified by a OneStep RT-PCR kit (Qiagen, Hilden, Germany) with real-time detection using SybrGreen I fluorescent dye. Reaction conditions were: reverse transcription at 50 °C for 30 min, initial activation at 95 °C for 15 min, cycling: denaturation at 94 °C for 15 sec, annealing at 53°C for 20 sec, extension at 72 °C for 30 sec. The final extension step was held for 10 min at 72°C. The real-time RT-PCR reactions were run in duplicates, with all samples (oocytes and all embryo stages) in the same reaction. The experiments were carried out on RotorGene 3000 (Corbett Research,

Mortlake, Australia/Qiagen). Fluorescence data were acquired at 3 °C below the melting temperature to distinguish the possible primer dimers.

The relative concentration of template in different samples was determined using comparative quantification in analysis software (Corbett Research/Qiagen). The results were normalized according to the relative concentration of the external standard (Luciferase). Products were verified by melting analysis and gel electrophoresis on 1.5 % agarose gel with ethidium bromide staining. Experiment was repeated three times.

Alpha-amanitin treatment

To block RNA polymerase II dependent transcription, α -amanitin (Sigma-Aldrich) was added to the culture medium at a final concentration of 100 μ g/ml from 4-cell stage to late 8-cell stage, 44 to 92 hpf. After the α -amanitin treatment, the embryos were washed with PBS, immediately frozen, and stored at -80 °C. Control embryos were collected at the same time interval as their treated counterparts, from the same fertilization/cultivation group, washed with PBS, immediately frozen, and stored at -80 °C. All pools were done in triplicate and contained 20 embryos.

Synthesis of dsRNA

The RNA for nucleophosmin DNA template synthesis was isolated from bovine fibroblasts using RNeasy Mini Kit (Qiagen). The template was synthesized using primers “*Npml* dsRNA” (see Table A). The identity of fibroblastic and embryonic sequence was verified by sequencing. These primers generated amplicons corresponding to the bovine cDNA sequence in GenBank (NM_001035441.1). The green fluorescent protein (*Gfp*) DNA template was amplified from empty p-Bluescript-GFP vector (kindly donated by M. Anger and P. Šolc) using primers “*Gfp* dsRNA” [34] (see Table A). Both pairs of primers were fused with the T7 promoter.

The reverse transcription and the PCR reaction was performed using two-step Phusion RT-PCR kit (Finnzymes, Vantaa, Finland) for nucleophosmin template synthesis; the sole PCR reaction was performed using Phusion Hot Start II DNA Polymerase (Finnzymes) for *Gfp* DNA template synthesis. The reverse transcription was performed with oligo(dT) primers and reaction conditions were: primer extension at 25°C for 10 min, cDNA synthesis at 50°C for 60 min, reaction termination at 85°C for 5 min. The reaction conditions for PCR reaction were: initial denaturation at 98°C for 3 min cycling: denaturation at 98°C for 10 s,

annealing at 55°C for 5 s, extension at 72°C for 30 s. The final extension step was held for 5 min at 72°C. The PCR product was purified using QIAquick PCR Purification Kit (Qiagen) and the identity was confirmed by sequencing.

The DNA template coupled with T7 promoter was transcribed in vitro using MEGAscript RNAi Kit (Ambion). An amount of 1 µg of DNA template was used for each reaction. The reaction mixture was incubated for 5 h at 37°C and the sense and antisense strands were transcribed in the same reaction. The residual DNA template and ssRNA were digested and the dsRNA was purified according to the manufacturer's instruction. 1 µl of RNA acquired by in vitro transcription and 1 µl of final dsRNA were resolved by electrophoresis on 1.5% agarose gel to confirm the integrity of the dsRNA and efficiency of the annealing step.

Zygote microinjection

The zygotes were injected 20 h post fertilization at the stage of two pronuclei. dsRNAs were dissolved in RNase-free water to a final concentration of 800 ng/µl. Two control groups were established – the uninjected group and a group injected with *Gfp* dsRNA.

Zygotes were microinjected with ~ 5 pl of the dsRNA using an MIS-5000 micromanipulator (Burleigh, Exfo Life Sciences, Canada) and PM2000B microinjector (MicroData Instrument, South Plainfield, NJ). Pipettes for microinjection were made using P97 Pipette Puller (Sutter Instrument Company, Novato, CA).

In total 19 independent experiments were performed. Embryos were categorized into the following groups: 1) Embryos injected with nucleophosmin dsRNA (928 zygotes); 2) embryos injected with *Gfp* dsRNA (665 zygotes) and 3) uninjected embryos (795 zygotes). After microinjection, embryos were cultivated under standard conditions and collected at early 8-cell, late 8-cell 16-cell, morula or blastocyst stage (see above). The number of embryos that reached each developmental stage was counted and the morphological state of each embryo was determined using phase-contrast technique.

Evaluation of nucleophosmin mRNA degradation

The embryos were washed using FCW buffer (a component of FastLane Cell SYBR Green Kit; Qiagen) and stored dry and deep-frozen at -80 °C until used. Whole single embryos were lysed in 10 µl of the mixture of Buffer FCPL and gDNA Wipeout Buffer 2 (both components of FastLane Cell RT-PCR kit; Qiagen) according to the manufacturer's instructions and the lysate was directly used for the RT-PCR.

Quantitative RT-PCR was performed using One Step RT-PCR kit (Qiagen) with real time detection using SybrGreen I fluorescent dye. Reaction conditions were: reverse transcription at 50 °C for 30 min, initial activation at 95 °C for 15 min, cycling: denaturation at 94 °C for 20 sec, annealing at temperature according to the primer for 20 sec, extension at 72 °C for 30 sec. The final extension step was held for 10 min at 72 °C. The experiments were carried out on Rotor-Gene 3000 (Corbett Research/Qiagen). Fluorescence data were acquired at 3 °C below the melting temperature to distinguish the possible primer dimers. The qRT-PCR data were determined using serial dilutions; the standard curve was created using the takeoff points. The takeoff points were calculated by Internal RotorGene software (Corbett Research, Mortlake, Australia) and defined as the cycle at which the second derivative curve is at 20% of the maximum rate of fluorescence and indicates the transition to the exponential phase (RotorGene 3000 operation manual; Corbett Research). The starting amount of corresponding RNA in analysed samples was determined by appointing the takeoff points to the curve. Products were verified by melting analysis and gel electrophoresis on 1.5% agarose gel with ethidium bromide staining.

Immunofluorescence

Nucleophosmin staining

Embryos were fixed in 4% paraformaldehyde supplemented with 0.5% (v/v) TritonX-100 for 50 min at 4°C. Fixed embryos were processed immediately or stored in PBS up to 3 weeks at 4°C. After washing in PBS the embryos were incubated in 0.5% (v/v) TritonX-100 for 15 min. All subsequent steps were done in PBS supplemented with 0.3% (w/v) bovine serum albumin (BSA) and 0.05% (w/v) saponin (PBS/BSA/sap). Embryos were blocked with 2% (v/v) normal goat serum (NGS; Millipore Biosciences; St Charles, MO) for 1 h and incubated with mouse anti-nucleophosmin antibody (Invitrogen, Carlsbad, CA) 1:100 in PBS/BSA/sap overnight at 4°C. After thorough washing the embryos were incubated with goat anti-mouse antibody conjugated with Alexa 594 in PBS/BSA/sap for 1 h at room temperature darkling. Controls of immunostaining specificity were carried out by omitting primary antibody or using another species-specific secondary antibody conjugate.

Nucleophosmin and alpha-tubulin doublestaining

Embryos were fixed in 4% paraformaldehyde for 50 min at 4°C and subsequently permeabilized in 0.5% TritonX-100 for 10 min at room temperature. Fixed embryos were

processed immediately or stored in PBS up to 3 weeks at 4°C. All staining steps were done in PBS/BSA/sap. Embryos were blocked with 2% (v/v) NGS for 1 h and incubated with mouse anti-nucleophosmin antibody 1:100 in PBS/BSA/sap overnight at 4°C. After thorough washing the embryos were incubated with goat anti-mouse antibody conjugated with Alexa 594 in PBS/BSA/sap for 1 h at room temperature and from now on, all steps were performed darkling. After thorough washing, the embryos were incubated in 2% (v/v) NGS for 1 h and incubated with rabbit anti-alpha-tubulin antibody (Abcam, Cambridge, UK) 1:500 in PBS/BSA/sap overnight at 4°C. After thorough washing the embryos were incubated in goat anti-rabbit antibody conjugated with FITC (Santa Cruz Biotechnology, Santa Cruz, CA) for 1 h. Controls of immunostaining specificity were carried out by omitting one or both primary antibodies, while using both secondary antibodies.

The nuclei were stained and the embryos were mounted on glass slides using VECTASHIELD HardSet Mounting Medium with DAPI (Vector Laboratories, Peterborough, UK). The samples were examined with Leica TCS SP confocal laser-scanning microscope (Leica Microsystems AG, Wetzlar, Germany). The images were processed using the ImageJ software (NIH, Bethesda, MD; <http://rsb.info.nih.gov/ij>).

Western blotting

Unless otherwise indicated, chemicals were purchased from Sigma.

Embryos and oocytes (45 per extract for uninjected MII, 4c and morulas or 26 per extract for injected 4c and morulas and corresponding uninjected controls) were subjected to 10% SDS-PAGE; proteins were transferred from gels to Immobilon P membrane (Milipore Biosciences, Billerica, MA) using a semidry blotting system (Whatman Biometra GmbH) for 28 min at 5 mA/cm². The blocking of the membrane was performed in 5% nonfat milk in TBS-Tween buffer (TBS-T; 20mM Tris, pH 7,4, 137mM NaCl and 0.5% Tween 20) for 1 h and incubated overnight with mouse anti-nucleophosmin antibody (1:1000) in 5% nonfat milk/TBS-T. After washing in TBS-T, the membranes were incubated with horseradish peroxidase-conjugated donkey anti-mouse IgG antibody (1:7500; Jackson Immuno Research) in 3% nonfat milk/TBS-T for 1 h at room temperature. Proteins were visualised by the ECL-PLUS detection system (Amersham Biosciences) according to the manufacturer's instruction. The data were processed using Quantity One software (Bio-Rad, Hercules, CA)

Statistical analyses

The data were analysed using SigmaStat 3.0 software (Jandel Scientific, San Rafael, CA). The Student's t-test or Mann-Whitney Rank Sum tests were used. $P \leq 0.05$ was considered as statistically significant.

Results

The expression of nucleophosmin mRNA from embryonic genome starts at late 8-cell stage
qRT-PCR analysis of the expression pattern of nucleophosmin transcript during *in vitro* culture (from MII oocyte stage until blastocyst stage) showed a slow decrease in transcript level from MII oocyte till early 8-cell stage embryo and increase in late 8-cell stage embryo. The mRNA level then remained approximately the same until the blastocyst stage. To confirm that the detected transcript represents newly synthesized mRNA, embryos were cultured from 4-cell till 8-cell stage in the presence of RNA polymerase II inhibitor α -amanitin at a final concentration of 100 $\mu\text{g/ml}$. A significant decrease in nucleophosmin transcript abundance was detected in α -amanitin-treated late 8-cell stage embryos in comparison to controls. (Fig. 1)

The dynamics of nucleophosmin localization and expression throughout bovine preimplantation development

Since there were some contradictory studies concerning nucleophosmin localization during early embryo development of cattle [28, 35], we performed the immunofluorescence analysis of in-vitro cultured embryos from MII oocyte to blastocyst stage (Fig. 2).

We did not detect any nucleophosmin staining in MII oocytes using immunofluorescence. The accuracy of staining was verified by holding a few cumulus cells as a positive control. However, in pre-EGA embryos (2-cell and 4-cell embryos), nucleophosmin was very abundant and was distributed mainly in the nucleoplasm. During mitosis, the protein dispersed throughout whole blastomere with a very slight colocalization with chromatin. With the formation of nucleolus, nucleophosmin formed shell-like structures (early 8-cell stage) and consequently, as the nucleolus became functionally active, the localisation pattern shifted to be typical for somatic cell nucleoli (late 8-cell stage and beyond, i.e. after EGA). By contrast to mitotic blastomeres of pre-EGA embryos and somatic cells, we did not detect colocalization of nucleophosmin and chromatin in post-EGA embryos, and the staining in mitotic blastomeres was generally much weaker. In late blastocysts (starting

with day 7) nucleophosmin localized predominantly to the trophectoderm (TE). The difference became most apparent in hatched blastocysts.

Further, we analysed MII oocytes, 4-cell embryos and morulas using western blot (Fig. 3). In contrast to immunofluorescence results, we detected a clear band in MII oocytes. In comparison to the embryos, the oocyte band migrated markedly more slowly, which suggests phosphorylation of the protein. The abundance of the nucleophosmin increased from 4-cell stage embryos to morulas.

Maternal nucleophosmin is stored throughout the whole preimplantation development

To reveal whether nucleophosmin mRNA expression is required for early embryo development, we silenced nucleophosmin mRNA by microinjection of nucleophosmin dsRNA into bovine zygotes. The microinjection of nucleophosmin dsRNA efficiently (Fig. 4) and specifically (Fig. 5) caused degradation of nucleophosmin mRNA in bovine preimplantation embryos.

The nucleophosmin mRNA was reduced by 86.8% ($P < 0.001$) in comparison to uninjected control and by 83.6% ($P < 0.001$) in comparison to *Gfp* dsRNA injected control. No significant difference was found in the abundance of nucleophosmin mRNA between the uninjected group and *Gfp* dsRNA injected group ($P > 0.05$). The experiment was repeated four times.

To verify the specificity of nucleophosmin mRNA degradation, we measured the level of mRNA of two control genes: centromeric protein F (*Cenpf*) and C-type lectin domain family 2, member D (*Clec2d*). We did not find any significant difference in mRNA levels between individual groups ($p > 0.05$ in each case). The experiment was repeated four times.

When analysed using immunofluorescence, we detected neither reduction of protein abundance nor protein localization changes in embryos injected with nucleophosmin dsRNA when compared to both control groups whether in embryos arrested in early stages or normally developing embryos (Fig. 6). We only detected a slight delay in nucleophosmin relocalization from nucleoplasm to nucleoli. In 8-cell stage only 5 of 60 blastomeres (8.3%) in uninjected group and 3 of 53 blastomeres (5.6%) in *Gfp* dsRNA injected group still displayed entirely nucleoplasmic localisation, while the same was true for 18 of 73 blastomeres (24.6%) in nucleophosmin dsRNA injected embryos. Nevertheless, the

localization was purely nucleolar already at the 16-cell stage in all three experimental groups.

However, the results concerning protein amount were based solely on visual observation. Since we found that the protein amount increases from 4-cell embryos to morulas, we wanted to see whether this increase is present also in the embryos injected with nucleophosmin dsRNA. We therefore performed immunoblotting analysis, which revealed considerable decrease in protein abundance in nucleophosmin dsRNA injected embryos compared to uninjected control and a decrease in protein amount from 4-cell embryos to morulas in injected embryos (Fig. 7).

Developmental competence of nucleophosmin dsRNA injected embryos is not significantly diminished

To investigate the effect of nucleophosmin mRNA silencing on preimplantation development, we monitored the capacity of embryos in all three experimental groups to develop from 2-cell stage to blastocyst stage. We found a slight decrease in the number of embryos injected with nucleophosmin dsRNA that reached the blastocyst stage. This deterioration was clearly noticeable in comparison to both control groups (mean \pm S.D.: uninjected control: 31.67% \pm 4.78; *Gfp* dsRNA injected control: 26.76% \pm 6.64; nucleophosmin dsRNA injected: 13.96% \pm 4.20) but the difference was not statistically significant. (A significant, however boundary, p-value ($p=0.05$) was found when comparing nucleophosmin dsRNA injected group and uninjected group) (Fig. 8). The experiment was repeated four times.

Of several defects found in *Npm1*^{-/-} cells and embryos [30, 31, 32, 33], we focused on the defect in tubulin polymerization. We wanted to know whether the decrease in protein abundance proven by western blot causes some developmental defects or whether the residual protein is sufficient. We did not detect any nucleus shape defect or cytoskeleton deformation (Fig. 9).

Discussion

The function of nucleophosmin in somatic cells and the presently available results concerning its expression in early embryos suggest its potential importance during preimplantation development [21, 29, 30, 31]. To provide an experimental basis for this assumption, we determined the level of nucleophosmin mRNA expression in individual

developmental stages of early embryogenesis with special emphasis on the EGA stage. The expression profile of genes in individual stages reflects their importance during preimplantation development, genes activated immediately at EGA being assumed to be the most important. Since we found that the embryonic transcription starts from nucleophosmin gene at late 8-cell stage, the transcription of nucleophosmin from embryonic genome seems to be necessary and hence we proceeded to further analysis.

We wanted to determine the expression and localization pattern of nucleophosmin protein during the whole preimplantation development from MII oocyte to the blastocyst stage. In agreement with Fair et al. [35], we did not detect any immunofluorescence staining in MII oocytes. Since there was a strong assumption that the protein is handed down from oocyte to embryo [21, 29], we verified the results using western blot. By this method, we detected a clear band, which displayed an evident mobility shift in MII oocytes when compared to 4-cell embryos and morulas (Fig. 3). This shift is likely caused by phosphorylation, which is characteristic for mitotic nucleophosmin in somatic cells [36, 37]. Since we have used a monoclonal antibody targeted to the C-terminus of the protein, the phosphorylation could hinder the antibody binding to the epitope during immunofluorescence staining. Similarly we found only very weak staining in post-EGA mitotic blastomeres (Fig. 2H-H'). In the following embryo development, nucleophosmin localization clearly reflected the formation of the nucleolus. In embryos before EGA (pre-EGA embryos), where no functional nucleolus is present, the protein was dispersed throughout the nucleoplasm and during mitosis it diffused all over the blastomere (Fig. 2B-C'). Our immunofluorescence results in pre-EGA embryos are in strong contrast with those of Laurincik et al. [28] and Svarcova et al. [21], who show nucleophosmin staining from the 4-cell stage, and only in some embryos. These discrepancies can however be caused by different culture media, which strongly influence gene expression [9] or by the usage of different antibodies [38].

As the vacuolized nucleoli are being formed at 8-cell stage, nucleophosmin generates the so called shell-like structures (Fig. 2D-E'). After EGA, functionally active nucleolus is present from the beginning of the cell-cycle and nucleophosmin displays its typical localization pattern characteristic for somatic cells. From day 7 blastocyst, nucleophosmin tended to localize mainly to trophectoderm cells and the distinction was apparent especially in hatched blastocysts. Since nucleophosmin is overexpressed in rapidly dividing cells and its

downregulation suppresses proliferation [39, 40, 41, 42], the elevated expression in TE cells is likely in connection with preparing embryo for implantation. Correspondingly, Colombo et al. [33] and Grisendi et al. [32] showed that the placental structures in *Npm1*^{-/-} mice embryos are smaller, even though normally developed. Interestingly, Johansson and Simonsson [43] reported that nucleophosmin forms complexes with ICM markers POU5F1, Sox2 and Nanog in embryonic stem (ES) cells. It is possible that in these protein interactions one protein silences its binding partner or that nucleophosmin is still needed for ICM development, but low amount is sufficient in this phase.

Svarcova et al. [21] in bovine embryos and Bjerregaard et al. [29] in porcine embryos reported that maternal nucleophosmin is stored at least over the EGA stage, but it is not able to localize to the nucleoli. However, they both used general transcription inhibitor α -amanitin. Hence, it cannot be distinguished whether maternal nucleophosmin is naturally preserved or whether it is just not degraded due to the absence of another protein. Similarly, it cannot be distinguished whether maternal protein is not able to translocate to the nucleolus or whether this is caused by the absence of some nucleophosmin translocating protein, or maybe by a general nucleolar biogenesis defect. The very intensive nucleophosmin staining in pre-EGA embryos (Fig. 2B'-C'') speaks in favour of hoarding long-term reserves of the protein. To see for how long maternal protein can stand for embryonic nucleophosmin, we performed an RNAi experiment. Both maternal and embryonic mRNA is silenced using this method. We showed that although a large portion of the protein is degraded (Fig. 7), an amount still sufficient for normal development is preserved (Fig. 6 and 8) and that only temporal delay in relocalization to nucleoli can be detected. We observed no nuclear-shape or cytoskeleton defects reported by Amin et al. [30] (Fig. 9) and only an undistinguished difference in the developmental competence. This likely shows that the preserved amount of maternal protein is mostly sufficient. However, since the mRNA expression in single preimplantation embryo is very variable (see standard derivation bars in Fig. 4) and the cell number increases, the protein level might become insufficient for some embryos with lower starting amount of the protein, which causes the slight decrease in developmental competence. In favour of the protein preservation speaks also the result on murine *Npm1*^{-/-} mutants [32, 33]. The *Npm1*^{-/-} embryos arrest their

development at around midgestation and until then, they likely utilize the pool of nucleophosmin protein synthesized from maternal mRNA.

In conclusion, we show that the transcription of nucleophosmin mRNA from embryonic genome is activated at late 8-cell stage. The protein is present from the beginning of embryonic development and its localization reflects the formation of the nucleoli. A small amount of maternal protein is preserved throughout the whole preimplantation development and enables almost normal growth of embryos with silenced nucleophosmin mRNA.

Acknowledgement

The authors are indebted to Pavla Karabinova and Lucie Liskova for their helpful comments and expert assistance during the experiments, to Monika Kopcikova, Jaroslava Kankova, Jitka Klucinova, Jaroslava Sestakova and Jaroslava Supolikova for the excellent technical assistance and to Ondrej Sebesta for his help with the confocal microscope.

References:

1. Memili E, First NL. Developmental changes in RNA polymerase II in bovine oocytes, early embryos, and effect of alpha-amanitin on embryo development. *Mol Reprod Dev* 1998; 51:381-389.
2. Kanka J. Gene expression and chromatin structure in the pre-implantation embryo. *Theriogenology* 2003; 59:3-19.
3. Nganvongpanit K, Müller H, Rings F, Gilles M, Jennen D, Hölker M, et al. Targeted suppression of E-cadherin gene expression in bovine preimplantation embryo by RNA interference technology using double-stranded RNA. *Mol Reprod Dev* 2006; 73:153-163.
4. Nganvongpanit K, Müller H, Rings F, Hoelker M, Jennen D, Tholen E, et al. Selective degradation of maternal and embryonic transcripts in in vitro produced bovine oocytes and embryos using sequence specific double-stranded RNA. *Reproduction* 2006; 131:861-874.

5. Toralová T, Susor A, Nemcová L, Kepková K, Kanka J. Silencing CENPF in bovine preimplantation embryo induces arrest at 8-cell stage. *Reproduction* 2009; 138:783-791.
6. Salilew-Wondim D, Hölker M, Rings F, Phatsara C, Mohammadi-Sangcheshmeh A, Tholen E, et al. Depletion of BIRC6 leads to retarded bovine early embryonic development and blastocyst formation in vitro. *Reprod. Fertil Dev* 2010; 22:564-579.
7. Hamatani T, Carter MG, Sharov AA, Ko MSH. Dynamics of global gene expression changes during mouse preimplantation development. *Dev Cell* 2004; 6:117-131.
8. Kanka J, Kepková K, Nemcová L. Gene expression during minor genome activation in preimplantation bovine development. *Theriogenology* 2009; 72:572-583.
9. Kepkova KV, Vodicka P, Toralova T, Lopatarova M, Cech S, Dolezel R, et al. Transcriptomic analysis of in vivo and in vitro produced bovine embryos revealed a developmental change in cullin 1 expression during maternal-to-embryonic transition. *Theriogenology* 2011; 75:1582-1595.
10. Borer RA, Lehner CF, Eppenberger HM, Nigg EA. Major nucleolar proteins shuttle between nucleus and cytoplasm. *Cell* 1989; 56:379-390.
11. Savkur RS, Olson MO. Preferential cleavage in pre-ribosomal RNA by protein B23 endoribonuclease. *Nucleic Acids Res* 1998; 26:4508-4515.
12. Hingorani K, Szebeni A, Olson MO. Mapping the functional domains of nucleolar protein B23. *J Biol Chem* 2000; 275:24451-24457.
13. Okuwaki M, Tsujimoto M, Nagata K. The RNA binding activity of a ribosome biogenesis factor, nucleophosmin/B23, is modulated by phosphorylation with a cell cycle-dependent kinase and by association with its subtype. *Mol Biol Cell* 2002; 13:2016-2030.
14. Swaminathan V, Kishore AH, Febitha KK, Kundu TK. Human histone chaperone nucleophosmin enhances acetylation-dependent chromatin transcription. *Mol Cell Biol* 2005; 25:7534-7545.

15. Yung BY, Bor AM, Yang YH. Immunolocalization of phosphoprotein B23 in proliferating and non-proliferating HeLa cells. *Int . Cancer* 1990; 46:272-275.
16. Valdez BC, Perlaky L, Henning D, Saijo Y, Chan PK, Busch H. Identification of the nuclear and nucleolar localization signals of the protein p120. Interaction with translocation protein B23. *J Biol Chem* 1994; 269:23776-23783.
17. Chen D, Huang S. Nucleolar components involved in ribosome biogenesis cycle between the nucleolus and nucleoplasm in interphase cells. *J Cell Biol* 2001; 153:169-176.
18. Adachi Y, Copeland TD, Hatanaka M, Oroszlan S. Nucleolar targeting signal of Rex protein of human T-cell leukemia virus type I specifically binds to nucleolar shuttle protein B-23. *J Biol Chem* 1993; 268:13930-13934.
19. Fankhauser C, Izaurralde E, Adachi Y, Wingfield P, Laemmli UK. Specific complex of human immunodeficiency virus type 1 rev and nucleolar B23 proteins: dissociation by the Rev response element. *Mol Cell Biol* 1991; 11:2567-2575.
20. Li YP, Busch RK, Valdez BC, Busch H. C23 interacts with B23, a putative nucleolar-localization-signal-binding protein. *Eur J Biochem* 1996; 237:153-158.
21. Svarcova O, Laurincik J, Avery B, Mlyncek M, Niemann H, Maddox-Hyttel P. Nucleolar development and allocation of key nucleolar proteins require de novo transcription in bovine embryos. *Mol Reprod Dev* 2007; 74:1428-1435.
22. Camous S, Kopecný V, Fléchon JE. Autoradiographic detection of the earliest stage of [3H]-uridine incorporation into the cow embryo. *Biol Cell* 1986; 58:195-200.
23. King WA, Niar A, Chartrain I, Betteridge KJ, Guay P. Nucleolus organizer regions and nucleoli in preattachment bovine embryos. *J Reprod Fertil* 1988; 82:87-95.
24. Kopecný V, Fléchon JE, Camous S, Fulka J Jr. Nucleologenesi and the onset of transcription in the eight-cell bovine embryo: fine-structural autoradiographic study. *Mol Reprod Dev* 1989; 1:79-90.

25. Pavlok A, Kopecný V, Lucas-Hahn A, Niemann H. Transcriptional activity and nuclear ultrastructure of 8-cell bovine embryos developed by in vitro maturation and fertilization of oocytes from different growth categories of antral follicles. *Mol Reprod.Dev* 1993; 35:233-243.
26. Biggiogera M, Bürki K, Kaufmann SH, Shaper JH, Gas N, Amalric F, et al. Nucleolar distribution of proteins B23 and nucleolin in mouse preimplantation embryos as visualized by immunoelectron microscopy. *Development* 1990; 110:1263-1270.
27. Spector DL, Ochs RL, Busch H. Silver staining, immunofluorescence, and immunoelectron microscopic localization of nucleolar phosphoproteins B23 and C23. *Chromosoma* 1984; 90:139-148.
28. Laurincik J, Thomsen PD, Hay-Schmidt A, Avery B, Greve T, Ochs RL, et al. Nucleolar proteins and nuclear ultrastructure in preimplantation bovine embryos produced in vitro. *Biol Reprod* 2000; 62:1024-1032.
29. Bjerregaard B, Wrenzycki C, Strejcek F, Laurincik J, Holm P, Ochs RL, et al. Expression of nucleolar-related proteins in porcine preimplantation embryos produced in vivo and in vitro. *Biol Reprod* 2004; 70:867-876.
30. Amin MA, Matsunaga S, Uchiyama S, Fukui K. Depletion of nucleophosmin leads to distortion of nucleolar and nuclear structures in HeLa cells. *Biochem. J* 2008; 415:345-351.
31. Amin MA, Matsunaga S, Uchiyama S, Fukui K. Nucleophosmin is required for chromosome congression, proper mitotic spindle formation, and kinetochore-microtubule attachment in HeLa cells. *FEBS Lett* 2008; 582:3839-3844.
32. Grisendi S, Bernardi R, Rossi M, Cheng K, Khandker L, Manova K, et al. Role of nucleophosmin in embryonic development and tumorigenesis. *Nature* 2005; 437:147-153.
33. Colombo E, Bonetti P, Lazzarini Denchi E, Martinelli P, Zamponi R, Marine J-C, et al. Nucleophosmin is required for DNA integrity and p19Arf protein stability. *Mol Cell Biol* 2005; 25:8874-8886.

34. Anger M, Stein P, Schultz RM. CDC6 requirement for spindle formation during maturation of mouse oocytes. *Biol Reprod* 2005; 72:188-194.
35. Fair T, Hyttel P, Lonergan P, Boland MP. Immunolocalization of nucleolar proteins during bovine oocyte growth, meiotic maturation, and fertilization. *Biol Reprod* 2001; 64:1516-1525.
36. Peter M, Nakagawa J, Dorée M, Labbé JC, Nigg EA. Identification of major nucleolar proteins as candidate mitotic substrates of cdc2 kinase. *Cell* 1990; 60:791-801.
37. Negi SS, Olson MOJ. Effects of interphase and mitotic phosphorylation on the mobility and location of nucleolar protein B23. *J Cell Sci* 2006; 119:3676-3685.
38. Shinmura K, Tarapore P, Tokuyama Y, George KR, Fukasawa K. Characterization of centrosomal association of nucleophosmin/B23 linked to Crm1 activity. *FEBS Lett* 2005; 579:6621-6634.
39. Okuwaki M. The structure and functions of NPM1/Nucleophosmin/B23, a multifunctional nucleolar acidic protein. *J Biochem* 2008; 143:441-448.
40. Wang BB, Lu R, Wang WC, Jin Y. Inducible and reversible suppression of Npm1 gene expression using stably integrated small interfering RNA vector in mouse embryonic stem cells. *Biochem. Biophys Res Commun* 2006; 347:1129-1137.
41. Qing Y, Yingmao G, Lujun B, Shaoling L. Role of Npm1 in proliferation, apoptosis and differentiation of neural stem cells. *J Neurol Sci* 2008; 266:131-137.
42. Johansson H, Vizlin-Hodzic D, Simonsson T, Simonsson S. Translationally controlled tumor protein interacts with nucleophosmin during mitosis in ES cells. *Cell Cycle* 2010; 9:2160-2169.
43. Johansson H, Simonsson S. Core transcription factors, Oct4, Sox2 and Nanog, individually form complexes with nucleophosmin (Npm1) to control embryonic stem (ES) cell fate determination. *Aging (Albany NY)* 2010; 2:815-822.

Figure Legends

Figure 1

Relative abundance of nucleophosmin mRNA during bovine preimplantation development. The data were normalized according to the relative concentration of the external standard (luciferase mRNA, 1 pg per oocyte/embryo). Bars shows mean \pm S.D. ^{a,b}Values with different superscripts indicate statistical significance ($P < 0.05$). (MII – MII stage oocytes; 2c – 2-cell embryos; 4c – 4-cell embryos; e8c – early 8-cell embryo; L8c – late 8-cell embryo; L8c AA – late 8-cell embryo cultivated with α -amanitin; mor – morula; bl – blastocyst)

Figure 2

Confocal laser scanning microscopy of oocytes/embryos from MII oocyte to hatched blastocyst. Some of the cumulus cells were retained attached to the MII oocyte as a positive control (A-A'). In E-E' and H-H' single nucleus of early 8-cell and morula stage embryo is shown, respectively. The oocytes/embryos were labeled with mouse monoclonal anti-nucleophosmin antibody (A'-J') and the nuclei were stained with DAPI (A-J). In mergers (A''-J'') nucleophosmin is red, DNA blue. Asterisks in I'' and J'' indicate inner cell mass.

Figure 3

Western blot analysis for the presence of nucleophosmin protein in MII oocytes and embryos in 4-cell (4c) and morula stage. A mobility shift can be seen in MII oocytes.

Figure 4

Relative abundance of nucleophosmin mRNA after injection of nucleophosmin dsRNA. The relative abundance (y-axis) represents the amount of nucleophosmin mRNA in a single embryo normalized to the mean of mRNA expression in control embryos in each developmental stage. Bars shows mean \pm S.D. ^{a,b}Values with different superscripts indicate statistical significance ($P < 0.05$).

Figure 5

The expression of control genes after injection of nucleophosmin dsRNA. The relative abundance of A) *Cenpf* and B) *Clec2d*. The relative abundance (y-axis) represents the amount of mRNA in a single embryo. Bars show mean \pm S.D.

Figure 6

Confocal laser scanning microscopy of embryos injected with nucleophosmin dsRNA and corresponding controls. Nuclei (DAPI) – blue; nucleophosmin - red

Figure 7

Western blot analysis for the presence of nucleophosmin in bovine embryos at 4-cell and morula stage following nucleophosmin dsRNA injection. Different exposition times are shown, so that both difference in protein abundance between 4-cell stage and morula and the protein amount in nucleophosmin dsRNA injected morulas can be seen. (control 4c - 4-cell control embryos; *Npm1* dsRNA inj.- 4c – nucleophosmin dsRNA injected 4-cell embryos; *Npm1* dsRNA inj.- morula - nucleophosmin dsRNA injected morulas)

Figure 8

Developmental competence of embryos after injection of nucleophosmin dsRNA. Number of embryos reaching individual developmental stages (y-axis). The number of 2-cell stage embryos is considered as 100%. The developmental competence was followed up during 4 independent experiments. ^{a,b}Values with different superscripts indicate $P=0.05$. 2c -2-cell stage embryos; 4c -4-cell stage embryos; 8c – 8-cell stage embryos; 16c – 16-cell stage embryos

Figure 9

Confocal laser scanning microscopy of 8-cell stage embryos injected with nucleophosmin dsRNA and corresponding controls stained for nucleophosmin and alpha-tubulin as a cytoskeletal protein. Nuclei (DAPI) – blue; nucleophosmin – red; alpha-tubulin – green

Table 1 Primer details

primer	sequences	annealing temperature	amplicon size
<i>Npm1</i> (NM_001035441) dsRNA	5'AGGATCCTAATACGACT CACTATAGGGAGAACGAT GACGATGATGATGATG3'	55°C	583 bp
	5'ACTCGAGTAATACGACT CACTATAGGGAGAACAAG CAAAGGGTGGAGTTC3'		
<i>Gfp</i> dsRNA* (Anger et al., 2005)	5'AGGATCCTAATACGACT AACTATAGGGAGAATGGT GAGCAAGGGCGAGGA 3'	55°C	712 bp
	5'ACTCGAGTAATACGACT CACTATAGGGAGAGCGGC CGCTTTACTTGTACA 3'		
<i>Clec2d</i> (XM_869843)	5'CACATGCCACGGAACAG C3'	55°C	110bp
	5'CTGCGGAGGACAGATTC TTG3'		
<i>Npm1</i> (NM_001035441) degradation verification	5'ACAGCCAACGGTTTCTC TTG 3'	55°C	154 bp
	5'TTTCACCTCCTCCTCCTC CT 3'		
<i>Cenpf</i> (XM_612376)	5'AGATGAAAGCCAGGCTC ACCCAGGAGCTAC 3'	60°C	445bp
	5'TCCAGGTCAGCCAAGGC AAGCTTCAGTTTC 3'		
<i>Npm1</i> (NM_001035441) mRNA expression	5'CTGCTGGTTCCAATAGT AGTC3'	53°C	262bp
	5'CGCCTCTGCTTCAACAA C3'		

* Transcribed from empty p-Bluescript-GFP vector; kindly donated by M. Anger and P. Šolc

Figure 1

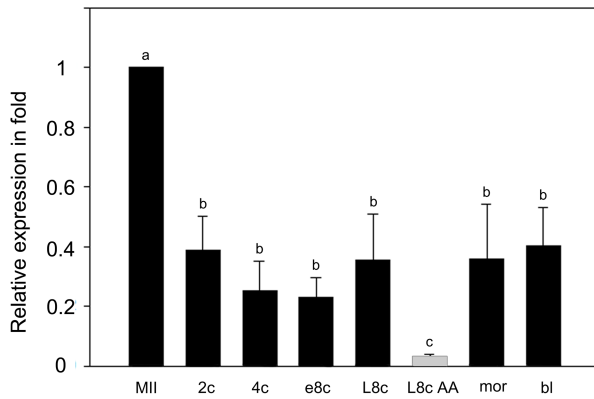


Figure 2

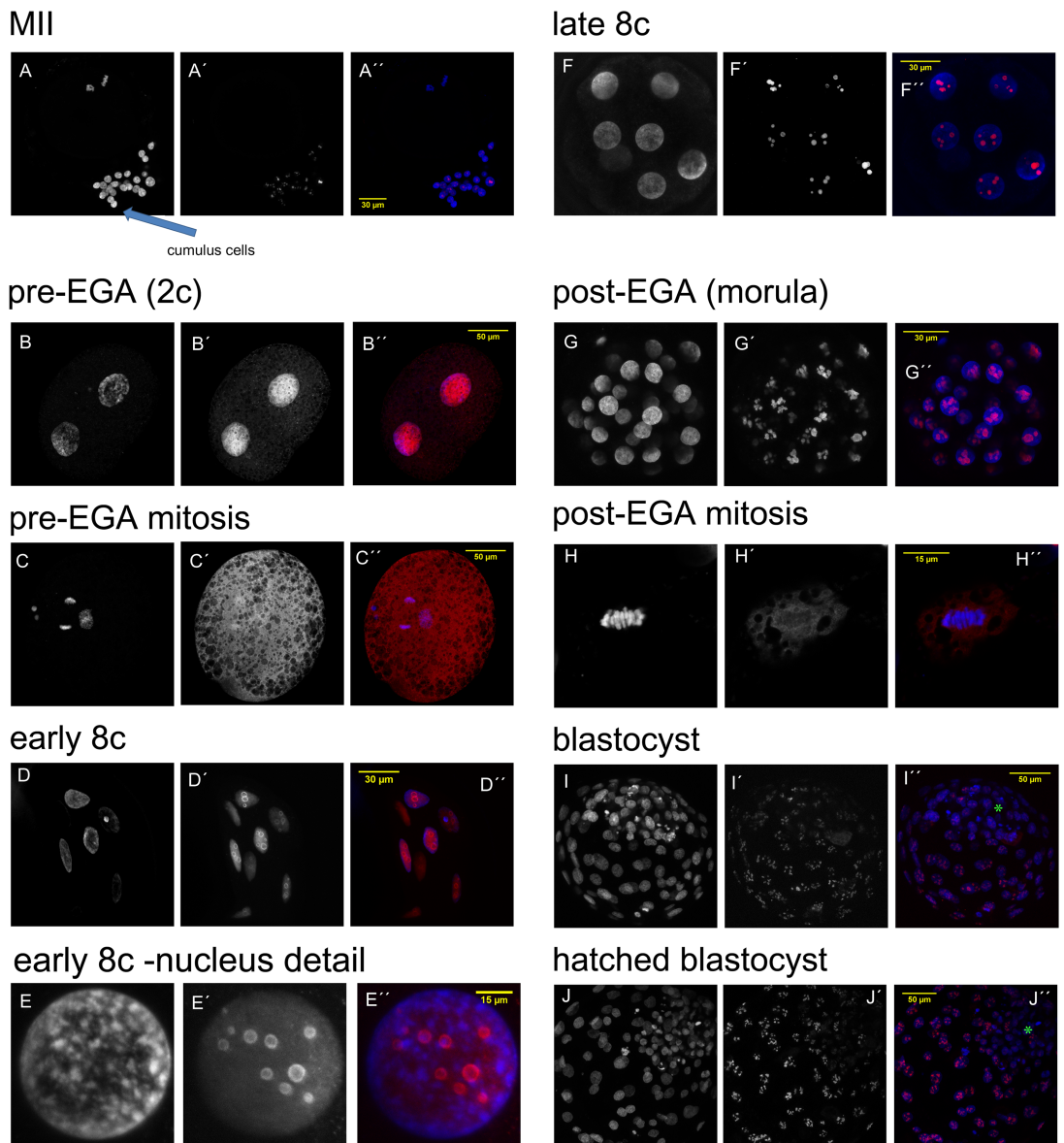


Figure 3

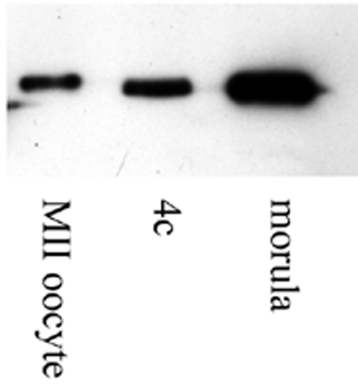


Figure 4

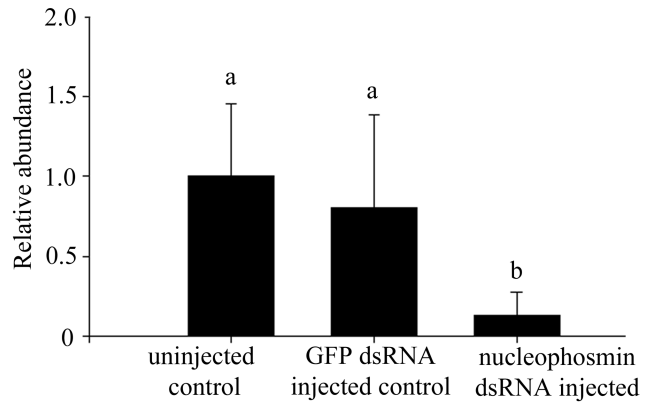


Figure 5

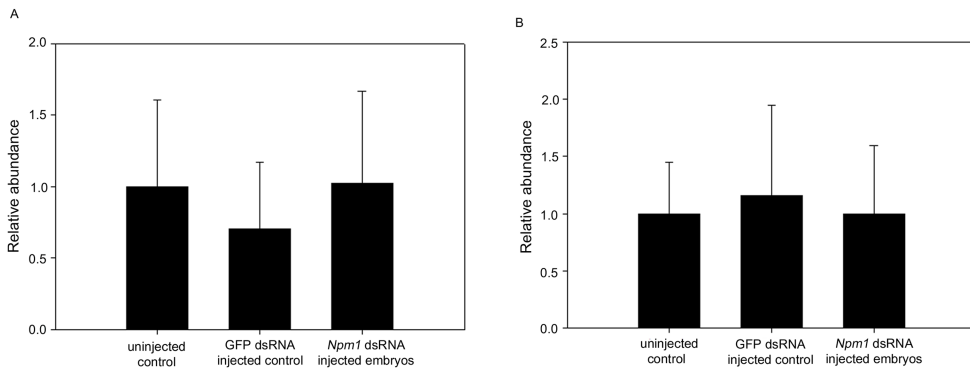


Figure 6

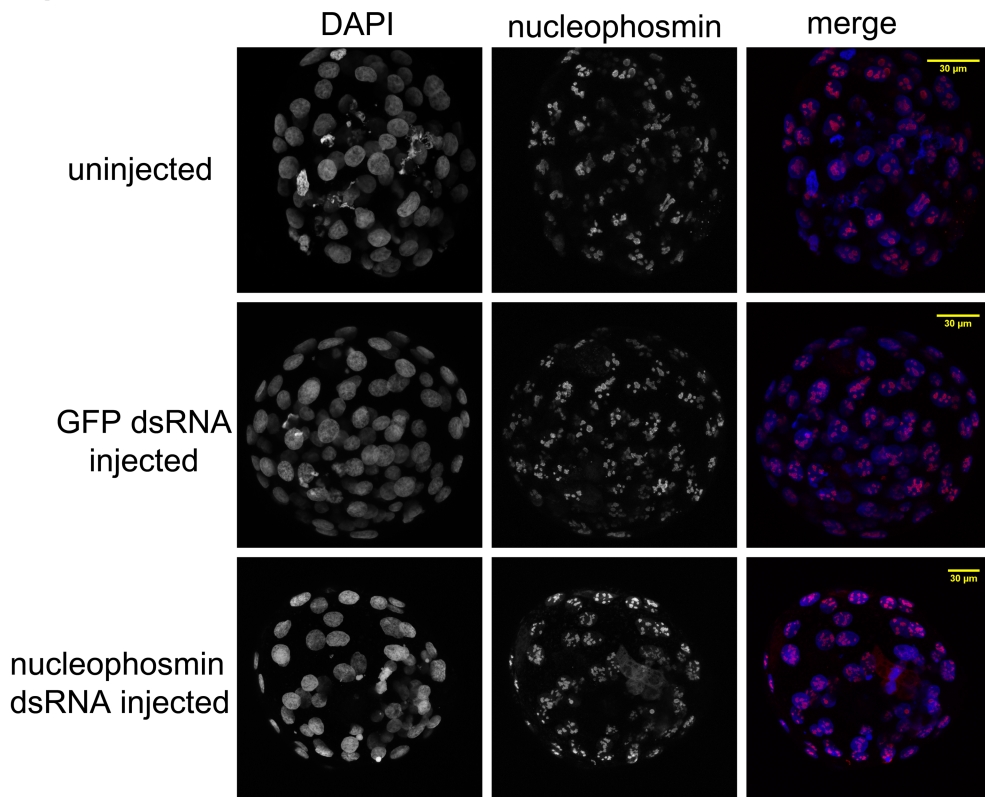


Figure 7

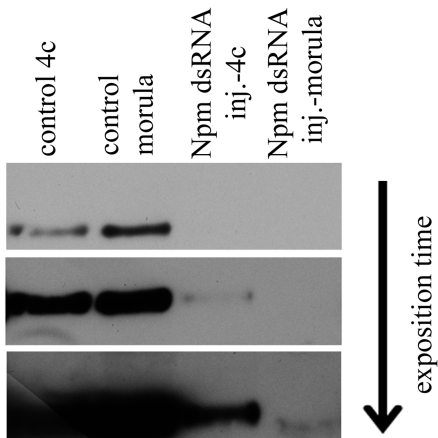


Figure 8

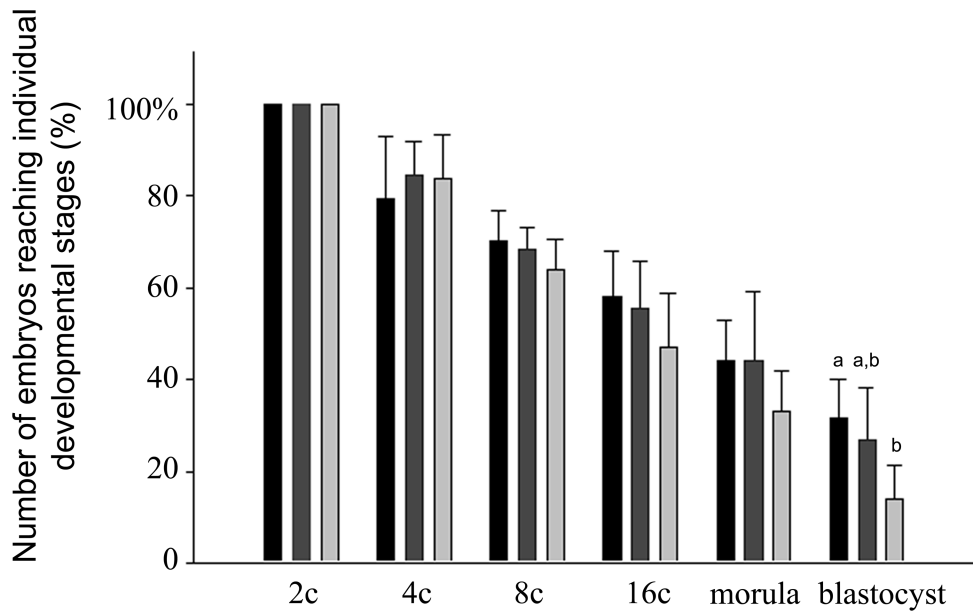


Figure 9

